Diversity in Notch ligand-receptor signaling interactions

Thesis by

Rachael Kuintzle

In Partial Fulfillment of the Requirements for the Degree of

PhD in Biochemistry and Molecular Biophysics

CALIFORNIA INSTITUTE OF TECHNOLOGY

Pasadena, California

2023

Defended May 2, 2023

Rachael Kuintzle
ORCID: 0000-0002-1035-4983

Acknowledgments

The research in this thesis comprises only one of three substantial facets of my professional development during my graduate studies, the other two being my creative writing and advocacy work. I have been surrounded in all these endeavors by wonderful people who are creative, passionate about science, and who labor tirelessly, often through volunteer service, to fight against injustice in their spheres of influence.

First, I'd like to thank my advisor, Michael Elowitz, for giving me the freedom to pursue the questions I was most curious to answer. I have learned much from watching you digest massive, complex sets of results into elegant principles and tidy diagrams that clearly communicate the most striking results.

Second, I acknowledge the colleague who contributed most significantly to the results presented here—my research partner-in-crime, Leah Santat, who wears many indispensable hats in the Elowitz Lab. Her unfailing enthusiasm for all things Notch signaling has kept me going through all the ups and downs of my PhD journey. I have been privileged to work so closely with such a skilled scientist, cell engineering miracle worker, and kind person for more than half a decade.

I thank other members and alumni of the Elowitz Lab, and especially of the "Signaling Subgroup," for helpful conversations and scientific advice—Yitong Ma, James Linton, Jacob Parres-Gold, Heidi Klumpe, Christina Su, Ron Zhu, and Lucy Chong. I am also grateful to my research mentees for their help with exploratory experiments: Rose Huang (rotation student), Giselle Venegas (i-STEM Scholars Summer Research Program), and Catherine Ko (Caltech's Freshman Summer Research Institute Program).

I think no biology-related dissertation from Caltech is complete without an acknowledgment of Justin Bois, whose excellent courses have made statistics and mathematical modeling intuitive and accessible to so many students among our ranks.

I would also like to extend gratitude to the members of the TechLit creative writing club for contributing in more subtle ways to this work by honing my writing skills over the years through rigorous critique of my fiction stories, and by giving me the privilege of editing their work. Thank you to my fellow writers and editors who dreamed that we could create Caltech's first science

fiction anthology, and then put in the work to bring it into existence in the form of *Inner Space and Outer Thoughts: Speculative Fiction From Caltech and JPL Authors*. I am grateful especially to my intrepid sci-fi coauthor, Samuel Clamons, who has an extraordinary gift for writing aliens. Small tides and large clutches, Sam.

I believe that service and advocacy are an important part of PhD training and of any stage of a scientific career. Some of the most valuable things I learned during graduate school were taught by my dear friends and advocacy mentors Sarah Sam and Nathan Waugh. I am honored to have served with fellow members of the Graduate Student Council Advocacy Committee, along with the leadership of Women in Biology and Bioengineering (WiBBE) and PRISM, to advance gender equity at Caltech through expanding support for student parents and improving gender inclusivity. I am grateful to the Steering Committee of Caltech Grad Students & Postdocs United, who are currently fighting for a better future for their colleagues. And I am forever humbled by all the student leaders from schools across the country who have believed that we could make meaningful change together, especially Katy Dupree, Flannery Currin, Justine Nguyen, and Sindupa De Silva.

Finally, thank you to my partner, Sharif Durzi, for keeping me fed during this weird thesis-writing period, as ever; for striving each day to fight against our species' destruction of the natural world; for your extremely effective encouragement, which has empowered me to accomplish things I didn't think were possible; and for mesonance.

Abstract

The ability to understand and predict signaling between different cell types is a major challenge in biology. The Notch pathway enables direct signaling through membrane-bound ligands and receptors, and is used in diverse contexts. While its canonical molecular signaling mechanism is well characterized, its many-to-many interacting pathway components, the complexity of their expression patterns, and the presence of same-cell (cis) as well as inter-cellular (trans) receptor-ligand interactions, have made it difficult to predict how a given cell will signal to others. Here, we use a cell-based approach, with Chinese hamster ovary (CHO-K1) cells and C2C12 mouse myoblasts, to systematically characterize trans-activation, cis-inhibition, and cis-activation efficiencies for the essential receptors (Notch1 and Notch2) and activating ligands (Dll1, Dll4, Jag1, and Jag2), in the presence of Lunatic Fringe (Lfng) or the enzymatically dead Lfng D289E mutant. All ligands trans-activate Notch1 and Notch2, except for Jag1, which competitively inhibits Notch1 signaling, and whose Notch1 binding strength is potentiated by Lfng. For Notch1, cis-activation is generally weaker than trans-activation, but for Notch2, cis-activation by Delta ligands is much stronger than trans-activation, and Notch2 cis-activation by Jag1 is similar in strength to trans-activation. Cis-inhibition is associated with weak cis-activation, as Dll1 and Dll4 do not cis-inhibit Notch2. Lfng expression potentiates trans-activation of both Notch1 and Notch2 by the Delta ligands and weakens trans-activation of both receptors by the Jagged ligands. The map of receptor-ligand-Fringe interaction outcomes revealed here should help guide rational perturbation and control of the Notch pathway.

Table of Contents

List of Figures and Tables

Chapter I: Introduction

1.1 Notch signaling amplitude controls cell fate decisions and cell states in nearly every tissue

The Notch signaling pathway is a juxtacrine signaling system, evolutionarily conserved from fruit flies to humans, that allows neighboring cells to communicate with each other through direct contact between a membrane-bound ligand on one cell and a receptor on the surface of a proximal cell (Artavanis-Tsakonas, Rand, and Lake 1999; Kopan and Ilagan 2009; Bray 2016; Henrique and Schweisguth 2019). It controls cell fate decisions in nearly every tissue and plays major roles in stem cell quiescence (Engler et al. 2018), activation of the progenitor pool in response to injury (Yao et al. 2018), cell proliferation, symmetry-breaking during cell fate branching points during development (Sjöqvist and Andersson 2019), and diversification of terminal cell subtype selection (Rocha et al. 2009; G. C. Tan, Mazzoni, and Wichterle 2016). In some cases, Notch also maintains the fate of terminally differentiated cells, as in the adult lung, where loss of Notch signaling results in transdifferentiation of club cells to ciliated cells (Lafkas et al. 2015).

In mammals, there are four Notch receptors (Notch1-4) and five canonical, membrane-bound ligands including the purely cis-inhibitory ligand Dll3 (Bochter et al. 2022; Ladi et al. 2005; Sewell et al. 2009) and four activating ligands that mediate Notch signaling at junctions between cells in direct contact: Delta-like 1 and 4 (Dll1, Dll4) and Jagged 1 and 2 (Jag1, Jag2). All four ligands are able to bind Notch1 and Notch2 (Kakuda et al. 2020), the only receptors essential for development in mice (Krebs et al. 2003; Kitamoto et al. 2005; Krebs et al. 2000; McCright et al. 2001; Hamada et al. 1999; Swiatek et al. 1994; Conlon, Reaume, and Rossant 1995). Yet, regardless of which ligand activates a given receptor, the downstream molecular events are thought to be the same. Activation of a ligand-receptor complex initiates trans-endocytosis of the ligand and the bound extracellular domain (ECD) of the Notch receptor by the sending cell (Langridge and Struhl 2017; Lovendahl, Blacklow, and Gordon 2018). This endocytic process exerts a force on the receptor, which results in unfolding of the negative regulatory region (NRR) and exposure of the S2 metalloproteinase cleavage site (Gordon et al. 2015). Following release of the Notch ECD, the receptor undergoes a second proteolytic cleavage event (S3-cleavage) by gamma-secretase—recently reported to occur in an intracellular compartment rather than at the cell surface (Martin et al. 2022)—that releases the intracellular domain (ICD) into the cytoplasm. The Notch ICD

subsequently translocates into the nucleus, where it assembles into a transcription factor complex with CBF1–Suppressor of Hairless–LAG1 (CSL or RBPJ) and co-activator Mastermind (MAML) to activate expression of target genes (Bray 2016).

The identity of the NICD produced via signaling appears to matter in some contexts, such as in the regulation of osteoclastogenesis, where the Notch2 ICD (N2ICD) may bind different cofactors than Notch1 ICD (N1ICD) does, conferring a qualitatively different function (Sekine et al. 2012; Yu and Canalis 2020). However, Notch1 and Notch2 ICDs are thought to be largely functionally equivalent in their binding partners and in the genes they regulate. Many tissues develop normally in mice when the two NICDs are swapped, including the kidneys, lung, liver, inner ear, and others, and developmental abnormalities are attributed to differences in surface receptor levels and NICD half-life (Zhenyi Liu et al. 2013, 2015; Kraman and McCright 2005).

What the downstream target genes, and cell state, seem to care about is the level of Notch signaling, rather than the identity of the receptor or ligand that transduced it. Indeed, Notch is an exquisitely dose-sensitive pathway. Different levels of Notch signaling elicit different responses in cells. Some cells can distinguish at least three signaling amplitudes: 'off,' 'low,' and 'high.' For example, in pancreatic progenitors (Ninov, Borius, and Stainier 2012) and CNS stem cells (Guentchev and McKay 2006), Notch inhibition ('off') promotes differentiation, while expression of 'low' levels of constitutively active NICD promote proliferation, and 'high' levels of NICD cause cells to exit the cell cycle. The level of Notch signaling also affects the ratios of different cell types derived from progenitor cells; for example, it dictates the ratios of three different cell types derived from hematopoietic progenitors (Dallas et al. 2005). Finally, a higher NICD dose can upregulate target transcription factors earlier in a developmental trajectory, depending on the target's enhancer architecture (Falo-Sanjuan and Bray 2019).

Cells have many methods of tuning Notch signaling levels: up- or down-regulation of ligands and receptors, expression of ligand activity modulators (like ubiquitin ligase Mindbomb1) (Baek et al. 2018), expression of post-translational modifiers of the Notch extracellular domain (like the Fringe glycosylatransferase enzymes) (Hicks et al. 2000; Kakuda et al. 2020; Stanley 2007), relocalization of expressed Notch components (Driessen et al. 2018), enhancer activity (Kuang et al. 2020), contact geometry between signaling cells (Khait et al. 2016; Shaya et al. 2017), antagonism of the

NICD by other factors (Sánchez-Iranzo, Halavatyi, and Diz-Muñoz 2022; Kim et al. 2011), and more.

The present work focuses on how cells may control Notch signaling amplitude via careful expression of specific Notch receptors, ligands, and factors that modify their interaction strengths, which all appear in highly regulated spatiotemporal patterns during development (Gasperowicz, Rai, and Cross 2013; Ramos et al. 2010).

1.2 Notch ligands can inhibit and activate receptors both intercellularly and cell-autonomously, with different strengths

Notch ligands function redundantly in some contexts and non-redundantly in others. For example, Dll4 knocked into the Dll1 locus cannot replace Dll1 function in many tissues, leading to embryonic lethality in mice (Preuße et al. 2015). Moreover, ectopic Dll1 and Dll4 expressed in the neural crest have opposite effects on muscle differentiation (Rios et al. 2011; Cappellari et al. 2013). Functional differences are attributed to the ligand extracellular domain, and are thought to arise from differences in their interactions with receptors (Tveriakhina et al. 2018)—specifically, differences in their activation strengths (Abe et al. 2010; Andrawes et al. 2013). Dll4 is reported to activate Notch1 more strongly than Notch2, while Dll1 and Jag1 activate Notch2 as efficiently or more strongly than Notch1 (Tveriakhina et al. 2018; Kakuda et al. 2020). It is therefore not surprising that Dll4 and Jag1 are the predominant activating ligands for Notch1 and Notch2, respectively, during mouse development (Hozumi 2019).

Signaling strength can be modulated by Fringe enzymes, which glycosylate the Notch extracellular domain and modify the strength of interactions between receptors and ligands (Kakuda et al. 2020; Kakuda and Haltiwanger 2017). For example, Lunatic Fringe (Lfng), which is essential for development in mice (Zhang, Norton, and Gridley 2002; Moran et al. 2009; Evrard et al. 1998), potentiates Notch1-Dll1 signaling and attenuates Notch1-Jag1 signaling, although their are conflicting reports of its effects on other receptor-ligand combinations (Shimizu et al. 2001; Hicks et al. 2000; Kakuda et al. 2020).

When ligands are coexpressed with receptors (in cis) instead of separately in adjacent cells (in trans), they can inhibit receptor activation by competing for receptor binding with an activating ligand presented in trans ("cis-inhibition") (Sprinzak et al. 2010; Fiuza et al. 2010; Becam et al.

2010; Palmer, Jia, and Deng 2014). In this configuration, the receptor and ligand are thought to interact through the same interface (Cordle et al. 2008), enabling competition between cis and trans ligand for receptor binding, but without an obvious way for the cis-ligand to generate the force needed to activate the receptor.

Cis-inhibition can mediate sharp fate decisions in adjacent cells in a process called lateral inhibition, for example, when daughter cells asymmetrically inherit ligand or receptor (Sjöqvist and Andersson 2019; Miller, Lyons, and Herman 2009). In such cases, asymmetries in ligand:receptor ratios create asymmetries in Notch signaling (Sprinzak et al. 2010), which can be amplified by negative feedback mechanisms (Notch signaling can downregulate Delta ligand expression) (del Álamo, Rouault, and Schweisguth 2011; Collier et al. 1996). Feedback may be essential for emergence of strong 'senders' and 'receivers' for tissue patterning. Cis-inhibition is best understood in the context of *Drosophila* wing boundary formation (Klein, Brennan, and Arias 1997; Micchelli, Rulifson, and Blair 1997; LeBon et al. 2014).

More recently, the phenomenon of cis-activation was observed in vitro—Dll1 and Dll4 ligands activated Notch1 and Notch2 receptors in vitro when a ligand and receptor pair were coexpressed (Nandagopal, Santat, and Elowitz 2019). Though its mechanism remain unknown, cis-activation requires ligand-receptor binding at the cell surface and is blocked by γ-secretase inhibitors, similar to canonical trans-activation. At least for Notch1, cis-activation shows a nonmonotonic ligand dose response, which a recent report suggests is generated via the inverse dependence of ligand activating potential on ligand-receptor stoichiometry (D. Chen et al. 2023). Specifically, mutations in the Dll4 EGF repeats that facilitate homodimerization decreased its cis-inhibitory potential, and this mechanism is consistent with a mathematical model that successfully recapitulated the nonmonotonic cis-activation curve for the Notch1-Delta combinations (Nandagopal, Santat, and Elowitz 2019).

It is possible that ligand oligomerization at high ligand concentrations is inhibitory in trans as well as in cis. High Delta levels in *Drosophila* inhibit signaling in adjacent neighbors, allowing clusters of adjacent high-Delta cells to emerge (Yatsenko and Shcherbata 2021; Zamfirescu, Yatsenko, and Shcherbata 2022). Modeling experiments have demonstrated how an inverse relationship between signaling strength and Delta levels in the high ligand range enable the emergence of clusters of adjacent cells expressing high Delta levels (Hadjivasiliou, Hunter, and Baum 2016). However, a

better understood mechanism of intercellular, ligand-mediated Notch inhibition ("trans-inhibition") is exemplified by the Notch1-Jag1 combination. Multiple reports show that Lfng increases the strength of Notch1-Jag1 binding while simultaneously decreasing their activation potential (Hicks et al. 2000; Kakuda and Haltiwanger 2017; Taylor et al. 2014; Yang et al. 2005). This is consistent with reports that Jag1 is an essential and Lfng-dependent trans-inhibitor of Dll4-Notch1 signaling in angiogenesis (Pedrosa et al. 2015; Benedito et al. 2009) and of Dll1-Notch1 signaling in the embryonic pancreas (Golson et al. 2009). It is unknown whether Lfng may enhance the inhibitory potential of other ligand-receptor pairs.

An essential role for cis-activation or cis-inhibition of Notch receptors by mammalian ligands has yet to be demonstrated in vivo, with the exception of the purely cis-inhibitory ligand Dll3 (Bochter et al. 2022; Ladi et al. 2005; Sewell et al. 2009). However, cell atlas data demonstrate that Notch receptors and their activating ligands are frequently coexpressed and able to interact within the same cell (Granados, Kanrar, and Elowitz 2022; Rusanescu and Mao 2014; Mitra et al. 2020; Xu et al. 2023; Negri et al. 2019). Thus, to predict the functions of individual Notch ligands in any given context, the signaling consequences of cis interactions between different ligands and receptors must be studied and taken into account.

1.3 Why are Notch components predominantly expressed in complex combinations?

Recent analysis of Notch pathway gene expression in publicly available single cell RNA-seq datasets has identified recurrent "motifs" of Notch components frequently coexpressed in the same cell across multiple different tissues (Granados, Kanrar, and Elowitz 2022). The vast majority of the 16 most prevalent motifs include Notch1 and Notch2, at least one ligand, and at least one Fringe enzyme. Several motifs express show substantial levels of five or more receptors and ligands, such as motif 12 (in Figure 5C) which shows high Notch1, Notch2, Notch4, Dll4, Jag1, and Rfng, with moderate levels of Dll1 and Jag2. This motif appears in cells of kidney, lung, large intestine, and other tissues.

Loss of function studies suggest that not all essential ligands and receptors play essential roles in every cell type where they are expressed. For example, in the intestinal crypt, Notch1 and Notch2 are functionally redundant, as individual loss of function maintains normal tissue homeostasis, but

inactivation of both receptors simultaneously results in depletion of the progenitor pool (Riccio et al. 2008).

In addition to including components that serve redundant functions, it is possible that complex Notch expression profiles in snapshots of developmental stages reflect the recent usage history of signaling components upregulated during a developmental trajectory to potentiate or attenuate Notch signaling amplitude. Expression of Notch components is precisely and dynamically modulated throughout a differentiation trajectory, especially in contexts where Notch controls many different decisions in a fate decision tree. For example, Jag2 is transiently expressed in motor neuron progenitors (pMNs) to inhibit differentiation (Rabadán et al. 2012), and Dll4 is upregulated later than Dll1 in differentiating neurons of the embryonic mouse retina and pV2 domain of the spinal cord (Rocha et al. 2009). It is possible that, in addition to rapidly increasing Notch signaling, upregulation of additional ligands in some cases could inhibit signaling—for example, upregulation of Jag1 in trans (Pedrosa et al. 2015; Benedito et al. 2009) or in cis (LeBon et al. 2014) could present an efficient and rapid method for dampening Notch1 signaling activity. Indeed, Golson et al. reported that Jag1 is upregulated after Dll1 to inhibit it in the pancreas (Golson et al. 2009).

Finally, complex Notch expression profiles theoretically enable more precise temporal regulation of Notch signaling. For example, in pancreatic progenitor cells, Notch signaling oscillations drive proliferation of multipotent progenitors (MPCs), and are mediated by feedback regulation between the Notch target gene/transcription factor Hes1 and Dll1, which both oscillate with ~90 periods (Seymour et al. 2020). Jag1 is constitutively expressed in these cells, and loss of Jag1 yields the opposite phenotype to loss of Dll1. Thus, Jag1 acts as a Notch1 inhibitor in this context, dampening and/or sharpening Notch signaling oscillations by sequestering receptor some portion of the receptor pool away from oscillating Dll1. This mechanism could be used in other tissues as well, since Notch signaling also exhibits asynchronous oscillations in developing neural progenitor cells (Shimojo, Ohtsuka, and Kageyama 2008; Kageyama et al. 2008) and muscle progenitors (Lahmann et al. 2019).

The differential ability of ligands to activate or inhibit specific receptors in cis or in trans presents many possible ways for cells to tune Notch signaling for regulation of cell state and fate via upregulation of additional Notch components. Characterizing the nature of those interactions for

all receptor-ligand combinations could shed light on the logic underlying changes in Notch gene expression profiles throughout cell fate decision trees.

1.4 The Notch pathway's diverse biological roles and the context-dependent functions of its signaling components have made it a challenging drug target

Mutations in Notch genes and misregulation of Notch component expression result in developmental diseases such as Alagille syndrome, congenital scoliosis, osteoarthritis, and CADASIL as well as numerous cancers including T cell acute lymphoblastic leukemia (T-ALL), Hepatocellular carcinoma, and glioma (Penton, Leonard, and Spinner 2012; Aster, Pear, and Blacklow 2017; Zhou et al. 2022). Although simple in its architecture, with only four receptors, five ligands, and a linear signal transduction mechanism with no second messengers, the combinatorial complexity of the interactions between Notch ligands and receptors, as well as the dependence of their functional roles on other molecular factors and cellular context, have made it a challenging target of pharmaceutical intervention.

Notch can play both oncogenic and tumour suppressive roles in various cancers, and in small cell lung cancers, Notch signaling has been discovered to both promote and inhibit tumour growth in different cell subpopulations within the same tumour (Aster, Pear, and Blacklow 2017; Kamath et al. 2012; Zhou et al. 2022). Multiple pan-Notch inhibitors were tested in clinical trials but have largely been discarded due to toxicity. Majumder et al. wrote in their recent review, "We are learning that the inherent complexity of Notch biology will require more precise and sophisticated approaches to the development of Notch-based therapeutics" (Majumder et al. 2021). Some promising cancer therapies target specific Notch receptor and ligand combinations (Zhou et al. 2022). Additionally, since cis-interactions may involve additional ligand-receptor contacts compared with trans-activation (Brendan D'Souza, Meloty-Kapella, and Weinmaster 2010), it is theoretically possible to design drugs that precisely block cis but not trans interactions between specific ligand-receptor pairs. However, the functional natures of the interactions between many receptor-ligand combinations remain unknown, especially when these components are coexpressed in the same cell, as previously described.

In Chapter 2, we present research providing a quantitative assessment of interactions between all essential Notch receptors, their activating ligands, and key modulators of receptor-ligand

interactions, paving the way for more rational approaches to perturbation of Notch signaling. Specifically, we measured the signaling activation strength of all pairwise combinations of essential receptors and ligands, both in cis and in trans, and assess the dependence of their activity and binding strength on Lfng expression. These data suggest that the Delta ligands preferentially cis-activate rather than cis-inhibit Notch2 receptors, even when competing with activating ligands supplied in trans, but all other ligand-receptor combinations can mediate cis-inhibition. Though future work is needed to quantitatively compare binding strengths, determine whether biophysical synergies impact their interactions when more than one receptor and ligand are coexpressed, and assess the generalizability of these interaction modes in vivo, our findings provide the first complete, functional map of interactions between the essential receptor, ligand, and Fringe interactions both in cis and in trans.

Chapter II: Diversity in Notch ligand-receptor signaling interactions

Rachael Kuintzle[1], Leah Santat[2], and Michael Elowitz[2]

[1]Division of Chemistry and Chemical Engineering, Caltech, Pasadena, CA

[2]Howard Hughes Medical Institute, and Division of Biology and Biological Engineering, Caltech, Pasadena, CA

2.1 Summary

The Notch pathway uses families of membrane-bound ligands and receptors to transmit signals at short length scales. These components are expressed in diverse combinations, interact in a many-to-many fashion, employ both intracellular (cis) and intercellular (trans) interactions, and are further modulated through receptor glycosylation by Fringe enzymes. A fundamental question is how the strength of Notch signaling depends on which pathway components are expressed, at what levels, and in which cells. Here, we used a quantitative, bottom-up, cell-based approach to systematically characterize trans-activation, cis-inhibition, and cis-activation signaling efficiencies across a range of ligand and Fringe expression levels in two different mammalian cell lines. Each ligand (Dll1, Dll4, Jag1, and Jag2) and receptor variant (Notch1 and Notch2) analyzed here exhibited a unique profile of interactions, Fringe-dependence, and signaling outcomes. All four ligands were able to bind receptors in cis and in trans, and all ligands trans-activated both receptors except for Jag1, which failed to activate Notch1. Cis interactions were predominantly inhibitory, with the exception of the Dll1- and Dll4-Notch2 pairs, which exhibited cis-activation stronger than trans-activation. Lfng strengthened Delta-mediated trans-activation and weakened Jagged-mediated trans-activation for both receptors, and in most but not all cases, Lfng effects on cis-activation were similar to those on trans-activation. Lfng effects on binding were sometimes decoupled from effects on activation, most notably in the case of Notch1-Jag1 and -Jag2, for which Lfng increased binding strength while decreasing activation strength. The map of receptor-ligand-Fringe interaction outcomes revealed here should help guide rational perturbation and control of the Notch pathway.

2.2 Introduction

The Notch signaling pathway controls stem cell differentiation and proliferation, plays key roles in numerous diseases, and represents a major drug target. It uses multiple membrane-bound ligands and receptors that interact with one another in a many-to-many fashion, as well as Fringe glycosyltransferases (Fringes) that modulate those interactions. In mammals, the Notch pathway consists of four receptors (Notch1-4), four canonical activating ligands (Delta-like 1 and 4 (Dll1 and Dll4) and Jagged 1 and 2 (Jag1 and Jag2)), at least one predominantly inhibitory ligand (Dll3, (Ladi et al. 2005; Serth et al. 2015)), and non-canonical ligands (Gera and Dighe 2018; B. D'Souza, Miyamoto, and Weinmaster 2008; Fiddes et al. 2018; Falix et al. 2012). Ligands and receptors interact both within the same cell (in cis) and between adjacent cells (in trans). Either configuration has the potential to activate or inhibit signaling (Nandagopal, Santat, and Elowitz 2019; del Álamo, Rouault, and Schweisguth 2011; Sprinzak et al. 2010). The level of signaling in a Notch expressing cell generally depends on which ligand, receptor, and Fringe variants are expressed in the cell and its neighbors. These components are expressed in various combinations in different cell types (Granados, Kanrar, and Elowitz 2022). However, it remains difficult to predict signaling strength—how strongly a given cell will signal to another cell—based on their expression profiles of Notch pathway components. It similarly remains challenging to rationally and predictably perturb signaling for therapeutic and tissue engineering purposes.

As a direct signal transduction pathway lacking second messengers, downstream transcriptional changes are sensitive to the amplitude and duration of Notch signaling. In the canonical trans-activation mechanism, binding of ligands on one cell to receptors on an adjacent cell triggers ligand endocytosis, which generates mechanical strain on the receptor, exposing a metalloproteinase recognition site (Lovendahl, Blacklow, and Gordon 2018; Langridge and Struhl 2017). S2 cleavage by ADAM10 results in shedding of the receptor extracellular domain (NECD) and permits a subsequent S3 cleavage by γ-secretase to release the Notch intracellular domain (NICD). The free NICD directly translocates into the nucleus and binds cofactors MAML and RBPjκ to activate target genes. Downstream target genes appear to be indifferent to NICD composition, responding similarly to NICD originating from the Notch1 or Notch2 receptors (Zhenyi Liu et al. 2013, 2015; Kraman and McCright 2005). However, they are sensitive to the concentration of NICD. In pancreatic progenitors (Ninov, Borius, and Stainier 2012) and central nervous system

(CNS) stem cells (Guentchev and McKay 2006), complete Notch inhibition permits differentiation, while 'low' levels of NICD promote proliferation, and 'high' levels induce quiescence. Notch signaling amplitude can also influence the timing of developmental transitions, with higher NICD concentrations activating master transcription factors earlier than lower concentrations, depending on the target's enhancer architecture (Falo-Sanjuan et al. 2019).

The Notch pathway provides numerous ways to quickly and precisely tune signaling amplitude. Fringe enzymes can alter receptor-ligand binding and activation strengths, sometimes in opposite directions (Kakuda and Haltiwanger 2017; Hicks et al. 2000; Kakuda et al. 2020). Upregulation of a cis-inhibitory ligand theoretically enables rapid, cell-autonomous suppression of Notch signaling (Sprinzak et al. 2010; Fiuza et al. 2010; Becam et al. 2010) and can simultaneously induce activation of receptors on neighboring cells. Growing evidence suggests that some ligands can inhibit signaling intercellularly ("trans-inhibition") by binding receptors strongly without activating them (Golson et al. 2009; Luna-Escalante, Formosa-Jordan, and Ibañes 2018; Benedito et al. 2009), as may be the case for Jag1 and Lunatic Fringe (Lfng)-modified Notch1 (Kakuda and Haltiwanger 2017; Hicks et al. 2000). Ligands can also activate receptors on the same cell ("cis-activation") (Nandagopal, Santat, and Elowitz 2019). Though its mechanism and natural function remain unknown, cis-activation requires ligand-receptor binding at the cell surface and is blocked by γ-secretase inhibitors, similar to canonical trans-activation. Thus, the Notch pathway architecture allows for receptor-ligand interactions to result in either activation or inhibition of signaling, in a manner dependent on the cis versus trans binding orientation. For the majority of the possible interaction pairs, relative activation and inhibition strengths have not been measured in both cis and trans; therefore, individual components' functions cannot currently be predicted in any natural contexts where receptors and ligands are coexpressed.

For the majority of possible interaction pairs, relative activation and inhibition strengths have not been measured in both cis and trans. Consequently, it is difficult to predict signaling outcomes in natural contexts where receptors and ligands are not only known to be coexpressed, but known to be expressed in various combinations (with multiple homologs) in different cell types (Granados, Kanrar, and Elowitz 2022)difficulty of predicting signaling strength (Notch signaling amplitude) based on expression profiles of Notch pathway components. Hence, it also remains challenging to rationally and predictably perturb signaling for therapeutic and tissue engineering purposes.

Therefore, to address the above-mentioned challenges, we developed a set of engineered cell lines and co-culture reporter assays to systematically characterize trans-activation, cis-inhibition, and cis-activation efficiencies across a range of cis-ligand and Fringe expression levels using Notch1 and Notch2 receptors in Chinese hamster ovary (CHO-K1) cells and C2C12 mouse myoblasts. We first systematically mapped trans interactions, and their modulation by Lfng, across multiple ligand-receptor combinations in CHO-K1 cells, and verified that key results generalized to a second, unrelated cell line derived from C2C12 mouse myoblasts to show that results were not specific to one cell background. We then performed a similar systematic analysis of cis interactions, and identified strong diversity among seemingly similar components. Finally, we delved into more complex cis-trans configurations of ligands, receptors, and Fringes.

We find that no receptor-ligand combination is alike in terms of its trans-activation strength, cis-activation strength, and its modulation by Lfng. We find that all ligands can trans-activate Notch1 and Notch2 except for Jag1, which cannot activate Notch1. Despite its impotence as a Notch1 activator, Jag1 efficiently cis-inhibits Notch1 and plate-bound Jag1 extracellular domain (Jag1-ext-IgG1) efficiently activates Notch1, suggesting that Jag1 binds the receptor without productive activation. Lfng further increases Jag1's inhibitory potential by strengthening its binding to Notch1 while weakening its Notch1 activation potential, in agreement with previous reports (Hicks et al. 2000; Kakuda and Haltiwanger 2017). By comparing the effects of Lfng expression on signaling activity for all receptor-ligand pairs, we find Lfng potentiates intercellular activation for all Delta-Notch combinations and attenuates activation for all Jagged-Notch combinations, but its effects on cis-activation sometimes differ from those on trans-activation. When receptors and ligands are coexpressed and allowed to engage in both cis- and trans-activation, trans-activation dominates over cis-activation, but the converse is true for the Notch2-Dll1 and -Dll4 pairs. In general, combinations that cis-activate weakly show efficient cis-inhibition in competition with sender cells supplying ligands in trans, although the relative strength of cis-inhibition depends in a complex manner on the identities of the receptor, the cis-inhibiting ligand, and the trans-activating ligand.

Together, these data define a ranking of receptor-ligand-Fringe activation strengths for both essential Notch receptors and all activating ligands in cis and in trans, as well as their dependence on Fringe enzyme expression. This information should enable prediction of Notch pathway

behaviors based on the expression profiles of other Notch proteins in a given cell or tissue context, and may help guide more rational, targeted perturbation of signaling activity.

2.3 Results

2.3.1 Engineered "receiver" and "sender" cell lines enable quantitative comparison of receptor-ligand-Fringe interactions

To systematically analyze all pairwise cis and trans receptor-ligand interactions, and their dependence on Fringe enzyme expression, we engineered a set of over 50 different stable cell lines (Supplementary Table 1). Collectively, they provide quantitative readouts of Notch signaling activity, receptor level, and ligand level. They also enable precise modulation of ligand expression. As a base cell line, we used CHO-K1 cells, which exhibit low levels of endogenous expression of most Notch pathway components (Supplementary Table 2) (Singh, Kildegaard, and Andersen 2018). In this background, we constructed three types of cell lines:

First, to read out Notch signaling, we created monoclonal "receiver" cells, similar to those described previously (Sprinzak et al. 2010; LeBon et al. 2014; Nandagopal, Santat, and Elowitz 2019) (Figure 1A). These cells expressed a chimeric human Notch receptor, whose intracellular domain was replaced with a minimal Gal4 transcription factor ("Gal4esn"). This coding sequence was followed by H2B-mTurq2, with an intervening ribosomal skipping "T2A" sequence, for cotranslational readout of receptor expression. It was stably integrated in the host cell genome using piggyBac transposition (System Biosciences, Methods). The cells also contained an insulated UAS promoter driving expression of H2B-mCitrine, such that mCitrine production reflects Notch activity.

Second, to analyze same-cell (cis) ligand-receptor interactions, we used lentivirus to stably integrate each of the four activating human Notch ligands (Dll1, Dll4, Jag1, Jag2) into the receiver cells (Figure 1A). All ligand constructs contained a cotranslational H2B-mCherry reporter for readout of expression (using T2A). Ligand expression was controlled by the Tet-OFF system, allowing the use of the doxycycline analog 4-epi-tetracycline (4-epi-Tc) to titrate relative ligand:receptor levels. In these lines, 4-epi-Tc tuned expression unimodally across two orders of magnitude (Figure 1—figure supplement 1), and ligand mRNA expression reached stable levels after 48 hours of incubation in media containing a low 4-epi-Tc concentration (Figure 1—figure supplement 2A). However, ligand expression from the Tet-OFF promoter showed a modest (<2-fold) dependence on cell culture density at fixed 4-epi-Tc concentrations (Figure 1—figure supplement 2B). Additionally, to control for non-specific effects of ligand overexpression, we also

constructed parallel negative control cell lines expressing H2B-mCherry or human nerve growth factor receptor (NGFR)-T2A-H2B-mCherry constructs in place of ligands. NGFR has been used in other Notch studies as a surface-detectable co-expression reporter or marker (Taghon et al. 2009; Sakata-Yanagimoto et al. 2008; Romero-Wolf et al. 2020; Del Real and Rothenberg 2013). Together, these cell lines enabled control and readout of cis ligand levels.

Third, we engineered a repertoire of "sender" cell lines (Figure 1A). One set enabled inducible expression of each of the four ligands under control of the Tet-OFF system. A second set provided constitutive expression of each ligand at a variety of different levels.

To limit combinatorial complexity, we focused on two essential receptors, Notch1 and Notch2, four canonical activating ligands (Dll1, Dll4, Jag1, and Jag2), and one Fringe (Lfng). We omitted Notch3, since Notch3 knockout mice are viable with minor vascular defects (Krebs et al. 2003; Kitamoto et al. 2005), and because Notch3 receptors are hypersensitive to activation during cell passaging, yielding elevated background signaling. We also omitted Notch4, which has no knockout phenotype in mice (Krebs et al. 2000), does not appear to activate in coculture with ligand-expressing cells (Groot et al. 2014; Lafkas et al. 2015; James et al. 2014), and has been suggested to inhibit Notch1 activation in cis (James et al. 2014). Among the best-studied ligands, we omitted Dll3 which is essential and believed to be purely cis-inhibitory (Bochter et al. 2022). Finally, we focused on Lunatic Fringe (Lfng), which we perturbed using siRNAs and transient plasmid transfection (Figure 1C), because it is the only Fringe enzyme that is essential in mice (Zhang, Norton, and Gridley 2002; Moran et al. 2009; Evrard et al. 1998)its effects dominate over those of Radical and Manic Fringe (Rfng and Mfng, respectively) when coexpressed (Pennarubia et al. 2021). Together, these cell lines enabled systematic analysis of ligand-receptor binding, trans-activation, cis-activation, and cis-inhibition (Figure 1B, Methods).

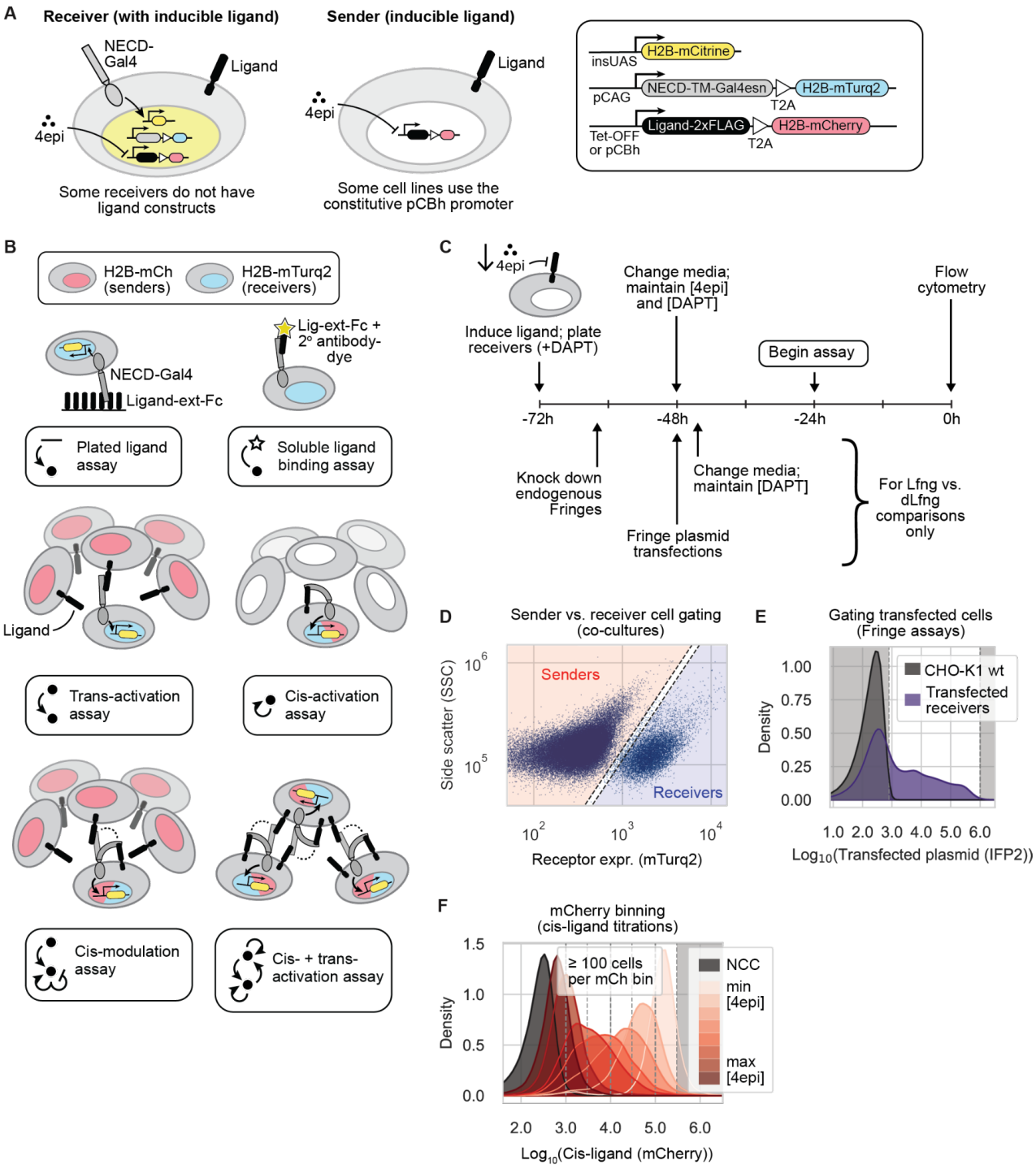

Figure 1: Engineered "receiver" and "sender" cells enable quantitative comparison of receptor-ligand interactions

(**A**) Cell line schematics. (Left) Engineered receiver cell lines enable readout of Notch signaling and receptor expression. CHO-K1 cells were engineered with a stably integrated construct containing a chimeric Notch receptor composed of the receptor extracellular and transmembrane domains fused with the minimal

Gal4 transcription factor ("Gal4esn," henceforth "Gal4") in place of the endogenous intracellular domain, followed by a T2A-H2B-mTurq2 cassette, enabling quantitative cotranslational readout of Notch receptor expression. Upon receptor activation, Gal4 is released and activates expression of the stably integrated insulated H2B-mCitrine cassette under the control of the UAS promoter. To create receiver cells containing cis-ligand, an additional construct containing a Notch ligand-2xFLAG-T2A-H2B-mCherry cassette under the control of the 4-epi-tetracycline (4-epi-Tc) suppressible Tet-OFF system was stably integrated into the originally engineered receiver cell lines. (Right) Engineered sender cell lines enable control and cotranslational readout of ligand expression levels. CHO-K1 cells were engineered to stably express a construct containing each of the four activating Notch ligands fused to 2xFLAG and followed by T2A-H2B-mCherry, under the control of the 4-epi-Tc suppressible Tet-OFF system or constitutively expressed by the CBh promoter. The T2A-H2B-mCherry enables quantitative cotranslational readout of ligand expression levels.

(**B**) Various cellular assays enable quantitative analysis of relative Notch-ligand binding strengths and Notch signaling activity mediated by ligands expressed in cis and/or trans. (From left to right): The plated ligand assay records Notch receivers' responses to various levels of plated recombinant ligand extracellular domains tagged at the C-terminus by a human Fc domain ("ligand-ext-Fc" or "lig-ext-Fc"). The soluble ligand binding assay enables the quantification of an experimental perturbation's effect on the strength of receptor binding to ligand-ext-Fc preclustered with secondary antibody. The trans-activation assay, where receiver cells are cultured with excess sender cells, enables the quantification of canonical trans-activation strengths for each receptor-ligand pair. The cis-activation assay enables quantification of cis-activation strengths by low-density plating of receivers expressing a range of cis-ligand levels with an excess of surrounding cells expressing no ligands. The cis-modulation assay is identical to the cis-activation assay, except that receiver cells are surrounded by excess senders to determine whether expressed cis-ligands increase or decrease (cis-inhibit) total signal activity relative to trans-activation alone. The cis- + trans-activation assay is similar to the cis-activation assay, except that receiver cells are plated in a confluent monoculture allowing cells to make intercellular contacts, and thus to signal in trans as well as in cis. See also Methods.

(**C**) Experimental workflow for cell culture experiments with flow cytometry readout. Ligand expression is induced in either sender or receiver cells by reducing the 4-epi-Tc concentration in the culture medium to the desired level, and receivers are incubated in the Notch signaling inhibitor DAPT to prevent reporter activation during this preinduction phase. Prepared cells, which may also undergo siRNA knockdown and/or plasmid transfection during the ligand preinduction phase, are replated without DAPT according to the chosen experimental scheme in (B) and allowed to signal for 22-24 hr before cells are detached and analyzed by flow cytometry. (**D-F**) Data plots show example flow cytometry data processing. Gates used in data processing are shown as dashed lines. Datapoints in grey-shaded regions were discarded.

(**D**) Senders and receivers are separated computationally in the flow cytometry data in a 2D plane of cell size (Side Scatter, A.U.) vs. cotranslational receptor expression (mTurquoise2, A.U.).

(**E**) Plasmid-transfected cells are gated on fluorescence levels of a cotransfected infrared fluorescent protein (IFP2, A.U.).

(**F**) Receiver cells coexpressing ligands are binned into discrete intervals of mCherry expression (A.U.) to generate curves sampling evenly across the ligand range.

2.3.2 Lfng potentiates Notch-Delta trans-activation and attenuates Notch-Jagged trans-activation

We first sought to analyze canonical Notch trans-activation and its dependence on Lfng activity for each receptor-ligand pair. Previous investigations reached conflicting conclusions about how strongly and even in what direction Fringes affect different ligand-receptor interactions (Kakuda et al. 2020; Yang et al. 2005; Hicks et al. 2000; Shimizu et al. 2001). However, these studies either focused on a small subset of ligand-receptor combinations, or in some cases used plate-bound ligands, which could potentially differ from expressed ligands in terms of their Fringe-dependence.

In order to compare cells with minimal Fringe expression to those expressing Lfng, we first suppressed endogenous Rfng and Lfng in receiver cells via siRNA knockdown (Figure 1C; Figure 2—figure supplement 1A; Supplementary Table 2). Approximately 16 hours later, we removed siRNAs and transfected plasmids encoding wild-type mouse Lfng or, as a negative control, a catalytically inactive mutant Lfng (D289E, denoted "dLfng") (Luther, Schindelin, and Haltiwanger 2009). We also co-transfected an additional marker, infrared fluorescent protein IFP2, to allow gating on transfected cells. After a 16-20 hour post-transfection recovery period, we cocultured these receivers with an excess of sender cells, previously sorted into various bins of stable ligand expression (Figure 2A), in a trans-activation assay. Finally, we measured Notch activity in receivers by flow cytometry after 22-24 hours of signaling. By gating on IFP2 positive cells (Figure 1E), we compared receiver cells expressing ectopic Lfng or dLfng. (Note that surface Notch1 levels differed by less than 25% between the dLfng- and Lfng-transfected samples (Figure 2—figure supplement 1B)). To enable robust quantification of Lfng effects, we used multiple monoclonal cell lines for each receptor (Figure 2B, Methods).

The effects of Lfng were similar for Notch1 and Notch2, but differed between Delta and Jagged ligand classes. Specifically, Lfng significantly enhanced Notch1 and Notch2 trans-activation by both Dll1 and Dll4. Its greatest effect was on Dll1-Notch1 (3-fold increase) followed by Dll4-Notch2 (2.5-fold increase) (Figure 2B,C). By contrast, Lfng significantly decreased trans-activation of both receptors by Jag1 (>2.5-fold) and, to a lesser extent, Jag2 (~1.4-fold).

Thus, Lfng strengthens Delta-mediated trans-activation and weakens Jagged-mediated trans-activation for both Notch1 and Notch2.

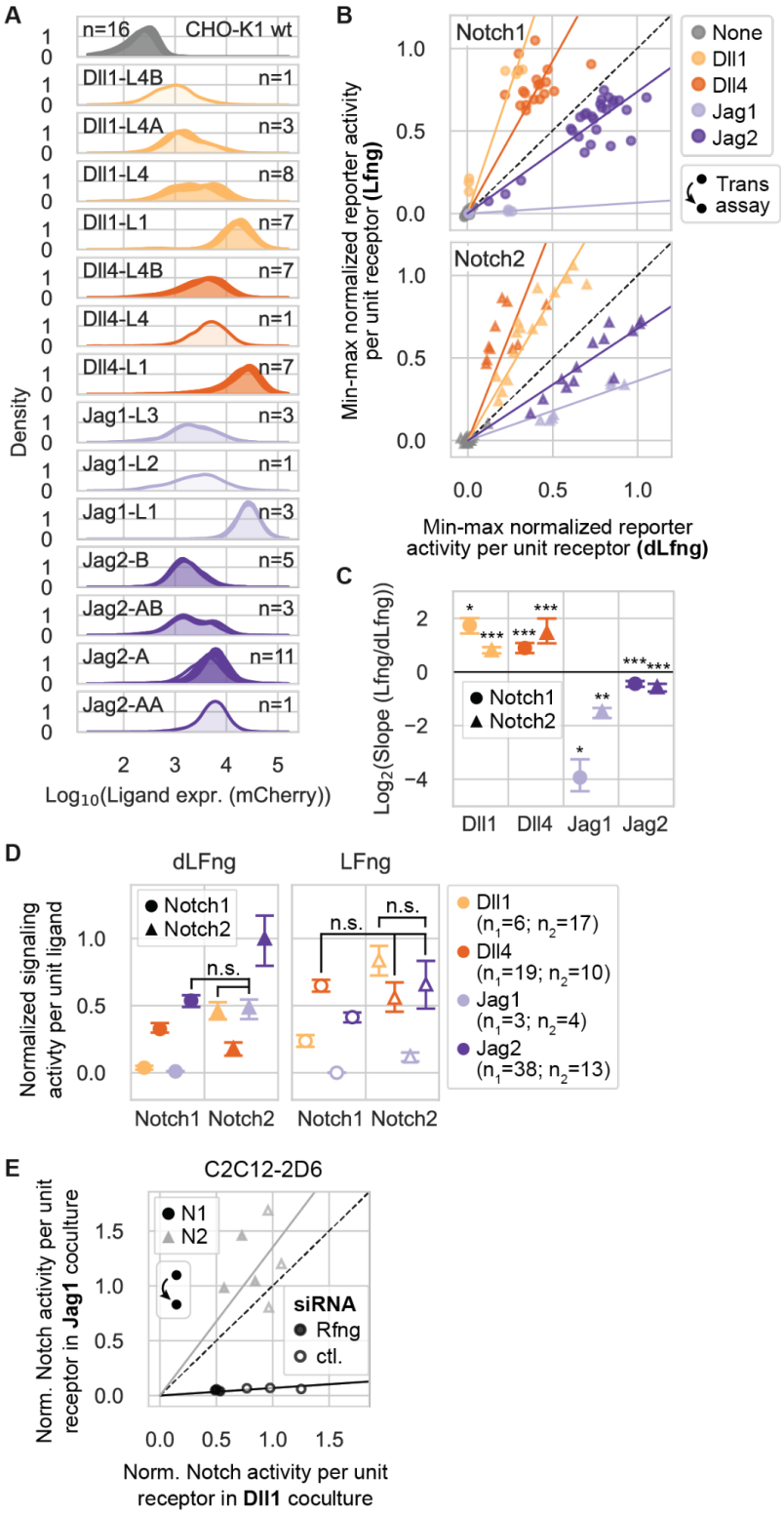

Figure 2: Lfng potentiates Delta- and attenuates Jagged-mediated trans-activation

(**A**) Histograms of single-cell distributions of cotranslational ligand expression (mCherry, A.U.) in the CHO-K1 sender populations used for Figure 2 experiments. Each histogram is a biological replicate, with a total of *n* replicates per plot.

(**B**) Scatterplots showing the effects of Lfng vs. dLfng (catalytically dLfng) on Notch1 (top) and Notch2 (bottom) signaling in the trans-activation assay, where endogenous CHO-K1 Rfng and Lfng were knocked down via siRNA and mouse Lfng or dLfng were added via transient plasmid transfection. Colors indicate the ligand expressed by the sender cells cultured in excess with the receivers for a given datapoint. X and y-axis values are signaling activity (reporter activity, mCitrine, divided by cotranslational receptor expression, mTurq2), background subtracted and normalized to the strongest signaling activity measured for each receiver clone in this experiment. Saturated data points, defined as those with normalized signaling activity over 0.75 in both dLfng and Lfng conditions, were excluded. Data are from five different Notch1 receiver clones and three different Notch2 clones, with at least three biological replicates per clone (Supplementary Table 4); cis-ligand expressed was suppressed with high 4-epi-Tc concentrations in receivers with integrated ligands. Colored lines are least-squares best-fits, and the black dashed line is y=x.

(**C**) Log2 fold difference in the slope of the best-fit line in (B) with Lfng expression relative to dLfng. Asterisks denote the p-value of the test statistic from a one-sided Wilcoxon signed-rank test (* p-val < 0.05; ** p-val < 0.01; *** p-val < 0.001), reflecting whether the slope is greater or lesser than 1. Error bars are 95% confidence intervals on best-fit slopes computed for 10k bootstrap replicates of the data points in (B).

(**D**) A ranking of ligand-receptor signaling strengths. Normalized signaling activities for non-saturated data points from (B) were further normalized to the mean expression of the sender population (A) cocultured with each receiver. Only senders with mCherry levels < 75% of the maximum sender expression were used, due to nonlinearities in normalized signaling activity with extremely high ligand expression. Error bars are 95% confidence intervals on the mean value of n data points across 10k bootstrap replicates, where n is given in the legend (n_1 corresponds to Notch1 receivers and n_2 to Notch2 receivers). The significance of pairwise differences in the signaling potential of each receptor-ligand-Fringe combination was evaluated by testing whether data for each pair come from distributions with the same mean, via permutation testing with 10k bootstrap replicates (Methods). Except where labeled with "n.s.," all signaling strengths within each subplot are significantly different (p-val < 0.05) from all other receptor-ligand combinations within the same Lfng or dLfng subplot. P-values for all 64 pairwise receptor-ligand-Fringe combination comparisons are given in Figure 2—figure supplement 2.

(**E**) Scatterplot showing the normalized Notch signaling strength in C2C12-Nkd Notch1 (black) or Notch2 (grey) receivers cultured with Jag1 vs. Dll1 senders in a trans-activation assay. Receivers were treated with negative control (unfilled markers) or mouse Rfng (filled markers) siRNAs prior to the assay. X and y-axis values are signaling activity (reporter activity, mCitrine, divided by cotranslational receptor expression, mTurq2), background subtracted and normalized to the max signaling activity—the average signal in Dll1 coculture with negative control siRNA treatment for each receiver. Solid lines are the least-squares best fit through all points for a given receiver. Both slopes were significantly greater or less than 1 according to a one-sided Wilcoxon signed-rank test (p-vals < 0.05). The black dashed line is y=x.

2.3.3 Trans-activation strength depends on both ligand and receptor identities

Previous quantitative, coculture-based measurements of Notch signaling compared relative receptor-ligand activation strengths for just the Dll1 and Dll4 ligands with Notch1 and Notch2, without analysis of Fringe dependence (Tveriakhina et al. 2018; Kakuda et al. 2020). The data described above (Figure 2B,C) enable quantitative comparison of signaling strengths across a matrix of 16 receptor-ligand-Fringe combinations. To make this comparison, we controlled for variation in ligand expression across sender populations by normalizing signaling activity by fluorescence of a cotranslational mCherry reporter, similar to an approach used previously (Tveriakhina et al. 2018).

Signaling strength varied widely across the 16 Notch-ligand-Fringe combinations. In the dLfng condition, Dll4 activated Notch1 9-fold stronger than Dll1 did (Figure 2D; Figure 2—figure supplement 2), in agreement with previous results from E14TG2a mouse embryonic stem cells (Tveriakhina et al. 2018) and likely reflecting the ~10-fold advantage in Notch1 binding affinity

of the recombinant Dll4 ligand extracellular domain over that of Dll1 (Andrawes et al. 2013). However, Dll4's signaling advantage over Dll1 was reduced in the Lfng condition to 2.7-fold. Without Lfng (with dLfng), Jag2 was the strongest sender for both receptors, but with Lfng, Dll4 and Dll1 surpassed or matched Jag2 in trans-activation strength for Notch1 and Notch2, respectively. All ligands signaled more strongly to Notch2 than to Notch1 regardless of Fringe expression, except for Dll4, which signaled more strongly to Notch1 than Notch2 in the dLfng condition but activated Notch1 and Notch2 to similar levels with Lfng. Strikingly, Jag1 failed to activate Notch1 in either the dLfng or Lfng conditions, despite activating Notch2 as well as Dll1 did in the dLfng condition (Figure 2D). With dLfng, Dll1 activated Notch1 almost as weakly as Jag1 did, showing that Dll1 depends on Fringe expression to activate Notch1.

Together, these results establish a quantitative measurement of relative trans-activation strengths, defining receptors' ligand preferences, ligands' receptor preferences, and their dependence on Lfng expression, for all essential Notch receptors and activating ligands.

2.3.4 Similar ligand-receptor signaling features occur in a distinct cell line

Effective Notch-ligand interactions could depend on cell context. To test this possibility, we constructed receiver and sender cell lines in an unrelated C2C12 mouse myoblast background, which is distinct from CHO-K1, allows control of Notch component expression without altering cell fate or morphology, and has routinely been used to investigate the role of Notch signaling in muscle cell differentiation (Shawber et al. 1996; Dahlqvist et al. 2003; Nofziger et al. 1999; Gioftsidi, Relaix, and Mourikis 2022). Because C2C12 cells express Notch receptors, ligands, and Fringes (Sassoli et al. 2012; Liang et al. 2021; Shimizu et al. 2001) (Figure 2—figure supplement 3A), we first constructed a C2C12 base cell line, dubbed C2C12-Nkd, for "Notch knockdown." We used two rounds of CRISPR/Cas9 editing to target Notch2 and Jag1, the most abundant receptor and ligand, for deletion (Methods, Figure 2—figure supplement 3). The resulting clone (C2C12-Nkd) showed a loss of Notch2 protein by Western blot (Figure 2—figure supplement 3B) and a loss of Jag1 mRNA by RT-PCR (Figure 2—figure supplement 3C). Additionally, it exhibited an impaired ability to upregulate Notch target genes, including Notch1 and Notch3 (Castel et al. 2013), relative to wild-type C2C12 (Figure 2—figure supplement 3A, right). We then engineered

sender and receiver cells in the C2C12-Nkd background with the ligand and receptor constructs used above.

To compare C2C12-Nkd responses to those of CHO-K1 cells, we repeated the trans-activation assay described previously (Figure 1B,C) in the C2C12-Nkd background. In these assays, to minimize residual expression of endogenous Notch components, we also inserted a transient knockdown step in the assay, in which we used siRNAs to suppress any remaining mRNA transcripts of endogenous Notch receptors and Rfng (Figure 2—figure supplement 3D, Methods).

We focused on one ligand of each Delta and Jagged class, Dll1 and Jag1, to test whether these ligands would exhibit similar relative abilities to trans-activate Notch1 and Notch2 in two distinct cell types. In the C2C12-Nkd background, Jag1 senders failed to activate Notch1 receivers, despite activating Notch2 receivers well (Figure 2E), just as we observed in CHO-K1 (Figure 2D). Dll1 senders activated both Notch1 and Notch2 C2C12-Nkd receivers well, with a slight preference for Notch2 over Notch1, also consistent with results in CHO-K1.

These results demonstrate that key quantitative features of Notch signaling generalize across at least two cell types and, in particular, suggest that weak activation of Notch1 by Jag1 is likely to be an intrinsic property of the ligand and receptor. Future studies will be necessary to see whether this is true generally across a broader range of cell lines.

2.3.5 Notch signaling is modestly ultrasensitive and sometimes exhibits nonmonotonic ligand dependence

In principle, receptor-ligand pairs could differ in other trans-activation signaling properties, such as ultrasensitivity. Ligand dose-response curves can reveal EC50, saturating activity, and ultrasensitivity in signaling. We measured these curves in receiver cells expressing endogenous levels of Rfng and Lfng (see Methods and Figure 2—figure supplement 4 for an analysis of endogenous Fringe effects in CHO-K1). First, we titrated ligand expression in Tet-OFF inducible sender cells across a range of levels by varying 4-epi-Tc concentration (Figure 2—figure supplement 5A), and cocultured these senders with a minority of receiver cells. We then fit the resulting dose-response curves to Hill functions, and computed relative EC50s, saturating trans-activation strengths, and ultrasensitivities for each receptor-ligand combination (Figure 2—figure

supplement 5B-E). The exception was Jag1-Notch1, which lacked sufficient signaling activity, as observed previously (Figure 2D).

Dose-response curves were modestly ultrasensitive with Hill coefficients of ~2 (Figure 2—figure supplement 5D), possibly reflecting effects of clustering of Notch receptors and ligands, as has been observed in other signaling systems (Tetzlaff et al. 2018; Narui and Salaita 2013; Bardot et al. 2005; Radhakrishnan et al. 2012; Gopalakrishnan et al. 2005; Duke and Graham 2009; Cattoni et al. 2015). Ligands' relative saturating activities were broadly similar (with ≤1.5-fold differences) for both Notch1 and Notch2 (Figure 2—figure supplement 5E). Relative inverse EC50s (Figure 2—figure supplement 5C) showed <2-fold differences (with the exception of the non-activating Jag1-Notch1 combination), in contrast with the >10-fold range of relative trans-activation strengths measured previously (Figure 2D). This difference, as well as differences in the patterns of relative signaling strengths across ligand-receptor pairs observed here (Figure 2—figure supplement 5C) vs. previously (Figure 2D), could be explained, at least in part, by the presence of endogenous CHO-K1 Fringes (see Methods).

Notably, at the highest ligand expression level, Dll1 signaling decreased for both receptors (Figure 2—figure supplement 5B), reminiscent of receiver cells' nonmonotonic ligand dose-response curves previously observed for Notch1 cis-activation by Dll1 and Dll4 (Nandagopal et al. 2019).

Together, these results suggest that intercellular Notch signaling is modestly ultrasensitive, that ligands can exhibit minor discrepancies in saturating activities for different receptors, and that differences in relative EC50s are small (≤2-fold) in the presence of endogenous CHO-K1 Fringes.

2.3.6 Plated Jag1 ligands activate Notch1 more efficiently than expressed Jag1 ligands

Plate-bound ligands provide a convenient method to assay Notch signaling (Kakuda et al. 2020), but differ from cell-expressed ligands in their Notch activation mechanism. We therefore sought to determine whether the method of ligand presentation (plate-bound or expressed by cells) affects ligands' relative receptor preferences. We analyzed CHO-K1 receiver cells' responses to titrated levels of plated recombinant ligand extracellular domains tagged at the C-terminus by a human Fc domain ("ligand-ext-Fc") and fit the dose response curves to Hill functions with the maximum activity fixed to the highest reporter activity measured for each receptor (Figure 2—figure

supplement 6A-C). Because many factors can impact the activity of recombinant ligands, we compared the relative ability of individual ligands to activate different receptors, but did not directly compare activities between ligands.

Ligands' receptor preferences were qualitatively, but not quantitatively, consistent between the plated ligand assay and trans-activation coculture assay. All plated ligands activated Notch2 more strongly than Notch1 except for Dll4-ext-Fc, which favored Notch1 over Notch2 (Figure 2—figure supplement 6B), in agreement with our previous results from coculture with sender cells (Figure 2D). However, plated Dll4-ext-Fc showed a stronger preference for Notch1 over Notch2 than the Dll4 in the coculture assay.

Of the eight receptor-ligand combinations, Notch1 activation by plated Jag1-ext-Fc deviated most strongly from Notch1 activation by Jag1 senders. Whereas Jag1 senders failed to activate Notch1 above background (Figure 2D; Figure 2—figure supplement 5B), plated Jag1-ext-Fc activated Notch1 only 4-fold less efficiently than it activated Notch2 (Figure 2—figure supplement 6B). This suggests that the natural endocytic activation mechanism, or potential differences in tertiary structure between the expressed and recombinant Jag1 extracellular domains, could play roles in preventing Jag1-Notch1 signaling in coculture.

Hill coefficients were sometimes lower in this plated ligand assay (Figure 2—figure supplement 6C) than in the coculture-based trans-activation assay (Figure 2—figure supplement 5D). For example, Notch1 activation by plated Dll1-ext-Fc and by expressed Dll1 had Hill coefficients of ~1 and ~2, respectively. These values are consistent with independent Notch binding by plated ligand-ext-Fc ligands, and cooperative binding by cell-expressed ligands (Cattoni et al. 2015).

Thus, while plate-bound ligands are undoubtedly useful, they differ in their Notch activation compared to ligands expressed on living cells. These results demonstrate the importance of coculture-based methods for quantitative analysis of Notch signaling.

2.3.7 Lfng strengthens binding and weakens activation of Notch1 by recombinant Jagged ligands

Although the activation of Notch receptors by plated recombinant ligands differs in notable ways from activation by the natural transendocytic mechanism (Figure 2D; Figure 2—figure supplement 5B; Figure 2—figure supplement 6B), recombinant Notch ligands enable analyses of receptor-ligand binding that are not possible with expressed ligands. By measuring the amount of these soluble ligands bound to receptor-expressing cells, others previously found that Lfng increases Jag1's Notch1 binding affinity while simultaneously reducing its Notch1 activation potential (Hicks et al. 2000; Kakuda and Haltiwanger 2017; Taylor et al. 2014; Yang et al. 2005). These reports also found that Lfng strengthened Dll1-Notch1 binding, in tandem with its activation potential. Another study suggested that Lfng reduced Notch2-Jag1 binding strength (Shimizu et al. 2001). Lfng effects on the binding strength of all other receptor-ligand combinations remains unknown.

To evaluate Lfng effects on relative ligand-receptor binding strengths for all eight receptor-ligand combinations, we incubated CHO-K1 receiver cells, or parental reporter cells expressing only endogenous receptors, with soluble ligand-ext-Fc fragments pre-clustered with a dye-conjugated antibody, as previously described (Kakuda and Haltiwanger 2017; Varshney and Stanley 2017) (Figure 1B, "Soluble ligand binding assay"). We then measured the amount of ligand bound to cells transiently expressing Lfng vs. dLfng, via flow cytometry.

Lfng did not decrease binding strength for any receptor-ligand pairs (Figure 3A,B). In agreement with previous results (Hicks et al. 2000; Kakuda and Haltiwanger 2017; Taylor et al. 2014; Yang et al. 2005), Lfng strengthened Notch1 binding to Dll1 and Jag1 (by 6.4-fold and 2.8-fold on average, respectively). Lfng also strengthened Notch1 binding to Jag2, by 1.6-fold. Lfng did not alter binding of Dll4 to either receptor, nor of Jag1 to Notch2 (in contrast with one previous report (Shimizu et al. 2001)). However, the Lfng effects measured here are minimum bounds on the true effect, since we did not titrate across a range of ligand concentration and may have selected ligand concentrations outside the linear range of binding for some receptor-ligand pairs. Thus, we cannot rule out the possibility that greater Lfng effects might be observed using lower ligand concentrations.

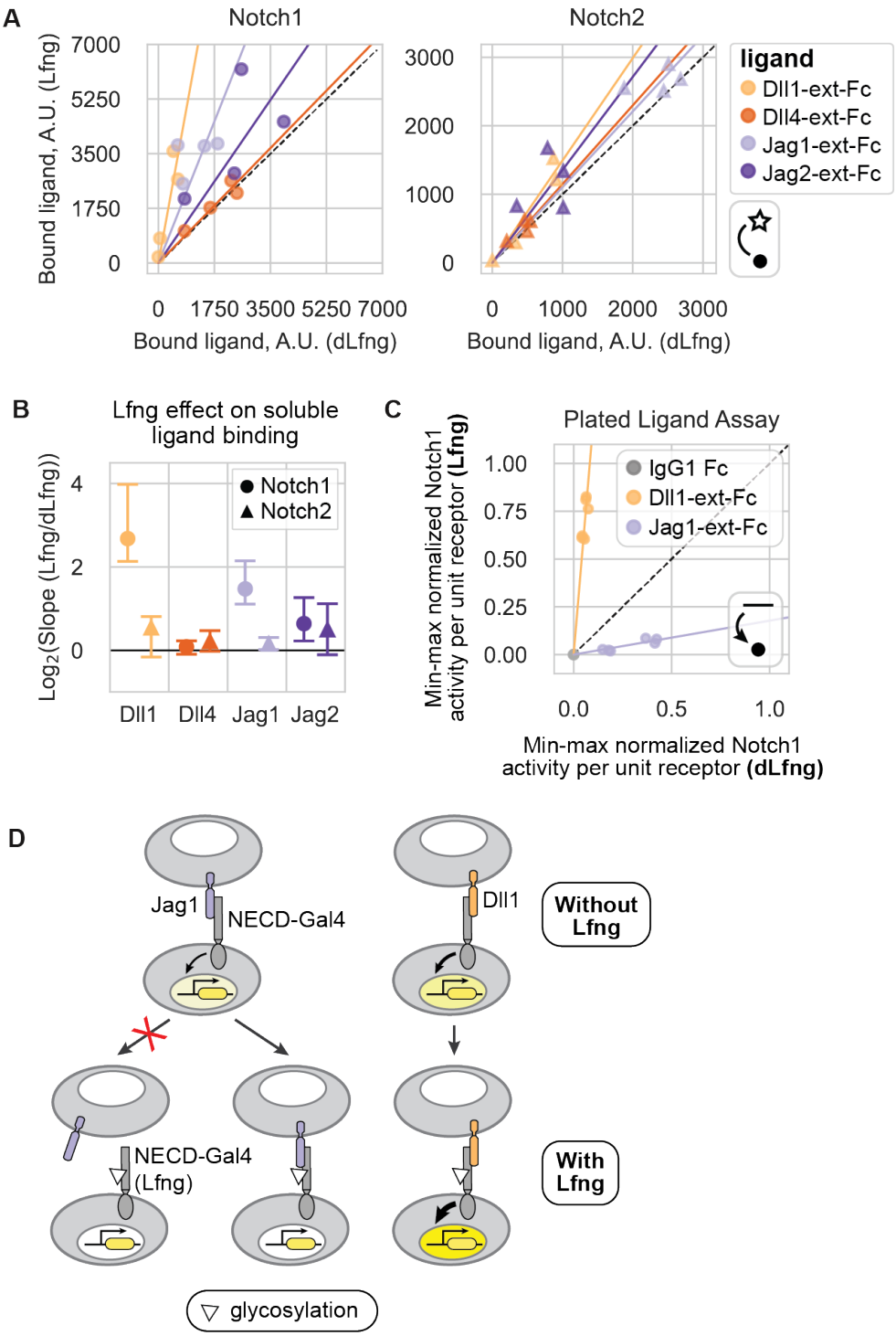

Figure 3: Lfng strengthens binding of Notch1 to Dll1 and Jag1, despite weakening Notch1 activation by Jag1

(**A**) Scatterplot of data from the soluble ligand binding assay (Methods) showing the amount of ligand-ext-Fc preclustered with AlexaFluor 594-conjugated secondary antibodies bound to CHO-K1 cells (median AF594 fluorescence (A.U.) from single-cell flow cytometry data) with Lfng (y-axis) vs. dLfng (x-axis)

expression. Fluorescence values were background-subtracted by subtracting the amount of ligand bound to parental reporter cells with no ectopic Notch receptors added, and negative values were set to zero. Solid lines are least-squares best-fits, and the black dashed line is y=x. The dot-and-arrow icon indicates the "Soluble ligand binding assay" type used to generate the data, as described in Figure 1B.

(**B**) Log2 fold difference in the best-fit slopes from (A) comparing receptor-ligand binding with Lfng vs. dLfng expression. Mean slopes and confidence intervals were computed from the distribution of least-squares line fits of 10k bootstrap replicates (n = 4 biological replicates).

(**C**) Scatterplot showing the normalized Notch signaling strength in CHO-K1 Notch1 receivers expressing Lfng or dLfng, plated on Dll1-ext-Fc (yellow) or Jag1-ext-Fc (purple) in a plated ligand assay (Methods). X and y-axis values are signaling activity (reporter activity, mCitrine, divided by cotranslational receptor expression, mTurq2), background subtracted and normalized to the max signaling activity—the average signal in the same receiver (+Lfng) plated on a high concentration of Dll4-ext-Fc. Solid lines are the least-squares best fits to six data points, representing three biological replicates for each of two plated ligand concentrations. Both slopes were significantly greater than or less than 1 according to a one-sided Wilcoxon signed-rank test (p-vals = 0.015 for both lines). The black dashed line is y=x. Bracketed numbers are the 95% confidence intervals on the best-fit slopes computed with 10k bootstrap replicates. Dot-and-arrow icons on individual plots indicate the assay type used to generate the data, as described in Figure 1B.

(**D**) Cell schematic depicting the effects of Lfng expression on Jag1 and Dll1 interactions with the Notch1 receptor. White triangles represent glycosylation modifications added by Lfng, and yellow saturation level in cell nuclei represents signaling activity. Lfng strengthens binding and activation of Notch1 by Dll1, but weakens activation while strengthening binding of Notch1 by Jag1. Therefore, rather than rendering Jag1 inert, Lfng enhances Jag1's ability to bind the Notch receptor without activating it, theoretically making it a stronger competitive inhibitor of Notch1 signaling.

In principle, the opposite effects of Lfng on Jag1- and Jag2-Notch1 binding (Figure 3A,B) vs. activation strength (Figure 2B,C; Figure 3C) could arise from potential molecular differences between full-length, expressed Jag1 protein and recombinant Jag1-ext-Fc fragments (post-translational modifications, oligomerization properties, folding, etc.). To test this possibility, we incubated dLfng- or Lfng-transfected Notch1 receivers on plated Dll1-ext-Fc and Jag1-ext-Fc. Lfng strongly increased Dll1-Notch1 signaling and weakened Jag1-Notch1 signaling in the plated ligand assay (Figure 3C), in agreement with the coculture results. Thus, Lfng has opposing effects on binding and activation of Notch1 by the same Jag1-ext-Fc fragment. This suggests that, rather than rendering Jag1 inert, Lfng strengthens Jag1's ability to competitively inhibit Notch1 activation by other ligands (Figure 3D).

While they do not rule out additional effects of Lfng on binding affinity for other ligand-receptor combinations, these results suggest that Lfng strengthens Notch1 binding to Dll1, Jag1, and Jag2. For Dll1, the Lfng effect on binding is associated with a similar potentiation of Dll1-Notch1

activation efficiency, but for Jag1 and Jag2, Lfng has opposite effects on Notch1 binding and activation.

2.3.8 Like trans interactions, cis interaction outcomes depend on both receptor and ligand identity

Single-cell RNA-seq datasets show that activating ligands are frequently coexpressed with Notch1 and/or Notch2, provoking the question of how ligands and receptors interact in the same cell (in cis), and more specifically whether they activate (cis-activation) or inhibit (cis-inhibition) signaling (Granados, Kanrar, and Elowitz 2022). Cis-interations are difficult to investigate in vivo (Henrique and Schweisguth 2019). However, in vitro studies in mammalian cells have demonstrated that Dll1 and Dll4 can cis-activate both Notch1 and Notch2 in CHO-K1 cells (Nandagopal, Santat, and Elowitz 2019), and that Dll1, Dll4, and Jag1 can cis-inhibit Notch1 (LeBon et al. 2014; Preuße et al. 2015; Sprinzak et al. 2010). Nevertheless, it has remained unclear whether other receptor-ligand combinations also engage in cis-activation and/or cis-inhibition. We therefore sought to analyze cis interactions more comprehensively.

We cultured cells at low density, amid an excess of "blank" cells with no Notch ligands or receptors. This configuration allows cis, but minimizes trans, interactions. We first pre-induced expression of cis-ligands for 48 hours by titrating 4-epi-Tc to the desired level in the presence of the γ-secretase inhibitor DAPT, as described previously (Nandagopal, Santat, and Elowitz 2019) (Figure 1C). We then cultured a minority of the pre-induced receiver cells with an excess of wild-type CHO-K1 cells (Figure 1B, "Cis-activation assay") to focus on cis interactions alone (Methods). In parallel, we cultured a minority of pre-induced receiver cells with an excess of sender cells constitutively expressing Dll1 (Figure 1B, "Cis-modulation assay") to probe the combined effects of cis and trans interactions (Methods). The constitutive Dll1 sender cells, denoted "high-Dll1 senders," stimulated strong Notch reporter activity when cultured with receiver cells expressing no cis-ligands (Figure 4—figure supplement 1). In both assays, cells were allowed to signal for 22-24 hours before flow cytometry analysis (Figure 1C-F). At these densities, trans interactions among the minority cells were minimal, activating to no more than 5% of maximum reporter activity (Figure 4A).

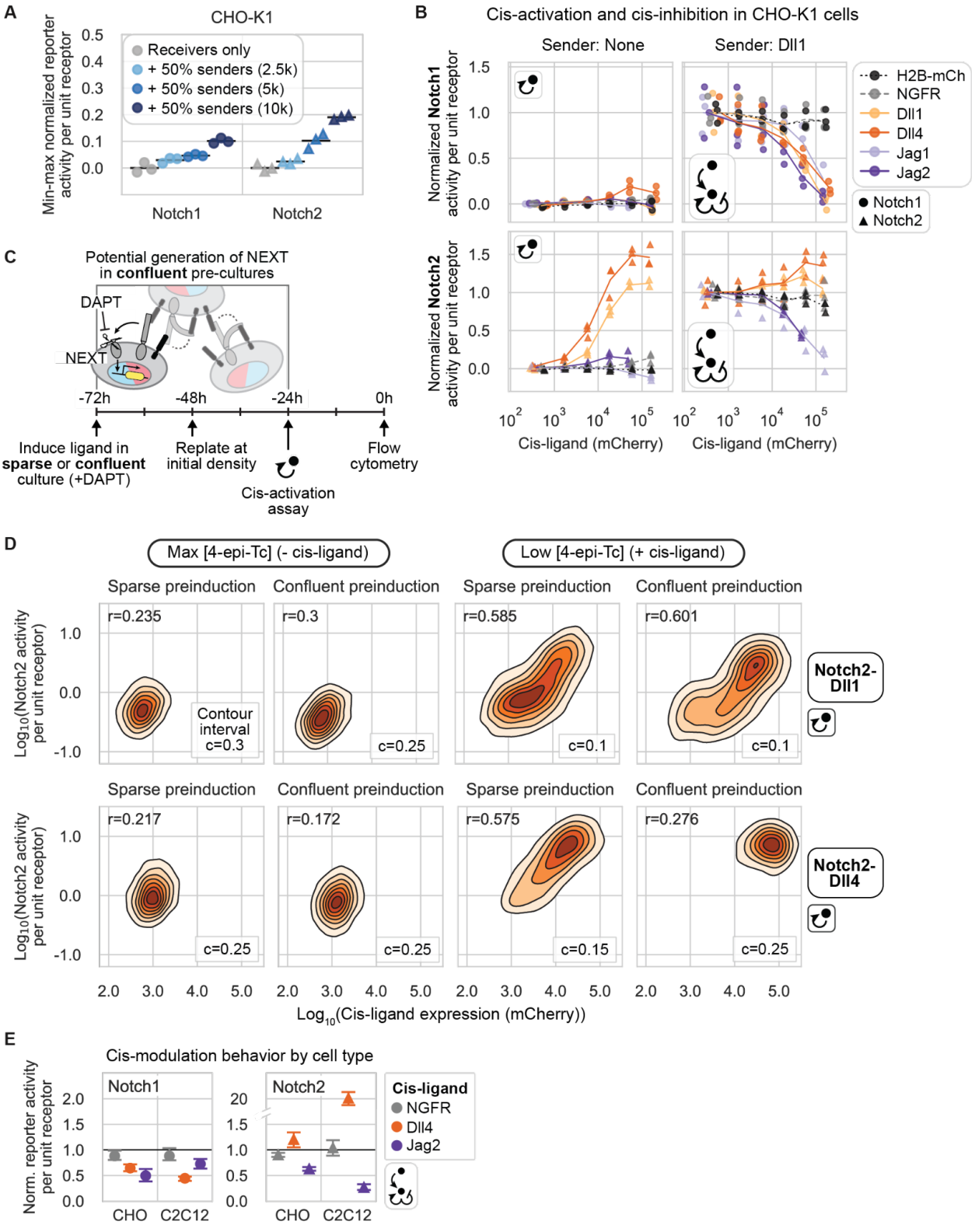

Figure 4: The Jagged ligands can cis-inhibit both receptors, but the Delta ligands can only cis-inhibit Notch1 *(caption on following page)*

(**A**) The cell density used in the cis-activation assay prevents intercellular signaling. CHO-K1 Notch1 or Notch2 receiver cells were plated sparsely at 2.5k, 5k, or 10k in a 24-well plate along with an equal number of high-Dll4 (for Notch1) or high-Dll1 (for Notch2) CHO-K1 sender cells, and surrounded by 150k CHO-K1 wild-type cells. Notch signaling activity is defined as the reporter activity (mCitrine, A.U.) divided by the cotranslational receptor expression (mTurq2, A.U.) in each cell, averaged across all cells in a given sample. Y-axis values are signaling activity minus signaling in the absence of ligand, divided by maximum signal (signaling level when receivers are cultured with a confluent excess of high-Dll4 or -Dll1 senders, for Notch1 and Notch2, respectively). The 2.5k receiver + 2.5k sender condition (lightest blue), matching the 5k total receivers used in the cis-activation assay, activated receivers to less than 5% of the maximal signal. Black bars are the mean of three biological repeats.

(**B-E**) Dot-and-arrow icons indicate the assay type used to generate the data, as described in Figure 1B.

(**B**) Results of cis-activation (left column) and cis-modulation (right column) assays for CHO-K1 Notch1 (top row) and Notch2 (bottom row) receivers coexpressing a Notch ligand or control protein at different levels corresponding to a range of 4-epi-Tc concentrations (see distributions in Figure 1—figure supplement 1). Individual receivers were sorted into discrete bins of mCherry and the mCitrine/mTurq2 (signaling activity, defined in (A)) and mCherry (cotranslational cis-ligand expression, A.U.) signals were averaged across all cells in that bin. Signaling activity on the y-axis was normalized as in (A), except that the maximum signal (y = 1) is the signaling activity of receivers with no cis-ligand (max [4-epi-Tc]) cocultured with sender cells expressing high levels of Dll1 (Dll1-L2 senders; see also Figure 6A) in the cis-modulation assay. Lines are interpolated through the mean of three biological replicates (individual data points) in each mCherry bin.

(**C**) Experimental workflow to assess the contribution of intercellular signaling during the 48 hr preinduction phase (from -72 hr to -24 hr) to the overall signal measured in the cis-activation assay at 0 hr. Cells preinduced sparsely were seeded at 5k cells per well, the same density used for the cis-activation assay. NEXT = Notch extracellular truncation, generated during the preinduction phase when the cell density enables intercellular ligand-receptor interactions but γ-secretase-mediated S3-cleavage of receptors is blocked by the inhibitor DAPT, as illustrated by the cell schematic. Red and blue colors in cell nuclei represent H2B-mCherry and H2B-mTurq2, cotranslational reporters of cis-ligand and receptor expression, respectively.

(**D**) 2D fluorescence distributions of signaling activity (mCitrine/mTurq2) versus cis-ligand expression (mCherry) in single-cell fluorescence distributions measured by flow cytometry according to the experiment in (C) performed with Notch2-Dll1 and -Dll4 receiver cells. Cell density in each discrete contour interval is indicated by color, and each contour level has a cell density range of n*c to (n+1)*c, where n is the contour level. The density interval below c is not shown. The Pearson's correlation coefficient r is shown in the top left of each plot, and all p-values were << 0.001. Cells with minimal cis-ligand (max [4-epi-Tc], 500 ng/mL) showed weak signaling activity regardless of their preinduction culture density. Cells with moderate cis-ligand expression (low [4-epi-Tc],10 ng/mL) showed strong positive correlations regardless of preinduction density. Both mCherry and mCitrine/mTurq2 distributions were shifted in the confluent vs. sparse preinduction density, likely because cell density affects expression from the Tet-OFF promoter (see also Figure 1—figure supplement 2B).

(**E**) Comparison of cis-ligand effects in the cis-modulation assay for CHO-K1 ("CHO") vs. C2C12-Nkd ("C2C12") cell types. Y-axis values are normalized signaling activities as defined in (B) for CHO-K1 cells and in Figure 4—figure supplement 2B for C2C12-Nkd cells. Specifically, signaling activities are the y-value corresponding to a cotranslational cis-ligand expression level equal to $3x10^4$ A.U., calculated by fitting a line between the x-axis cis-ligand level bins flanking $3x10^4$ A.U. Values are the mean, and error bars are 95% confidence intervals, of 10k bootstrap replicates.

Cis-activation strength was both ligand and receptor specific. Notch1 exhibited no cis-activation for any of the ligands, except for a modest response to Dll4, of no more than 20% of maximal trans-activation (Figure 4B, upper left). The lack of Dll1-Notch1 cis-activation is consistent with previous observations in wild-type CHO-K1 cells (Nandagopal, Santat, and Elowitz 2019). By contrast, Notch2 was cis-activated by both Dll1 and Dll4, to levels exceeding those produced by trans-activation by high-Dll1 senders (Figure 4B, lower left). Jagged ligands, on the other hand, showed little if any cis-activation of Notch2 in this assay (Figure 4B, lower left). (We note that in other assays using clones with lower background signaling, discussed further below, modest Jag1-Notch2 cis-activation was detectable.)

In contrast to cis-activation, the reciprocal phenomenon of cis-inhibition can only be detected in the context of basal Notch activation by other ligands. The cis-modulation assay provides this basal trans-signaling by Dll1 senders (Figure 1B, "cis-modulation assay"). The cis-modulation assay revealed that cis-inhibition strength, like cis-activation strength, depends on both receptor and cis-ligand identity. All ligands cis-inhibited intercellular Dll1-Notch1 signaling, achieving 75-100% inhibition in the highest cis-ligand expression bin (Figure 4B, top right). By contrast, intercellular Dll1-Notch2 signaling was cis-inhibited by Jag1 and Jag2, but not by Delta ligands, whose cis-activation further increased Notch2 signaling (Figure 4B, lower right). These results were not due to non-specific effects of ectopic cis protein expression, as Notch1 and Notch2 reporter activities showed no dependence on expression of negative control proteins H2B-mCherry or NGFR-T2A-H2B-mCherry, in either the cis-activation or cis-modulation assay (Figure 4B). Thus, Delta ligands show strikingly different cis-interactions for the two receptors while Jagged ligands show more similar cis effects on the two receptors.

2.3.9 Cis-activation signal does not arise from prior trans-activation

Since cis-activation in Delta-Notch2 receivers appeared to rival the strength of trans-activation, we considered the possibility that the cis-activation signal could be a misleading artifact of intercellular signaling occurring prior to the start of the assay. During the ligand preinduction phase, the γ-secretase inhibitor DAPT prevents S3, but not S2, receptor cleavage. Thus, intercellular contacts between receivers during preinduction culture could in principle generate S2-

cleaved receptor, also known as the Notch extracellular truncation (NEXT). NEXT could in principle undergo S3 cleavage after DAPT removal, contributing to the total observed signal.

To test this possibility, we carried out a control cis-activation assay in which receivers were cultured at both sparse and confluent densities during the 48 hour cis-ligand preinduction phase, and then replated sparsely or densely after 24 hours of preinduction to maintain the initial low or high cell density conditions (Figure 4C). If cis-activation signal resulted from intercellular signaling during preinduction, only cells preinduced in confluent culture (able to make intercellular contacts) would show a "cis-activation" signal 24 hours after DAPT removal. For Notch2-Dll1 and Notch2-Dll4, single cell reporter activities correlated with cis-ligand expression, regardless of whether cells were preinduced at a high or low culture density (Figure 4D). While confluent pre-culture did shift the signaling distributions to higher values relative to sparse pre-culture, it maintained the correlation between cis-ligand expression and reporter activity. This effect is consistent with elevated expression of cis-ligand at high cell density (Figure 1—figure supplement 2B). Together, this analysis rules out the possibility that Delta-Notch2 cis-activation signal arises from S3-cleavage of NEXT generated by intercellular signaling during the ligand preinduction phase.

2.3.10 Notch cis interactions exhibit similar properties in two distinct cell types

To determine whether the cis-interaction properties observed above (Figure 4B) are cell type-dependent, or whether they might reflect more general features of these receptor-ligand pairs, we repeated the cis-activation and cis-modulation assays described previously (Figure 1B,C) in the C2C12-Nkd background. Due to differences in cell size between CHO-K1 and C2C12, we first identified a sufficiently low working cell density—5,000 receiver cells per well in a 12-well plate—to prevent undesired intercellular signaling between C2C12-Nkd receivers (Figure 4—figure supplement 2A).

We focused on one ligand of each Delta and Jagged class, Dll4 and Jag2, to test whether the Delta ligand would cis-activate Notch2 strongly and cis-inhibit Notch1, and whether the Jagged ligand would cis-inhibit both receptors without cis-activating them, as observed in CHO-K1 cells. With Notch2, we observed strong cis-activation by Dll4 and cis-inhibition by Jag2, similar to results in

the CHO-K1 background, suggesting these interactions are similar in the two backgrounds. As a negative control, we also verified that overexpression of the NGFR cis-ligand in C2C12-Nkd Notch2 receivers did not affect signaling activity. With Notch1, Dll4 and Jag2 cis-inhibited Notch1 reporter activity in C2C12-Nkd cells relative to the NGFR cis-ligand negative control, similar to their behavior in CHO-K1 (Figure 4E; Figure 4—figure supplement 2B). Also similar to CHO-K1, Jag2 did not cis-activate Notch1 in this background. However, in contrast to CHO-K1, where Dll4 weakly cis-activated Notch1 (Figure 4B), we observed no cis-activation by Dll4 in C2C12-Nkd. This modest difference between the cell lines may be due to Rfng, which potentiates Dll4-Notch1 signaling (Stanley and Guidos 2009; Song et al. 2016; Benedito et al. 2009). Rfng is expressed in both cell line backgrounds (Singh, Kildegaard, and Andersen 2018) (Figure 2—figure supplement 3A), but was knocked down only in the C2C12-Nkd experiments. Together, these results indicate that the ligand-receptor signaling behaviors are broadly similar between CHO-K1 and C2C12 backgrounds.

2.3.11 Cis-activation dependencies on Lfng expression differ from those of trans-activation

Cis-activation and trans-activation share several similar features. For instance, like trans-activation, cis-activation requires receptor-ligand binding at the cell surface and depends on γ-secretase cleavage (Nandagopal, Santat, and Elowitz 2019). Additionally, these signaling modes show similar ligand-dependence in their responses to Rfng, which increased Notch1 cis-activation by Dll1 but not by Dll4 (Nandagopal, Santat, and Elowitz 2019), resembling its effects on trans-activation by the same plated ligands (Kakuda et al. 2020). We therefore asked whether similarities between the response of cis- and trans-activation to Lfng would extend to other ligand-receptor combinations.

To address this question, we repeated the cis-activation assay (Figures 2B) with or without Lfng (Figure 5A). We transiently transfected receiver cells with Lfng or dLfng plasmids following endogenous Rfng and Lfng knockdown (Figure 1C). Because reporter activity varied non-monotonically with cis-ligand for most receptor-ligand combinations (Figure 5A), we defined cis-activation strength as peak reporter activity in the cis-activation assay normalized to maximum trans-activation potential of the receiver cells without cis-ligands (Figure 5B).

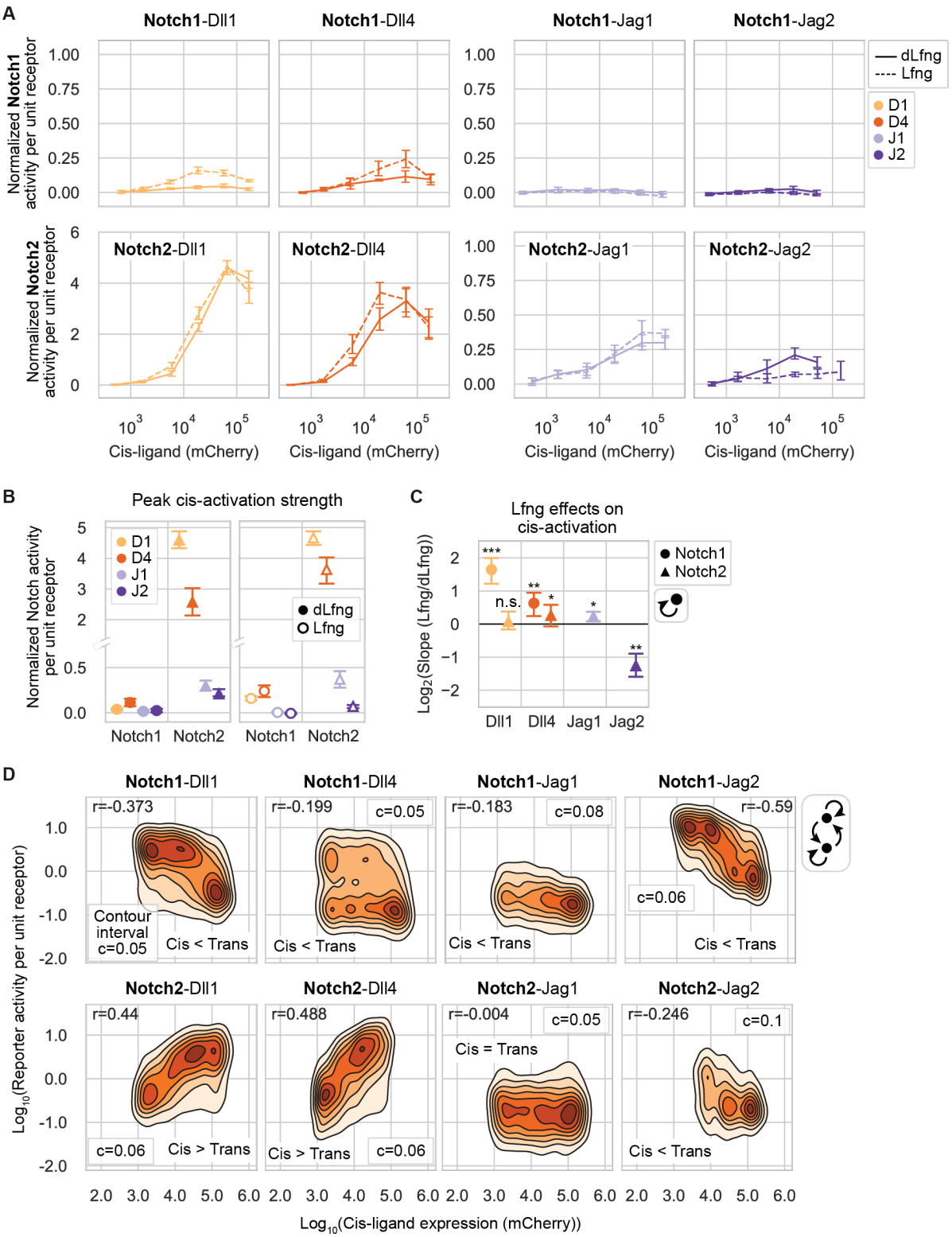

Figure 5: Lfng effects on weak cis-activation, but not strong cis-activation, consistently mirror its effects on trans-activation *(caption on following page)*

(**A**) Results of cis-activation assays for CHO-K1 Notch1 (top row) and Notch2 (bottom row) receivers coexpressing a Notch ligand at different levels corresponding to a range of 4-epi-Tc concentrations (see distributions in Figure 5—figure supplement 3). During ligand preinduction, endogenous Fringes were knocked down and cells were transfected with dLfng or Lfng (solid and dashed lines, respectively). X- and y-axis values are cis-ligand expression (mCherry, A.U.) and normalized Notch signaling activity (reporter activity (mCitrine, A.U.) divided by the cotranslational receptor expression (mTurq2, A.U.) in each cell), respectively, averaged across all cells in a given mCherry bin. Signaling activity on the y-axis was background subtracted and normalized to the "max" signaling in receivers with no cis-ligand (max [4-epi-Tc]) cultured with high-Dll1 or -Dll4 senders (for Notch2 and Notch1, respectively); see also Supplementary Table 4. Lines are interpolated through the mean of seven biological replicates in each mCherry bin. Error bars are 95% confidence intervals on the mean value across 10k bootstrap replicates. Colors indicate cis-ligand identity.

(**B**) Peak cis-activation strengths for each receptor-ligand pair with corresponding 95% confidence intervals defined from the curves in (A). Colors indicate ligand identity; in the legend, 'D' stands for 'Dll' and 'J' stands for 'Jag.'

(**C**) Lfng effects on cis- + trans-activation. Values are the log2 fold difference in the slope of the best-fit line to signaling activity (from A) in a scatterplot of Lfng vs dLfng; error bars are 95% confidence intervals on best-fit slopes computed for each of 10k bootstrap replicates. Asterisks denote the p-value from a Wilcoxon signed-rank test (one-sided) evaluating whether the slope of Lfng vs. dLfng is significantly greater than or less than 1 (* p-val < 0.05; ** p-val < 0.01; *** p-val < 0.001). Receptor-ligand combinations that did not activate above background levels were excluded.

(**D**) 2D fluorescence distributions of signaling activity (mCitrine/mTurq2) versus cis-ligand expression (mCherry) in single-cell flow cytometry data from the cis- + trans-activation assays described in (A). Each plot shows data from a single biological replicate at the single 4-epi-Tc concentration and Fringe expression context (Lfng or dLfng) corresponding to peak activation for each given receiver (Methods). 500-1000 data points were randomly sampled across each mCherry bin to generate the distributions shown here. Cell density in each discrete contour interval is indicated by color, and each contour level has a cell density range of n*c to (n+1)*c, where n is the contour level. The density interval below c is not shown. The Pearson's correlation coefficient *r* is shown in the top left of each plot, and all corresponding p-values were << 0.001 except for Notch2-Jag1, which was not significant.

Effects of Lfng on Notch1 cis-activation (Figure 5B) generally resembled those on trans-activation (Figure 2B,C). Lfng expression significantly increased Dll1-Notch1 cis-activation from 0.04 (with dLfng) to 0.16 (Figure 5B,C), a quantitatively similar fold-difference to its effect on Dll1-Notch1 trans-activation (Figure 2C). (Dll1 activation of Notch1 is very weak with dLfng both in cis and trans.) Lfng expression increased Dll4-Notch1 cis-activation by 1.5-fold, similar to the 1.8-fold boost observed for trans-activation. The Jagged ligands failed to cis-activate Notch1 in both dLfng and Lfng conditions.

In contrast to Notch1, Lfng's effects on Notch2 cis-activation sometimes differed from its effects on trans-activation. Dll1 and Dll4 showed negligible and weak (< 20%) increases in Notch2 cis-

activation strength, respectively, with Lfng vs. dLfng (Figure 5C), a much lower boost than that observed for trans-activation (Figure 2C). Lfng decreased Jag2-Notch2 cis-activation by more than 2-fold, a stronger effect than seen for trans-activation. Unlike in the cis-activation assay results in Figure 4B, Jag1 cis-activated Notch2 well above background levels (Figure 5A,B). This discrepancy may reflect our use of a different Notch2-Jag1 receiver clone ("2B7") for this experiment than for Figure 4B ("2B8"), since we switched to using 2B7 after finding it had lower background signal than 2B8; however, all of the Notch2-Jagged cell lines we generated had high backgrounds and low dynamic ranges relative to other receptor-ligand combinations (Figure 4—figure supplement 1; Figure 5—figure supplement 1). With the slightly enhanced sensitivity of Notch2-Jag1 clone 2B7, Jag1 cis-activated Notch2 up to a third of the max trans-activation signal (Figure 5A,B). Similar to the Delta ligands, Jag1-Notch2 cis-activation showed little to no dependence on Lfng, with a small (1.15-fold) but significant (p-val=0.018) increase in Lfng relative to dLfng (Figure 5C), despite the fact that Lfng attenuated Jag1-Notch2 trans-activation by 2.8-fold (Figure 2C).

These results identify differences in the dependence of Notch1 and Notch2 cis-activation on Lfng expression, suggest potential additional complexity in the mechanism of cis and/or trans-activation, underscoring the need for further mechanistic comparison of these two signaling modes.

2.3.12 Unlike Delta-Notch1, Delta-Notch2 cis-activation dominates over trans-activation

Many cell types coexpress ligands and receptors in the same cell (Granados, Kanrar, and Elowitz 2022). When such cells interact in a natural tissue context, do ligands preferentially activate receptors in cis, in trans, or both? To experimentally model this scenario, we cultured receiver cells coexpressing ligands in a confluent monoculture (Figure 1B; "Cis- + trans-activation assay"). By comparing signaling activity from this assay with signaling activity in the cis-activation-only assay, we measured receivers' abilities to signal intercellularly in the presence of cis-ligand.

For Notch1, but not for Notch2, signaling activity increased when intercellular contacts were allowed (cis- + trans-activation assay) relative to cis-activation alone, with some exceptions (Figure 5—figure supplement 2). Notch1-Dll1 receivers (with dLfng) and Jag1-Notch1 (with

dLfng and Lfng) did not activate in either culture scheme, consistent with the inability of these receptor-ligand-Fringe combinations to signal productively in cis or trans (Figure 2D; Figure 2—figure supplement 5B,C). Only Jag2, the strongest Notch2 trans-activator but weakest Notch2 cis-activator, gained a substantial (≥ 1.9-fold) signaling advantage from the ability to signal in cis and trans compared with cis-activation alone (Figure 5A).

Compared with its effects on cis-activation alone (Figure 5C), Lfng effects on the signaling in the cis- + trans-activation assay (Figure 5—figure supplement 2B) more closely resembled its effects on trans-activation (Figure 2C), as expected.

To quantify the relative strength of cis- vs. trans-activation for each receptor-ligand combination, we took advantage of the broadness of ligand expression distributions at intermediate 4-epi-Tc concentrations (Figure 5—figure supplement 3). (Despite heterogeneous cis-ligand expression, reporter activity vs. cis-ligand expression curves showed similar trends whether fluorescence values were averaged across cells from different wells sorted into the same bin of cis-ligand (mCherry) expression (Figure 5A) or across cells from the same well and 4-epi-Tc concentration (Figure 5—figure supplement 4).) Specifically, we calculated correlations between reporter activity and cis-ligand expression in single-cell fluorescence distributions using the flow cytometry data from the cis- + trans-activation assay described above. We reasoned that reporter activity and cis-ligand expression would show positive correlations if cis-activation is stronger than trans-activation, since cells expressing higher ligand levels would experience greater activation. Conversely, negative correlations would be observed where trans-activation is stronger than cis-activation, since cells with higher ligand expression would preferentially signal to cells with lower ligand levels.

Trans-activation was stronger than cis-activation for Notch1. Jag2, the strongest Notch1 trans-activator in dLfng (Figure 2D), showed a strong negative correlation (Pearson's correlation coefficient (r) = -0.59, p-val << 0.001) between reporter activity and cis-ligand expression (Figure 5D), consistent with Jag2's inability to cis-activate Notch1 even with dLfng (Figure 5A,B). Dll1, which is a moderate Notch1 trans-activator with Lfng but a weak cis-activator overall, likewise showed a strong negative correlation, though not as strong as Jag2 (r = -0.373, p-val << 0.001). The best Notch1 cis-activator, Dll4, showed a weaker, but still negative, correlation (r = -0.199, p-val << 0.001). Despite its impotence as a Notch1 activator in any positional orientation, Jag1

showed a negative correlation between reporter activity and cis-ligand expression ($r = -0.183$, p-val $<< 0.001$), consistent with previous reports that cis-inhibition suppresses even leaky (ligand-independent) Notch activity (Fiuza et al. 2010). In contrast with the negative correlations observed between Notch1 activity and cis-Delta expression in the cis- + trans-activation assay, these correlations were positive in the cis-activation-only assay (Dll1 $r \geq 0.18$, p-val $<< 0.001$; Dll4 $r = 0.32$, p-val $<< 0.001$), as expected for true cis-activation (Figure 5—figure supplement 5).

Unlike Notch1, Notch2 showed positive correlations between reporter activity and cis-ligand expression with Dll1 and Dll4 in the cis- + trans-activation assay (Figure 5D), with Pearson's correlation coefficients of 0.44 and 0.488, respectively ($p << 0.001$ for both combinations). This result demonstrates that Delta-Notch2 cis-activation dominates over trans-activation, since cells with high cis-ligand preferentially signal in cis rather than signaling to adjacent cells. The Jag1-Notch2 combination was unique among the eight receptor-ligand combinations in its ability to activate equally well in cis and in trans (Figure 5D), with a Pearson's correlation of roughly zero ($r = -0.004$). However, when compared with signaling between Jag1 senders and Notch2 receivers lacking cis-ligand, which achieved reporting-saturating activation (Figure 2—figure supplement 4), cis- + trans-activation was much weaker, achieving no more than 40% of purely-intercellular signaling capacity (Figure 5A,B). Thus, it appears likely that Jag1-Notch2 trans-activation in the cis- + trans-activation assay is impaired by competition with cis-ligand. Finally, Jag2-Notch2 showed a negative correlation between reporter activity and cis-ligand expression ($r = -0.246$, p-val $<< 0.001$), consistent with its strong Notch2 trans-activation potential (Figure 2D) and relatively weak cis-activation potential (Figure 5A,B).

In summary, when receptors and ligands are coexpressed, Delta-Notch2 cis-activation dominates over trans-activation, Jag1-Notch2 cis-activation is similar in strength to trans-activation, and Delta-Notch1 and Jag2-Notch2 trans-activation dominates over cis-activation. Confluent monocultures of Delta-Notch1 or Jag2-Notch2 receivers signal both in cis and trans, with a total activation level falling between that of pure cis-activation and pure trans-activation, suggesting that receptor-ligand combinations bind competitively in cis and in trans despite exhibiting vastly different activation potentials between the two orientations.

2.3.13 Cis-inhibition efficiencies depend on receptor, trans-ligand, and cis-ligand identities

The above work compared the signaling behaviors of receptor-ligand pairs; however, receptors and ligands are often expressed in complex combinations allowing for interactions between multiple ligands and multiple receptors (Granados, Kanrar, and Elowitz 2022). Because Notch trans-activation and cis-inhibition involve complex, oligomeric interactions (Narui and Salaita 2013; D. Chen et al. 2023), the strength of receptor-ligand interactions could, in principle, be altered by interactions with a third receptor or ligand. For example, in cis-inhibition, receptor-ligand binding strengths might depend in a more complex manner on the identity of the activating trans-ligand in addition to the identities of the cis-ligand and the receptor. To test this possibility, we repeated the cis-modulation assay (Figure 4B, right), coculturing each of the eight cis-ligand containing receiver cell lines (expressing endogenous CHO-K1 Fringes) with an excess of each of the four sender cell lines, for a total of 32 coculture combinations (Figure 6).

The sender populations selected for these assays differed in their ligand expression levels (Figure 6—figure supplement 1A,B) and trans-activation efficiencies (Figure 6—figure supplement 1C). High-Dll1 and -Dll4 senders ("Dll1-L2" and "Dll4-L2") showed similar cotranslational mCherry fluorescence (Figure 6—figure supplement 1A,B). mCherry expression in high-Jag1 ("Jag1-L1") and medium-Jag2 ("Jag2-A") senders was 25% and 60% lower than in high-Dll1 senders, respectively. In absence of cis-ligand expression, these senders activated Notch1 and Notch2 receivers with ≤2-fold differences in overall signaling activity, except for the Jag1-Notch1 combination, which failed to signal, as expected (Figure 6—figure supplement 1C; Figure 2—figure supplement 5).

Qualitatively, cis-inhibition of trans-activation by these senders did not depend on the identity of the trans-ligand (Figure 6A). Consistent with earlier results (Figure 4B), Jagged ligands cis-inhibited Notch1 and Notch2, while Delta ligands cis-inhibited Notch1 and cis-activated Notch2 (Figure 6A), regardless of the sender cells used. (Cis-inhibition of Jag1-Notch1 signaling could not be analyzed because trans-activation was too weak (Figure 6—figure supplement 1C).) Quantitatively, cis-inhibition behaviors depended strongly on the identities of both the trans-activating and cis-inhibiting ligand for Notch1 but not Notch2 (excluding the non-inhibitory Delta ligands for Notch2) (Figure 6B,C). Relative cis-inhibition strengths varied by almost two orders

of magnitude across the 12 cis- and trans-ligand combinations assayed for Notch1, but varied by <1.6-fold between the strongest and weakest cis-inhibiting combinations for Notch2.

Notch1 cis-inhibition strengths did not correlate with trans-activation strengths. For example, Jag2 cis-inhibited Notch1 6- to 17-fold stronger than Dll4 did, despite these ligands' equivalent abilities to trans-activate Notch1 in the presence of endogenous Fringes (Figure 2—figure supplement 5B). Conversely, Jag1 cis-inhibited Notch1 up to 1.6-fold stronger than Dll1 did, despite its unique and total inability to trans-activate Notch1. Dll4's unexpectedly weak cis-inhibition potential relative to Jag2 might reflect, to some extent, our observations that Dll4 cis-activated Notch1 but Jag2 did not (Figure 4B; Figure 6A). Jag1's relatively strong cis-inhibition potential reinforces the view that Jag1 binds Notch1 efficiently but without productive activation in either cis or trans (Figure 4B; Figure 2D), except via the noncanonical activation mechanism used in the plated ligand assay (Figure 2—figure supplement 6).

Unexpectedly, each ligand's ability to cis-inhibit Notch1 exhibited a complex dependence on the identity of the ligand competing in trans (Figure 6C). The same was not true for cis-inhibition of Notch2 signaling. Although Dll1-Notch1 trans-activation was most often the easiest signaling pair to cis-inhibit, and Dll4-Notch1 the hardest, the ranking of trans-ligands' relative susceptibilities to cis-inhibition differed for each of the four cis-ligands. For example, Dll1 cis-inhibited Notch1 activation by Dll1 senders ~2-fold more efficiently than it cis-inhibited Notch1 activation by Jag2 senders, but the reciprocal relationship was also true, to a lesser extent: Jag2 cis-inhibited Notch1 activation by Jag2 senders 1.4-fold more efficiently than it cis-inhibited activation by Dll1 senders. Similarly, Dll4 was the only ligand that cis-inhibited Dll4 trans-activation at least as well as Jag2 trans-activation (Dll1 and Jag1 were exceptionally poor inhibitors of Dll4-Notch1 signaling).

These observations suggest that each cis-ligand has a comparative advantage, relative to other cis-ligands, when competing against a trans-ligand of the same identity in the case of Notch1 binding ("like disrupts like"). However, this rule cannot account for all of the differences in Notch1 cis-inhibition strength patterns observed in Figure 6C. For example, it is not obvious why Jag1 cis-inhibited Dll1- and Jag2-Notch1 trans-activation equally well, given that Dll4 cis-inhibited Dll1 trans-activation better than it inhibited Jag2 trans-activation. Similarly, it is unknown how Jag2 could cis-inhibit Dll1- and Dll4-Notch1 trans-activation equally well, given that Jag1 cis-inhibited Dll1-Notch1 signaling better than Dll4-Notch1 signaling.

The Hill function fits to cis-inhibition curves in Figure 6A additionally provided insights into the biochemical nature of cis-inhibition via estimation of Hill coefficients. These values ranged from ~0.75-1.5 (Figure 6D), indicating less cooperativity in cis ligand-receptor binding than in trans, which showed Hill coefficients of ≥ 2 for all combinations analyzed (Figure 2—figure supplement 5D). (Note: we could not estimate Hill coefficients for Dll4-Notch1 cis-inhibition, except with Dll1 senders, due to nonlinearities in maximum signaling introduced by cis-activation (Figure 6D).)

Taken together, these data provide the first systematic comparison of Notch ligands' relative cis-inhibition strengths, and reveal previously unappreciated biochemical complexities in the mechanism of Notch cis-inhibition.

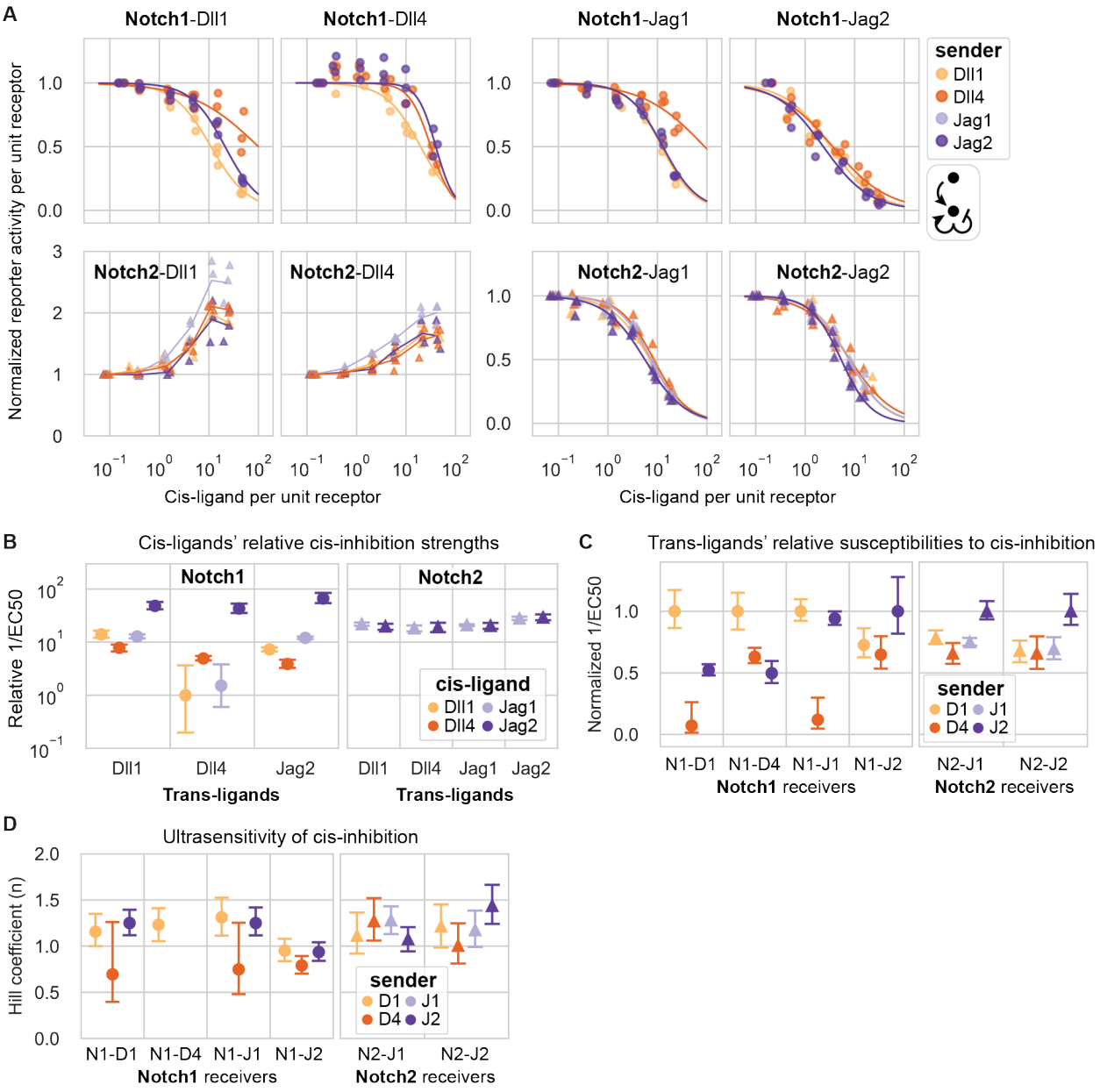

Figure 6: Cis-inhibition strengths depend on the identities of the receptor, the cis-ligand, and the trans-ligand

(**A**) Results of cis-modulation assays for CHO-K1 Notch1 (top row) and Notch2 (bottom row) receivers coexpressing a Notch ligand or control protein at different levels (Figure 6—figure supplement 1A,B) corresponding to a range of 4-epi-Tc concentrations. X- and y-axis values are flow cytometry fluorescence values averaged across all cells in a given mCherry bin. Specifically, the x-axis is cis-ligand expression (mCherry, A.U.) relative to (divided by) cotranslational receptor expression (mTurq2, A.U.); see also Methods. Y-axis values are Notch signaling activity (reporter activity (mCitrine, A.U.) divided by cotranslational receptor expression (mTurq2, A.U.). For each bioreplicate curve, signaling activity was normalized to the y-value with minimum cis-ligand (Figure 6—figure supplement 1C). Each curve on a

given plot corresponds to a different sender (Figure 6—figure supplement 1A,B) cocultured with the receivers. Cis-inhibition of Jag1-Notch1 signaling could not be analyzed because trans-activation was too weak (Figure 6—figure supplement 1C). For Notch2-Delta receivers, lines are interpolated through the mean of three biological replicates in each mCherry bin along the x-axis. For other receivers, curves are the least-squares fit of three biological replicates to an inverse Hill function with maximum y=1 (Methods), colored according to the sender cell type cocultured with the receivers. The dot-and-arrow icon below the legend indicates the assay type used to generate the data (Figure 1B).

(**B-D**) Mean fit parameters computed from least-squares fits of 10k bootstrap replicates of the curves in (A) to inverse Hill functions (Methods). Error bars are 95% confidence intervals.

(**B**) Relative 1/EC50 values were computed by dividing all values by the lowest 1/EC50 (Notch1 with trans-Dll4 and cis-Dll1). Colors indicate cis-ligand identity.

(**C**) Fitted 1/EC50 values were normalized to the maximum value for each receiver cell line to compare trans-ligands' relative susceptibilities to cis-inhibition by each of the different cis-ligands. Colors indicate trans-ligand (sender cell) identity; in the legend, 'D' stands for 'Dll' and 'J' stands for 'Jag.'

(**D**) Hill coefficients (*n*) from Hill fits in (A). Reliable Hill coefficients could not be computed for Notch1-Dll4 receivers with Dll4 or Jag2 senders because of the slight cis-activation observed at intermediate cis-ligand levels for those combinations.

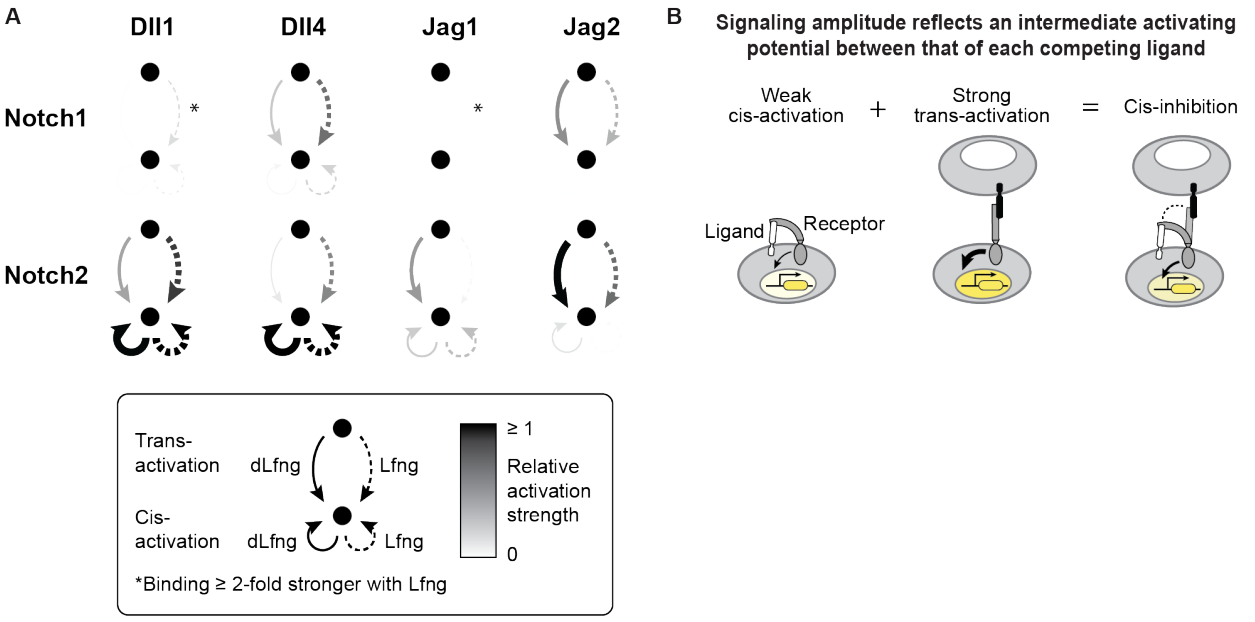

Figure 7: Each receptor-ligand combination has a unique activity profile

(**A**) Relative trans- and cis-activation strengths are shown for all eight receptor-ligand pairs both with dLfng (solid) and Lfng (dashed) expression. Signaling strengths, corresponding to the normalized trans-activation strengths summarized in Figure 2D and the normalized cis-activation strengths summarized in Figure 3B, are mapped linearly to both the greyscale color and line thickness of the arrows. (Missing or imperceptible arrows indicate weak signaling activities.) Combinations with binding strengthened by Lfng are indicated with an asterisk.

(**B**) Cell schematic illustrating that receptor-ligand pairs that cis-activate well do not exhibit cis-inhibition (i.e., Delta-Notch2 combinations). Black ligands represent strong activators and white ligands represent weak activators, which are still able to bind receptors. Yellow saturation levels in cell nuclei represent signaling activities. Our data support the view that Notch cis-inhibition mediated by the four primary activating ligands operates by competitive inhibition, wherein cis- and trans-ligands bind the same or overlapping sites on the receptor extracellular domain.

2.4 Discussion

The Notch signaling architecture allows ligands to either inhibit or activate receptors, and to do so both in cis and in trans. Systematic mapping revealed that each ligand is functionally unique in terms of its profile of signaling in cis and trans across the two Notch receptors, its inhibition abilities, and its response to Lfng (Figure 7A). Similarly, Notch1 and Notch2 are qualitatively distinct in terms of their interaction profiles with different ligands.

By analyzing Lfng effects on trans-activation, cis-activation, and relative binding strengths, we found that Lfng can alter these three properties in different ways even for the same receptor-ligand pair. Lfng potentiated Delta-mediated trans-activation and attenuated Jagged-mediated trans-activation for both receptors. However, Lfng strengthened binding of both Jag1 and Jag2 to Notch1, in addition to strengthening Dll1-Notch1 binding. This result is consistent with previous reports that Lfng strengthened binding of both Dll1 and Jag1 to Notch1 (Hicks et al. 2000; Kakuda and Haltiwanger 2017; Taylor et al. 2014; Yang et al. 2005). We did not observe any Lfng-mediated attenuation of Jagged-Notch binding. However, one previous report suggested that Lfng decreased Jag1-Notch2 binding strength (Shimizu et al. 2001), and our failure to detect an Lfng effect on Jag1-Notch2 binding at the single ligand concentration used here did not rule out the possibility that an effect might be observed at lower ligand concentrations. Nevertheless, Lfng showed opposite effects on Notch1 binding (potentiation) and activation (attenuation) by both Jag1 and, to a lesser extent, Jag2.

The mechanism by which Lfng modifications could strengthen Jag1-Notch1 binding while decreasing its activation is unknown, though the glycolsylation sites responsible for Lfng-mediated activation attenuation have been localized to Notch1 EGF repeats 6 and 36 (Kakuda and Haltiwanger 2017). Since Lfng weakened Notch1 activation by plated recombinant Jag1-ext-Fc (Figure 3C) as well as by cell-expressed Jag1 (Figure 2B), Lfng's ability to attenuate Jag1-Notch1 activation must not depend on the natural endocytic activation mechanism. Although Lfng modifications at the core binding interface increase receptor-ligand affinity under low tension, it is possible that Lfng modifications at other sites prevent formation of additional, essential intermolecular contacts made following initiation of ligand endocytosis. For example, might these Lfng-mediated modifications prevent formation of the "catch-bond" that allows the Jag1-Notch1

complex to endure the high tension conditions of force-mediated activation (Luca et al. 2017)? Further studies are needed to test this hypothesis.

Regardless of the mechanism, it is clear that Lfng's ability to strengthen Jag1-mediated inhibition of Notch1 signaling represents one of the enzymes's critical biological functions, since Jag1 is an essential and Lfng-dependent trans-inhibitor of Dll4-Notch1 signaling in angiogenesis (Pedrosa et al. 2015; Benedito et al. 2009) and of Dll1-Notch1 signaling in the embryonic pancreas (Golson et al. 2009).

Overall, our measurements of relative trans-activation strengths, and their modulation by Lfng, largely agree with existing data for the subset of receptor-ligand pairs previously analyzed (Stanley and Guidos 2009; Song et al. 2016; Benedito et al. 2009; Tveriakhina et al. 2018; Hicks et al. 2000; Kakuda et al. 2020). The literature provides contradictory reports of Lfng effects on Jagged-Notch2 signaling, with some finding Lfng had no effect (Kakuda et al. 2020), some finding Lfng increased Jag1-Notch2 signaling (Hicks et al. 2000), and others consistent with our finding that Lfng weakens Jag1-Notch2 signaling (Shimizu et al. 2001).

Our analysis of cis receptor-ligand interactions revealed that all Notch ligands interact with both Notch1 and Notch2 in cis, and they only cis-inhibit the receptors that they do not efficiently cis-activate (Figure 7B), resembling an existing mathematical model of competition between cis and trans Notch ligands (Formosa-Jordan and Ibañes 2014). For example, we found that Dll1 and Dll4 strongly cis-activated, but did not cis-inhibit, Notch2. For all other receptor-ligand pairs, ligands cis-inhibited receptors efficiently when competing with high levels of trans-activating ligands, and exhibited negligible or modest cis-activation in absence of trans-activating ligands. The above principle supports the view that cis-inhibition occurs via competition between the cis- and trans-ligand for binding to the same receptor domain (Brendan D'Souza, Meloty-Kapella, and Weinmaster 2010), and is consistent with reports that a highly conserved region of the Serrate ligand is required both for cis-inhibitory and trans-activating Notch interactions in *Drosophila (Cordle et al. 2008)*, and that synNotch ligands can cis-inhibit their receptors when expressed in the same cell (Morsut et al. 2016).

For Notch1, cis-inhibition by Jag2 exhibited some properties reminiscent of mutual-inhibition-like models of cis-inhibition (Sprinzak et al. 2010; LeBon et al. 2014; Xu et al. 2023), but other ligands did not. These models assumed much stronger receptor binding by the cis-ligand than the trans-

ligand, which allows the cis-ligand to linearly "titrate" the amount of receptor and enables cis-inhibition models to disregard direct competition between cis- and trans-ligands (del Álamo, Rouault, and Schweisguth 2011). Consistent with this model, Jag2-Notch1 cis-inhibition curves had Hill coefficients of ~1 (Figure 6D), and EC50 values showed relatively minimal dependence (<1.6-fold differences) on the identity of the trans-activating ligand or the strength of trans-activation (Figure 6C), suggesting that trans-ligands may not have been able to effectively compete with cis-Jag2 for receptor binding. Jag2 also exhibited the strongest Notch1 cis-inhibition by far, with EC50s roughly an order of magnitude smaller than those of the other ligands.

In contrast with our observations of Jag2-Notch1 cis-inhibition and with a previous model of Dll1-Notch1 cis-inhibition (Sprinzak et al. 2010), Dll1-Notch1 cis-inhibition efficiencies showed strong dependence (up to ~10-fold) on the identity of the trans-activating ligand, suggesting that in some cases, trans-ligands compete effectively with cis-Dll1 for receptor binding. Dll1-Notch1 cis-inhibition curves had Hill coefficients of up to ~1.5, better resembling a more recent model proposing that cis-inhibition requires ligand dimerization, suggesting ligand-receptor binding stoichiometries greater than 1:1 (D. Chen et al. 2023). A key difference between our experiments and those supporting mutual-inhibition-like Dll1-Notch1 behavior is that, in our experiments, trans-ligand was supplied via sender cells, whereas others measured cis-inhibition of Notch1 activation by plated recombinant Dll1-ext-Fc (Sprinzak et al. 2010). Indeed, we found that with canonical trans-endocytosis-mediated Notch1 activation, the Dll1-Notch1 trans-activation curve had a Hill coefficient of ~2 (Figure 2—figure supplement 5D), whereas in the plated ligand assay, the Dll1-Notch1 trans-activation curve had a Hill coefficient of ~1 (Figure 2—figure supplement 6C), consistent with independent, 1:1 binding between receptors and plated Dll1-ext-Fc ligands. The cooperative nature of the canonical intercellular Notch trans-activation mechanism, likely involving ligand-receptor clustering at the signaling interface (Narui and Salaita 2013), could account for observations that trans-ligands can compete with cis-Dll1 (as well as with cis-Dll4 and -Jag1) for receptor binding in our experiments.

Additionally, our results revealed new complexities to cis-inhibition that previous mathematical models have not accounted for. While existing models describe competitive inhibition of Notch signaling in terms of simple pairwise receptor-ligand binding affinities dependent only on binding orientation (cis vs. trans) (Luna-Escalante, Formosa-Jordan, and Ibañes 2018; Sprinzak et al. 2010;

del Álamo, Rouault, and Schweisguth 2011; LeBon et al. 2014; Formosa-Jordan and Ibañes 2014), our data suggest that each cis- or trans-ligand's ability to compete with another ligand for receptor binding depends in a more complex manner on identities of the receptor and both competing ligands. For Notch1 but not Notch2, we found that trans-activating ligands' relative susceptibilities to cis-inhibition exhibited distinct patterns for each of the four cis-ligands. Strikingly, all ligands showed a comparative advantage in their ability to cis-inhibit trans-activation by the same ligand compared with trans-activation by different ligands. Thus, future modeling of competitive Notch1 inhibition should utilize third-order binding affinities that depend on the identities and orientations of both competing ligands.

In addition to cis-inhibition, the present study provides new insights into the nature of cis-activation. Unlike in trans-activation, where endocytosis of the receptor-bound ligand generates mechanical strain that exposes the receptor's negative regularly region (NRR) to activating enzymatic cleavage (Langridge and Struhl 2017), same-cell interactions between receptors and ligands offer no obvious way to apply tensile strain. Though the biophysical mechanism of cis-activation remains a mystery, we observed some key differences between cis- and trans-activation that identify interesting avenues for future investigation. For example, although Lfng altered cis- and trans-activation in similar ways for the Delta-Notch1 and Jag2-Notch2 combinations, its effects differed by orientation (cis vs. trans) for a subset of other receptor-ligand pairs. Lfng enhancement of Delta-Notch2 activation was much stronger in trans than in cis. For the Jag1-Notch2 pair, Lfng weakened trans-activation but modestly strengthened cis-activation. Our finding that strong cis-activation differs from trans-activation in terms of its Lfng dependence suggests that the cis-activation mechanism, at least for most Notch2-ligand pairs, does not occur via canonical trans-endocytosis at contacts between potential folds in the membrane.

Another key difference between cis- and trans-activation for Notch2 was that, unlike trans-activation, the strength of Notch2 cis-activation showed an inverse correlation with the size of the ligands' extracellular domains (the strongly cis-activating Delta ligands are roughly half the size of the weakly cis-activating Jagged ligands (B. D'Souza, Miyamoto, and Weinmaster 2008)). In principle, cis-binding between Notch2 and the smaller Delta ligands in the same antiparallel orientation proposed for Notch1 (Luca et al. 2015; Kovall et al. 2017; Morsut et al. 2016) could apply sufficient mechanical strain through receptor bending to expose the receptor negative

regulatory region (NRR) to activating protease activity, in a manner theoretically independent of ligand endocytosis. If Notch2 cis- and trans-activation mechanisms differ in terms of the types of mechanical strain involved (for example, bending vs. tensile elongation), distinct Lfng dependencies might be expected. Mechanistic investigations are needed to elucidate the biophysical basis of cis-activation for both strong and weak cis-activating combinations, which could differ in fundamental ways.

In principle, cis-activation could depend to some extent on cell context or other factors specific to our experiments. Our observation that the Deltas cis-activate but cannot cis-inhibit Notch2, both in CHO-K1 and C2C12 cells, conflicts with a recent report that wild-type Dll4 cis-inhibited Notch2 in U2OS osteosarcoma cells, evidenced by lower luciferase reporter activity in cells with integrated Dll4 compared with cells only expressed Notch2 (D. Chen et al. 2023). It is possible that cell type-specific factors prevent Dll4 cis-activation of Notch2 in U2OS cells or that Dll4 cis-inhibition requires some interaction between Dll4 and the N2ICD (absent from our N2ECD-Gal4 receptors). Future work is needed to assess the outcome of cis interactions between Notch2 and the Delta ligands in vivo.

Our systematic, quantitative map of receptor-ligand-Fringe interactions, in cis and trans, could enable better predictions of the functional roles of Notch components in existing cell atlas data. However, it is not clear whether behaviors we observed for pairwise receptor-ligand interactions will hold in contexts where multiple receptors or ligands are coexpressed in the same cell. For example, one of the 16 most prevalent "motifs" of Notch component expression identified by Granados et al. (2022) using publicly available single-cell RNA-seq datasets (Granados, Kanrar, and Elowitz 2022) showed high levels of Notch1 and Notch2 as well as moderate levels of all four activating ligands. This motif appeared in multiple cell types within the heart, trachea, forelimb, and other tissues. Supposing the surface protein expression profile reflects the underlying mRNA profile with some fidelity, do the Delta ligands predominantly cis-activate Notch2 in these cells, or does Notch2 preferentially interact with the Jagged ligands instead? We still lack measurements of relative binding strengths for two or more ligands competing in cis for the same receptor. Moreover, pairwise cis-binding affinity measurements may still be insufficient, since we found that relative binding strengths (in the case of Notch1 cis-inhibition) depended not only on the receptor-ligand pair, but on the receptor-(cis-ligand)-(trans-ligand) triad.

Another open question is whether interaction synergies occur between coexpressed receptors competing for the same ligand. For example, when Dll4 is coexpressed with both Notch1 and Notch2, does it still predominantly cis-activate Notch2 and cis-inhibit Notch1 in competition with activating ligands expressed by a neighboring cell, or do biophysical synergies flip the interaction mode, enabling Dll4 to better cis-activate Notch1 or to cis-inhibit Notch2? Experiments using "double receivers" with orthogonal readout of Notch1 and Notch2 activity could shed light on this question.

Together, the work presented here offers new insights into the complex cellular language of Notch signaling, and paves the way for more rational perturbation of Notch signaling through context-specific targeting of specific receptor-ligand combinations.

2.5 Methods

Plasmid construction

The pEV-2xHS4-UAS-H2B-Citrine-2xHS4 reporter construct is the same base construct used in (Nandagopal, Santat, and Elowitz 2019) with the modification of the 2xHS4 insulating elements flanking each side of the expression cassette. All of the Notch receptor piggyBac constructs were derived from the vector PB-CMV-MCS-EF1-Puro (System Biosciences), with changes made to the promoter (CMV changed to PGK or CAG) and selection marker (Puromycin to Neomycin), as well as insertion of the NotchECD-Gal4esn-T2A-H2B-mTurq2 sequence into the MCS. The Lfng and Lfng(D289E) sequences were cloned into the MCS of the original PB-CMV-MCS-EF1-Puro plasmid to create the Fringe constructs, while the IFP2.0 sequence was cloned into the same base vector, but with the Puro resistance gene replaced by the Neomycin resistance gene. TetOff constructs were designed from the original pCW57.1-MAT2A plasmid obtained by Addgene. The sequence from the end of the TRE-tight promoter to the beginning of the Blast resistance gene promoter was removed and replaced with each of the activating Notch ligand sequences fused to a T2A-H2B-mCherry sequence or with an H2B-mCherry or NGFR-T2A-H2B-mCherry sequence in the case of the control plasmids. For the constitutively expressing ligand constructs, the TRE-tight promoter was also removed and replaced with the CBh promoter. The plasmids used to PCR the gRNA for the CRISPR-Cas9 mediated knockout of endogenous Notch2 and Jagged1 in C2C12 cells (see CRISPR section below) were the same plasmids used in (Nandagopal, Santat, and Elowitz 2019).

Cell culture and plasmid transfections

CHO-K1 cells (ATCC) were cultured in alpha MEM Earle's Salts (FUJIFILM Irvine Scientific) supplemented with 10% FBS (Avantor, VWR), and 1X Pen/Strep/L-glutamine (Thermo Fisher Scientific) as previously described (Elowitz, Santat, and Nandagopal 2018). Transfection of CHO-K1 cells was performed using Polyplus-transfection jetOPTIMUS DNA Transfection Reagent (Genesee Scientific) according to the manufacturer's instructions. Briefly, for cells plated in 24 wells the night before (to reach ~80% confluency at time of transfection), 500 ng of non-piggyBac DNA was used along with 0.5 ul of transfection reagent. For piggyBac constructs, 500 ng of DNA + 100 ng of the Super piggyBac transposase (System Biosciences) was used. For generation of

stable cell lines, cells were incubated in 0.5 ml media with DNA + transfection reagent overnight at 37ºC, 5% CO_2 before changing media the next day. For transient transfections, cells were incubated with DNA + transfection reagent for only 4-6 hours before media change.

C2C12 cells (ATCC) were cultured in DMEM with high glucose, no glutamine (Thermo Fisher Scientific) supplemented with 20% FBS, 1X Pen/Strep/L-glutamine, and 1X Sodium Pyruvate (Thermo Fisher Scientific). Cells were split to ensure that stock cell cultures never reached more than 80-90% confluency. Plasmid transfection of C2C12 cells was performed using the same protocol as used for CHO cells mentioned above.

All cell lines were originally tested by the manufacturer, ATCC, and determined to be free from mycoplasma contamination. Subsequent testing for mycoplasma contamination was also performed by our lab using the InvivoGen MycoStrip test kit and protocol. All cell lines were found to be free of mycoplasma contamination at the time of experiments.

Lentivirus production and infection

Lentivirus was produced using the ViraPower Lentiviral Expression System (Thermo Fisher Scientific). Briefly, 293FT producer cells in a T-25 flask were transfected with a pCW57.1 expression construct (1.3 ug DNA) along with a packaging plasmid mix consisting of pVSV-G, pLP1 and pLP2 in a 2:1:1 ratio (3.9 ug DNA total). 24 hr after transfection, cell media was changed with 4 ml of fresh media. 48 hr post-transfection, virus containing cell media was collected and centrifuged at 3K rpm for 15 min at 4ºC to remove cell debris and filtered through a 0.45 um PVDF filter (EMD Millipore). 200 ul unconcentrated viral supernatant was added to cells plated at 20K / 24-well the day before, in a total volume of 300 ul (100 ul media + 200ul virus) and incubated at 37°C, 5% CO2. 24 hr post-infection, virus containing media was removed and replaced with fresh media. At 48 hr post-infection, cells were placed under selection with media containing 10 ug/ml Blasticidin (Invivogen). After 2 cell passages in selection media, cells with high mCherry expression were sorted (see Cell line construction section) and used to screen for clones.

Cell line construction

CHO-K1 cells were engineered to produce Notch receiver cells, receiver cells with inducible ligand, and Notch ligand sender cells. Receiver cells were created by initial transfection of the 2xHS4-UAS-H2B-mCitrine-2xHS4 plasmid. After selection in 400 ug/ml Zeocin (Thermo Fisher Scientific), cells were placed into limiting dilution, and a single reporter clone was identified that activated well in response to transient expression of Gal4, and continued with. The reporter clone was then transfected with a chimeric Notch1 or Notch2 receptor, whose intracellular domain was replaced with a Gal4esn-T2A-H2B-mTurq2 sequence (Gal4esn = minimal Gal4 transcription factor). Transfected reporter cells were selected in 600 ug/ml Geneticin (Thermo Fisher Scientific) and placed into limiting dilution. A Notch1 or Notch2 receiver cell clone was chosen by its ability to demonstrate high mCitrine expression when plated on plate-bound ligand in culture. For receiver cells with inducible ligand, TetOff-ligand-T2A-H2B-mCherry was added to the receiver cells by lentiviral infection (see Lentiviral production and infection section above). Cells were selected in 10 ug/ml Blasticidin (Invivogen), and sorted (Sony MA900 Multi-Application Cell Sorter) for expression of Notch (mTurq2) and ligand (mCherry) in the absence of 4-epi-Tc. Sorted cells were placed into limiting dilution, and clones were selected that demonstrated good ligand induction range (mCherry levels) when treated with various amounts of 4-epi-Tc as well as expressed good levels of mTurq2 (Notch receptor). Sender cell lines, stably expressing each of the four ligands under control of the TetOff system or constitutively activated by the CBh promoter (Figure 1A) were created by infection of CHO-K1 cells with TetOff-ligand-T2A-H2B-mCherry lentivirus or CBh-ligand-T2A-H2B-mCherry lentivirus, respectively. After selection in 10 ug/ml Blastidicin, sorting for high mCherry levels and placement in limiting dilution, cell clones were chosen by their tunability of the Tet-Off ligand with 4-epi-Tc or by the level of ligand expression in the case of constitutively expressed ligand.

C2C12 receivers, receivers with inducible ligand, and sender cell lines were constructed in the same manner as the CHO-K1 cells with 1 major difference. C2C12 wildtype cells were first depleted of endogenous Notch2 and Jagged1 by CRISPR-Cas9 knockout before any cell lines were made (see CRISPR section below).

CRISPR-Cas9 knockout of endogenous C2C12 Notch2 and Jagged1

Endogenous Notch2 and Jagged1 genes were knocked out in C2C12 mouse myoblast cells using 2 rounds of transfection with RNPs (ribonucleoproteins) consisting of gRNAs targeting Notch2 and Jagged1 complexed with Cas9 protein, along with an empty plasmid containing the blasticidin resistance gene added to the transfection mixture. To make the RNPs, gRNA sequences were first placed into the pX330 CRISPR-Cas9 plasmid as described in Nandagopal et al. 2019. The gRNA sequences were then PCR amplified with a forward primer containing a T7 promoter and a reverse primer containing a small pA tail:

Notch2 gRNA primer sequences: (5' to 3')

T7 mN2C2 F

TCTACCTAATACGACTCACTATAGGGTGGTACTTGTGTGCC (T7 promoter)

mN2C2 R

AAAAGCACCGACTCGGTG

Jagged1 gRNA primer sequences: (5' to 3')

T7 mJ1C1 F

TCTACCTAATACGACTCACTATAGCGGGTGCACTTGCG (T7 promoter)

mN2C2 R

AAAAGCACCGACTCGGTG

Resulting PCR products were transcribed using the Megashortscript T7 transcription kit (ThermoFisher Scientific), following the manufacturer's directions. 125 ng of each gRNA was separately incubated with 250 ng of Cas9 protein (PNA Bio Inc) for 10 minutes at room temp, after which, the two gRNA/Cas9 mixtures were combined and used to transfect cells along with plasmid containing blasticidin resistance. Transfected cells were incubated for 24 hours before transfection media was replaced with media containing 10 ug/ml blasticidin (Invivogen). Cells were incubated for 30 hours, after which, selection media was removed and replaced with fresh

media without selection. After the selected cell population was grown to ~80% confluency, cells were placed into limiting dilution in 96-well plates, calculating for 1 cell/well. Single cell clones were identified and grown for ~10-12 days before expanding. Screening of C2C12 clones for reduced surface expression of Notch2 and Jag1 enabled identification of clone "Nkd" that showed a loss of Notch signaling with impaired upregulation of Notch target genes Hey1, HeyL, Notch1, Notch3, and Jag2, when cells were cultured on plated recombinant Dll1 (Dll1-ext-Fc) and analyzed by RNA-seq (Figure 2—figure supplement 3A). The C2C12-Nkd clone also showed loss of Notch2 protein by Western blot (Figure 2—figure supplement 3B) and a loss of Jag1 mRNA by RT-PCR (Figure 2—figure supplement 3C). Western blot was performed as described in (Nandagopal, Santat, and Elowitz 2019). For RT-PCR analysis, RNA from cell lines was extracted by using the RNeasy Mini Kit (Qiagen) with the cell-lysate first being homogenized through a QIAshredder column (Qiagen), as per the manufacturer's directions. RNA was then reverse-transcribed with the iScript cDNA Synthesis Kit (Bio-Rad), and PCR was carried out using the Jagged1 specific primers (5' to 3'):

mJ1 C1 F

CCAAAGCCTCTCAACTTAGTGC

mJ1 C1 R

CTTAGTTTTCCCGCACTTGTGTTT

RNA-sequencing data collection and analysis of C2C12 wild type and Nkd clone

C2C12-Nkd or C2C12 wild-type cells were plated at 80k cells/well in a 12-well plated treated with recombinant ligand (2µg/mL Dll1-ext-Fc in PBS) or PBS only (negative control, C2C12-Nkd only) in 10 µM DAPT (Notch signaling inhibitor) overnight in two biological replicates. The next morning, DAPT was washed out and cells were allowed to signal for 6 hours before cells were harvested for RNA extraction using QIAshredder columns (Qiagen) and the RNeasy Mini Kit per the manufacturer's instructions (see next section for further details of the plated ligand assay).

cDNA libraries were prepared according to standard Illumina protocols at the Millard and Muriel Jacobs Genetics and Genomics Laboratory at Caltech. SR50 sequencing (10 libraries/lane) with a sequencing depth of 20–30 million reads was performed on a HiSeq2500. TrimGalore was used to run Cutadapt to trim low-quality ends (with -q 28), to remove adapters, and to clip 3 bp from the 3' ends of reads after adapter/quality trimming, as well as to run FastQC for quality assessment. Data were then uploaded to Galaxy for subsequent processing. Reads were aligned to the Mouse Dec. 2011 (GRCm38/mm10) genome using HISAT2 with default parameters and transcript abundances were computed with StringTie using the GENCODE annotation of the mouse genome (GRCm38), version M22 (Ensembl 97), downloaded 2019-06-27.

Analysis of publicly available, pre-processed CHO-K1 transcriptomic data from RNA-sequencing

We computed mRNA expression levels for Notch genes in CHO-K1 cells (Supplementary Table 2) using processed RNA-sequencing data from CHO-K1 cells downloaded from the CHO gene expression visualization application (CGEVA) located at https://anksi.shinyapps.io/biosciences/ (Singh, Kildegaard, and Andersen 2018). Gene expression was given by the CGEVA application in units of normalized log2-transformed counts per million reads mapped (CPM), with normalization procedures previously described by the authors (Singh, Kildegaard, and Andersen 2018). For Notch genes of interest, we averaged expression measured in two different samples from CHO-K1 wild type cells, and converted Log2-transformed CPM values to CPM units by the transformation CPM = 2^(Log_2(CPM)).

Signaling assays with flow cytometry readout

Various cellular assays enabled quantitative analysis of relative signaling activity mediated by different receptor-ligand pairs expressed in cis and/or trans (see Figure 1B). The general workflow for all assays was as follows (see also Figure 1C): Ligand expression was induced in either sender or receiver cells by reducing the 4-epi-Tc concentration in the culture medium to the desired level (Supplementary Table 3), and receivers were incubated in the Notch signaling inhibitor DAPT to prevent reporter activation during this 48 hr preinduction phase. Media was changed after 24 hr to

maintain the desired 4-epi-Tc concentration and 1 μM or 2 μM DAPT for CHO-K1 and C2C12 receivers, respectively. For all assays with siRNA knockdown, siRNAs were applied 7-10 hrs after cell seeding such that cells were 30-50% confluent at time of transfection (see section "siRNA transfections") and siRNAs were removed after a ~16 hr incubation. Plasmid transfections (when applicable) were performed immediately after siRNA media change (24 hr before starting an assay) when cells were ~80% confluent. Per 0.5mL of medium in a 24-well, 500 ng of total plasmid was transfected including IFP2 plasmid only or 350 ng of an IFP2 plasmid cotransfected with 150 ng of a plasmid containing wild-type mouse Lfng or the Lfng D289E mutant (mutated catalytic aspartate, "dLfng"). Media was changed (replacing proper 4-epi-Tc and DAPT concentrations) 4-6 hours after transfection. To start the signaling assay, receivers (and sender cells, if applicable) were trypsinized using 0.25% Trypsin without EDTA and plated at a total cell density to reach confluence after 24 hours, either in a monoculture, coculture, or on plated ligand (see assay subtype details below). Senders used for each coculture assay experiment are listed in Supplementary Table 4. Cells were incubated for 22-24 hours in the proper 4-epi-Tc concentration (if applicable) but without DAPT to allow signaling, and with the IFP2 cofactor biliverdin for samples transfected with IFP2 plasmid. Cells were harvested by trypsinization and Notch activation was analyzed by flow cytometry. All assays were performed with at least three biological replicates. Procedural details specific to each assay subtype, including cell coculture ratios, are described below.

Plated ligand assay: For assays with CHO-K1 cells, wells of a 48-well plate were coated with recombinant ligand (Bio-Techne/R&D Systems) diluted in PBS to a volume of 150 ul/well and incubated at room temperature for 1 hour with rocking. For experiments with C2C12 cells, 24-well plates were used and volumes were scaled up accordingly. Either PBS alone or IgG1 Fc was plated as a negative control. The ligand or control solution was removed, and receiver cells were trypsinized using 0.25% Trypsin without EDTA and plated at 50k cells/well to start the assay. Plated ligand concentrations used for each experiment are given in Supplementary Table 5.

Trans-activation assay: Excess sender cells (stable or preinduced Tet-OFF senders) or negative control senders expressing no ligand (CHO-K1 wt or C2C12-Nkd parental cells, corresponding to the receiver cell type) were cocultured with receiver cells (trypsinized in 0.25% Trypsin without EDTA) in 48-well, 24-well, or 12-well plates with a sender:receiver cell ratio of 5:1 or greater and a total cell density equivalent to 150k total cells/well in a 24-well plate. When receiver clones with

Tet-OFF ligands were used, cis-ligand expression was suppressed with maximal [4-epi-Tc] (500-800 ng/mL). Signaling activity was analyzed by flow cytometry after 22-24 hours of signaling.

Cis-activation assay: Ligand expression was induced in receiver cells as described above. 150k cells expressing no ligand (CHO-K1 wt or C2C12-Nkd parental cells, corresponding to the receiver cell type) were cocultured with 5k receiver cells (trypsinized in 0.25% Trypsin without EDTA) in 24-well plates or 12-well plates for CHO-K1 and C2C12-Nkd cells, respectively.

To determine theto what extent to which the cell density used during the ligand preinduction phase contributes to Notch activity measured in the cis-activation assay, CHO-K1 Notch2-Dll1 and Notch2-Dll4 receivers cells were plated either at 29k in a 96-well plate (for dense conditions) or 25k in a 6-well plate (for sparse conditions). All cells were plated in 1uM DAPT with varying amounts of 4-epi-Tc (Supplementary Table 3). 24 hours post-incubation, cells were trypsinized with 0.25% Trypsin without EDTA. Cells were then counted and replated at the same cell numbers, using the same plating conditions used to initially seed the cells. After another 24 hours of incubation, the CHO cells were trypsinized, counted, and plated along with CHO-K1 cells as described above. 22 hours post-incubation, cells were run on the flow cytometer to measure Notch activation. Positive controls were set up using 5k receiver cells (treated with 500 ng/mL 4-epi-Tc) cultured with 150k Dll1-L1 sender cells. All conditions were performed and run in triplicate.

Cis-modulation assay: Ligand expression was induced in receiver cells as described above. 150k sender cells (stable or preinduced Tet-OFF senders) or negative control senders expressing no ligand (CHO-K1 wt or C2C12-Nkd parental cells, corresponding to the receiver cell type) were cocultured with 5k receiver cells (trypsinized in 0.25% Trypsin without EDTA) in 24-well plates or 12-well plates for CHO-K1 and C2C12-Nkd cells, respectively. Signaling activity was analyzed by flow cytometry after 22-24 hours of signaling. For Figure 6 experiments only, a slightly different culture format was used (10k receiver cells with 100k sender cells in a 48-well plate).

Cis-* + *trans-activation assay: Ligand expression was induced in CHO-K1 receiver cells as described above. 150k receiver cells were trypsinized in 0.25% Trypsin without EDTA and plated in a 24-well plate. Receiver cells treated with siRNA knockdown and plasmid transfection were plated at a higher density of 300k per well to reach confluence during the course of the assay

despite reduced cell viability following the transfections. Signaling activity was analyzed by flow cytometry after 22-24 hours of signaling.

Soluble ligand binding assay

CHO-K1 reporter cells and reporter cells with integrated Notch1 or Notch2 ("receiver" cells) were prepared with endogenous Fringe knockdown and Lfng or dLfng transfection (with IFP2 as a cotransfection marker) as described in the section above ("Signaling assays with flow cytometry readout"). Instead of beginning a signaling assay, cCells were then replated on non-tissue-culture-treated polystyrene plates from CellStar to reduce cell attachment to the bottom of the well, enabling detachment without trypsin. After a 24 hr incubation in medium supplemented with the IFP2 cofactor biliverdin, the ligand binding assay was carried out with slight modifications from protocols described previously (Kakuda and Haltiwanger 2017; Varshney and Stanley 2017). Cells were detached by pipetting and spun down for 5 minutes at 400xg at room temperature (same parameters used for all centrifugation steps), then blocked with blocking buffer (2% BSA + 100 µg/mL CaCl2 in 1X DPBS) for 15 minutes. Ligands were prepared by preclustering ligand-ext-Fc fragments (at 2X concentrations relative to the final concentrations given in Supplementary Table 5) with AlexaFluor 594-conjugated anti-human secondary antibodies (1:1000) in blocking buffer for 1 hr in the dark at 4C. After blocking, cells were spun down again, resuspended in 50 µL blocking buffer, and mixed with 50 µL 2X preclustered ligands, then incubated in the dark for 1hr at 4C. To evaluate Fringe effects on surface Notch levels, cells were incubated with 400 ng/mL PE-conjugated anti-Notch1 or -Notch1 antibodies (instead of ligands) in blocking buffer at room temperature in the dark for 30 mins. Cells were washed once by adding 1 mL blocking buffer before spinning down, aspirating buffer, and resuspending cells in 200 µL FACS Buffer for analysis by flow cytometry (see "Flow cytometry analysis" section for FACS Buffer composition).

siRNA transfections and qRT-PCR analysis

Cells were seeded in 24-well or 12-well plates at a density to reach 30-50% confluence at the time of transfection—either 7-10 hrs or 24 hrs after plating, depending on the experiment. For Fringe knockdown in CHO-K1 cells, 2 pmol each of siRNA targeting the endogenous Rfng and Lfng

transcripts, or 4 pmol total negative control siRNA (Allstars negative control, Qiagen), were transfected usingwith the Lipofectamine RNAiMAX Transfection Reagent (Thermo Fisher Scientific) according to the manufacturer's instructions. For all assays with C2C12 cells, the same reagent was used to transfect cells with either negative control siRNA (32 pmol), N1+N2+N3 siRNA (4 pmol + 20 pmol + 4 pmol, respectively, plus 4 pmol control siRNA) or N1+N2+N3+Rfng siRNA (4 pmol+20 pmol + 4 pmol + 4 pmol, respectively) in a 12-well plate. In all assays, siRNAs were incubated with cells for 16-24 hours before media change, and transfected cells were harvested for knockdown quantification by qRT-PCR or for use in signaling assays 24-36 hours after initial transfection. For analysis by qRT-PCR, cells were spun down by centrifugation at 1400 rpm for 3 min at room temperature. After supernatant removal, the cell pellets were stored at -80^{0}C for later RNA extraction using the RNeasy Mini Kit (Qiagen) with the cell-lysate first being homogenized through a QIAshredder column (Qiagen), per the manufacturer's directions, followed by cDNA synthesis with the iScript cDNA Synthesis Kit (Bio-Rad), and finally analyzed by qPCR using the qPCR primers in Supplementary Table 1. qPCR was performed on a CFX96 Touch Real-Time PCR Detection System (Bio-Rad).

Analysis of endogenous Fringe effects on signaling in CHO-K1 cells

CHO-K1 cells endogenously express low levels of Lfng and ~20-fold higher levels of Rfng (Supplementary Table 2) (Singh, Kildegaard, and Andersen 2018). To assess the effects of endogenous Fringes on receptor-ligand interactions, we expressed dLfng or Lfng while knocking down endogenous Rfng and Lfng with siRNA in CHO-K1 receiver cells (as described above), and compared these "No Fringe" and "high Lfng" conditions to wild-type levels of Fringe in a trans-activation assay with flow cytometry readout.

As a general trend, the magnitude of signaling in the presence of endogenous Fringes fell between the dLfng and Lfng signaling magnitudes. Jag1-Notch1 signaling was not potentiated by endogenous Fringes (as would be expected in the case of Rfng dominance), but showed 1.7-fold weaker with endogenous CHO-K1 Fringes than with dLfng, consistent with Lfng dominance (Kakuda et al. 2020; Yang et al. 2005; Pennarubia et al. 2021), despite the much lower expression of Lfng relative to Rfng (Figure 2—figure supplement 4). (Note: Near signal saturating conditions,

we observed very small (<1.3-fold) decreases in Delta-Notch signaling with endogenous Fringes compared with dLfng, suggesting the possibility of mild, nonspecific effects of the siRNA or plasmid treatment in the two conditions). Although endogenous Fringes showed overall weaker effects on signaling activity than transfected Lfng did, our results suggest that endogenous Lfng modestly weakens Jagged signaling and strengthens Dll1-Notch1 signaling.

Density optimization for the cis-activation assay

For CHO cells, Notch1 or Notch2 receiver cells were trypsinized using 0.25% Trypsin without EDTA (Thermo Fisher Scientific). Receiver cells were plated sparsely at 2.5k, 5k or 10k in a 24 well plate along with an equal number of CHO Dll4 sender L1 cells (for Notch1) or CHO Dll1 sender L1 cells (for Notch2), and surrounded by 150k CHO-K1 wild-type cells. Cell cocultures were incubated for ~22 hours and subsequently analyzed by flow cytometer to determine Notch activation (citrine levels) in the receiver cells. For positive controls, 5k receiver cells were plated with 150k sender cells (Dll4 with Notch1 cells, and Dll1 with Notch2 cells) in order to obtain maximal activation of the receivers. 5k receiver cells were plated with 150k CHO-K1 wild-type cells along with the gamma-secretase inhibitor DAPT (1uM, Sigma) for use as negative controls. All experiments were performed in triplicate.

For C2C12 cells, the assay was performed similarly to the CHO cell assay with a few key changes. C2C12 Notch1 and Notch2 receiver cells were first plated at 140k cells per 12-well. After ~6 hours post-plating, the cells were transfected with siRNAs targeting residual endogenous mouse N1, N2 and N3 (Figure 2—figure supplement 3D), using Lipofectamine RNAiMAX Transfection Reagent (Thermo Fisher Scientific), following the manufacturer's instructions. Each siRNA was used at a final amount of 4 pmol, except for N2 siRNA which was used at 20 pmol. Cell media was changed 24 hours after siRNA transfection. 48 hours post-transfection, receiver cells were cocultured in a 12 well plate at 2.5k, 5k or 10k with an equal number of C2C12 Dll1 sender c19 cells as well as with 150k C2C12-Nkd cells. Positive controls were set up with 5k receiver cells + 150k Dll1 sender c19 cells, and negative controls consisted of 5k receiver cells + 150k C2C12-Nkd cells along with 2uM DAPT.

Flow cytometry analysis

For analysis of cells by flow cytometry, cells were trypsinized in 0.05% or 0.25% Trypsin-EDTA (Thermo Fisher Scientific). Cells were resuspended in 1X FACS buffer: 1X Hanks Balanced Salt Solution (Thermo Fisher Scientific) supplemented with 2.5 mg/ml Bovine Serum Albumin (Sigma-Aldrich) and 200 U/mL DNAse I. Resuspended cells were filtered through 40 μm cell strainers (Corning Inc, Corning, NY) into U-bottom 96-well tissue culture-treated plates. Cells were analyzed on a Beckman Coulter Life Sciences CytoFLEX benchtop flow cytometer. Data were analyzed in Python using custom software according to the following workflow:

1. Cells were gated in a 2D plane of forward scatter (FSC) and side scatter (SSC) to select intact, singlet cells.
2. Cells were gated in a 2D plane of mTurq2 (PB450, A.U.) vs. SSC to separate out the +mTurq2 receiver cells from -mTurq2 senders or 'blank' parental cells.
3. Plasmid-transfected cells were gated in the APC700 channel to select cells expressing the cotransfection marker IFP2.
4. Receiver cells coexpressing ligand were gated into six consecutive bins of arbitrary mCherry (ECD) fluorescence units (Figure 1C).
5. Compensation was applied to subtract mTurq2 signal leaking into the FITC channel.
6. If applicable, reporter activity, mCitrine (FITC, A.U.) fluorescence was normalized to co-translational receptor expression by dividing mCitrine by the mTurq2 signal (PB450, A.U.). The resulting mCitrine/mTurq2 ratio is the "signaling activity" (reporter activity per unit receptor).
7. If applicable, cotranslational cis-ligand expression was normalized to co-translational receptor expression by dividing mCherry by the mTurq2 signal (PB450, A.U.). The resulting mCherry/mTurq2 ratio (cis-ligand expression per unit receptor) controls for slight

variations in receptor expression when quantitatively comparing ligands' cis-inhibition efficiencies (Figure 6).

8. Average bulk measurements for each sample were obtained by computing the mean signal across single-cell data for a given sample (and mCherry bin, if applicable). Cells treated with different 4-epi-tetracycline (4-epi-Tc) levels were pooled as technical replicates after mCherry binning. A minimum of 100 cells were required during averaging; mCherry bins with too few cells did not generate a bulk data point.
9. Background subtraction was performed by subtracting "leaky" reporter activity of the receiver (with minimal cis-ligand, if applicable) in coculture with "blank" senders (CHO-K1 wt or C2C12-Nkd parental cells, according to the receiver cell type).
10. Y-axis normalization was performed as described in each figure caption.

Statistics

At least three biological replicates were used for each flow cytometry and qRT-PCR experiment, where biological replicates are distinct samples prepared separately, sometimes in parallel on the same day and sometimes on different days. Two biological replicates were used for RNA-sequencing.

Least squares regressions to fit data to lines or Hill functions were computed using scipy.optimize.leastsq(). Hill functions are defined as $y = b * x^n / (K^n + x^n)$ where K = the EC50 and b is the curve maximum.

All 95% confidence intervals were computed based on 10,000 bootstrap replicates with at least n = 3 biological replicates. When bootstrapping confidence intervals on parameter estimates from nonlinear regressions to Hill functions, bootstrapped datasets were constructed by bootstrapping from biological replicates within each x-axis "bin," defined as the mCherry fluorescence window, the plated ligand concentration, or the 4-epi-Tc concentration, as relevant.

P-values were computed in two ways. To evaluate whether the correlation between two paired variables had a slope greater or less than 1, we used one-sided Wilcoxon signed-rank tests

implemented in scipy—scipy.stats.wilcoxon(). To test whether two sets of datapoints came from distributions with the same means, we used permutation testing following these steps:

1. Compute the true difference in means between the control and test datasets (of length *n* and *m*, respectively).
2. Pool the two datasets and scramble the order of data points.
3. Define the permutation sample by labeling the first *n* points from the scrambled data as "control" data and the next *m* points as "test" data.
4. Compute the difference in means between the control and test distributions from the permutation replicate versus the original data set.
5. Repeat many times. The p-value is the fraction of permutation replicates with a difference in means greater than the true difference in means.

P-values were computed using at least 10k permutation replicates with one-sided differences in mean.

2.6 Acknowledgments

R.K., L.S., and M.B.E. conceived and designed the experiments. R.K. and L.S. generated the cell lines and performed the experiments. R.K. and L.S. analyzed the experimental data. R.K., L.S., and M.B.E. wrote the paper. We thank Irwin Bernstein for generously sharing the recombinant Dll1-ext-Fc ligand, and Igor Antoshechkin in the Millard and Muriel Jacobs Genetics and Genomics Laboratory for assistance with RNA sequencing. We are grateful to Xun Wang and the Rothenberg Lab for providing the NGFR construct. This work was supported by the National Institutes of Health (NIH) (grant R01 HD7335C). R.K. was supported by an NIH Ruth L. Kirschstein NRSA predoctoral fellowship (F31 HD100185). M.B.E. is a Howard Hughes Medical Institute Investigator.

2.7 Supplementary Figures

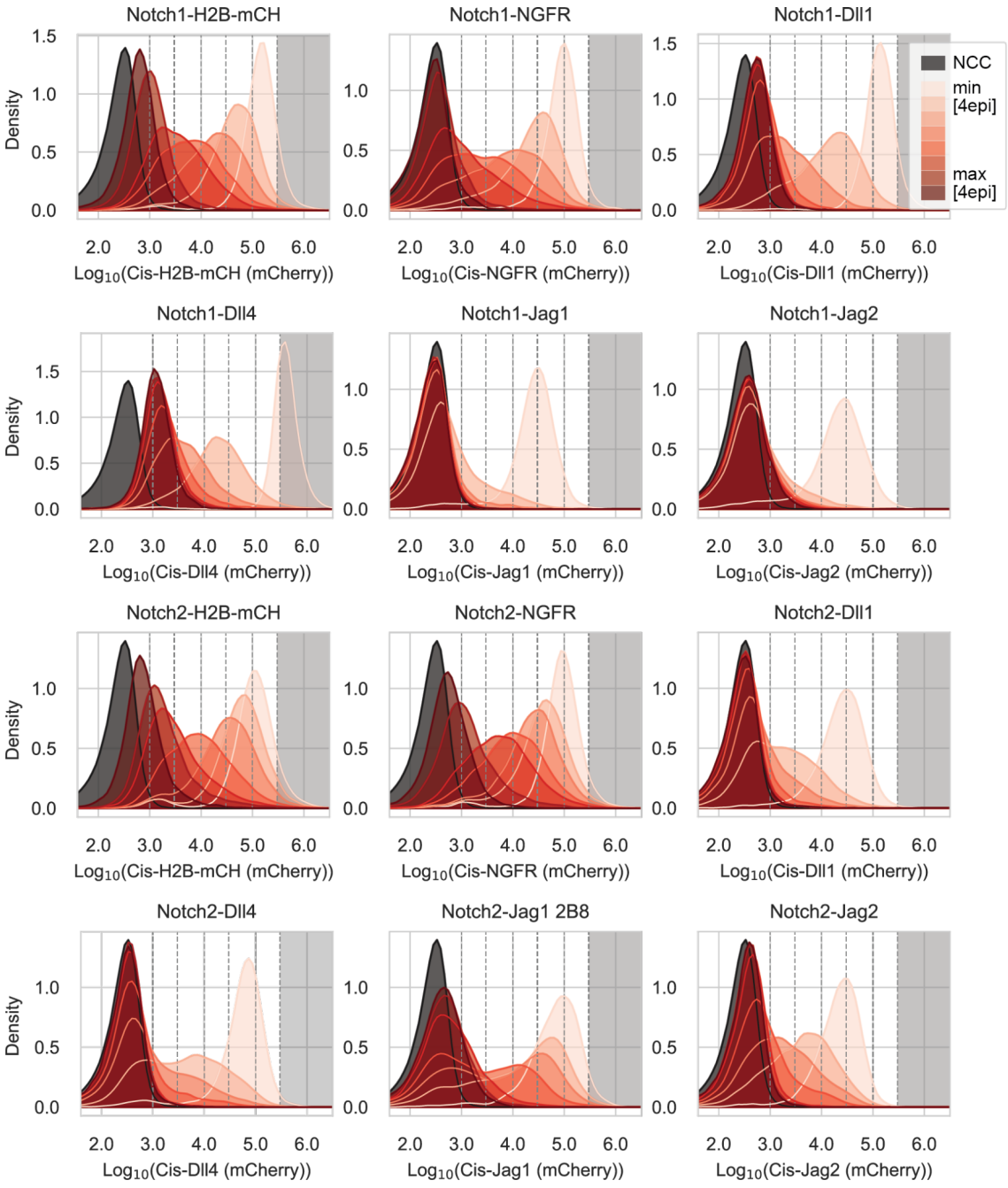

Figure 1—figure supplement 1: The Tet-OFF system enables unimodal titration of ligand levels

Distributions of cotranslational cis-ligand expression (mCherry, A.U.) in the receivers used to generate data in Figure 4. Each histogram contains data from three biological replicates corresponding to a specific 4-

epi-Tc concentration ranging from 0-500 ng/mL. Black histograms are CHO-K1 wild-type cells (NCC = no color control). To generate Figure 4B plots, receiver cells were binned into discrete intervals of mCherry expression indicated by the vertical dashed lines. Datapoints in the grey-shaded region were discarded.

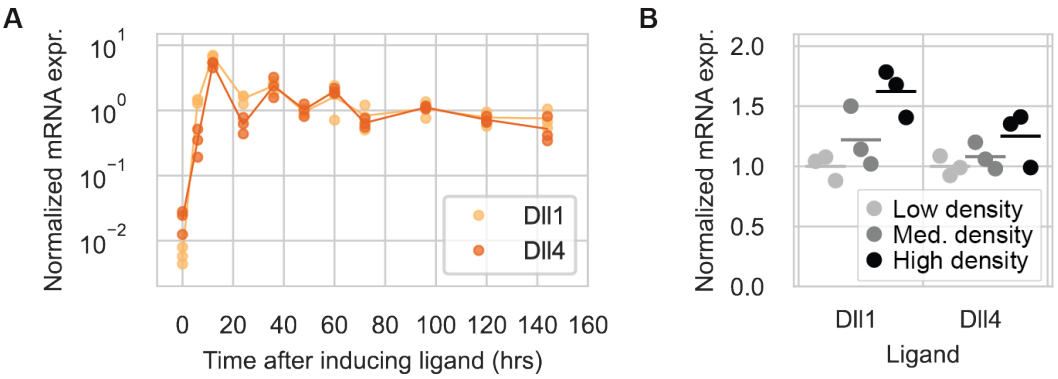

Figure 1—figure supplement 2: The Tet-OFF system achieves stable expression after 24-48 hours but cell density can affect expression

(**A**) mRNA expression from the Tet-OFF promoter reaches stable levels after 24-48 hours. CHO-K1 senders with integrated Dll1 or Dll4 ligands driven by the Tet-OFF promoter were seeded at a density that would reach confluence in a 24-well plate at the indicated time of collection. Seeded senders were induced to express ligand by reducing [4-epi-Tc] in the culture medium from 500 ng/ml to 5 or 10 ng/mL for Dll4 and Dll1 senders, respectively. Media was changed every 24 hr to replenish the proper 4-epi-Tc concentration, and cells were passaged every 72 hr, where applicable. At collection time, cells were spun down and RNA was extracted, followed by cDNA synthesis and qRT-PCR analysis. Y-axis values are $2^{-\Delta Cq}$ values quantifying mCherry transcript levels relative to the housekeeping gene beta-actin, normalized to the average of all data points after 36 hr for each ligand individually. Three biological replicates were collected for each cell type and time point.

(**B**) Cell density can affect Tet-OFF controlled ligand expression. 25k CHO-K1 Dll1 or Dll4 sender cells were seeded in a 24-well, 12-well, or 6-well plate (for high, medium, and low density, respectively) and induced to maximal ligand expression by removing 4-epi-Tc from the culture medium. Cells were collected 72 hr later and RNA expression was analyzed by qRT-PCR. Y-axis values were computed as in (A), except here they were normalized to transcript levels in the 'low' density condition. Horizontal bars are the mean of three biological replicates.

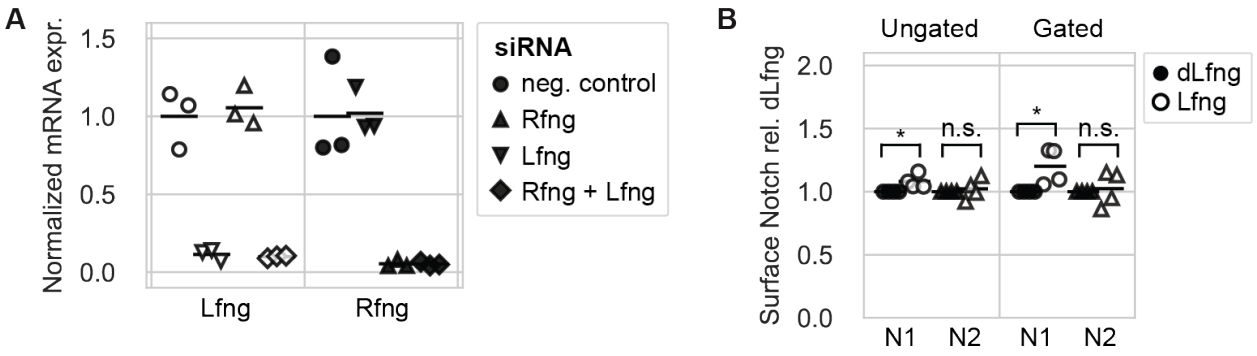

Figure 2—figure supplement 1: Knockdown of endogenous Lfng and Rfng in CHO-K1 cells

(**A**) qRT-PCR analysis of wild-type CHO-K1 Lfng and Rfng transcripts from cells treated with either a negative control siRNA, Rfng siRNA, Lfng siRNA, or Rfng and Lfng siRNAs. siRNA is indicated by marker shape as shown in the legend. Y-axis values are $2^{-\Delta Cq}$ values (computed using beta-actin as a housekeeping gene) normalized to the expression level in the negative control knockdown for each gene. Black bars are the mean of three biological replicates.

(**B**) Log2 fold-difference in the amount of surface Notch detected by staining with PE-conjugated antibodies (median PE fluorescence (A.U.) from single-cell flow cytometry data) in different Fringe expression conditions relative to Notch levels with dLfng expression (normalized within each bioreplicate). Marker shape denotes the receptor and marker fill denotes the Fringe construct transfected along with an IFP2 cotransfection marker. Asterisk-labeled brackets denote data sets unlikely (p-val < 0.05) to come from distributions with the same means according to permutation testing with 10k bootstrap replicates (Methods). Horizontal bars are mean of four biological replicates. On the x-axis, “N” stands for “Notch.” There is a small but significant increase in the amount of surface Notch1 detected (but not Notch2) with Lfng expression compared with dLfng, and this difference is slightly larger (but still <1.25-fold) when an IFP2 gate is applied to enrich for cells expressing the transfected Fringe constructs (“Gated”) than when no IFP2 gate is applied (“Ungated”) (Figure 1E; Methods).

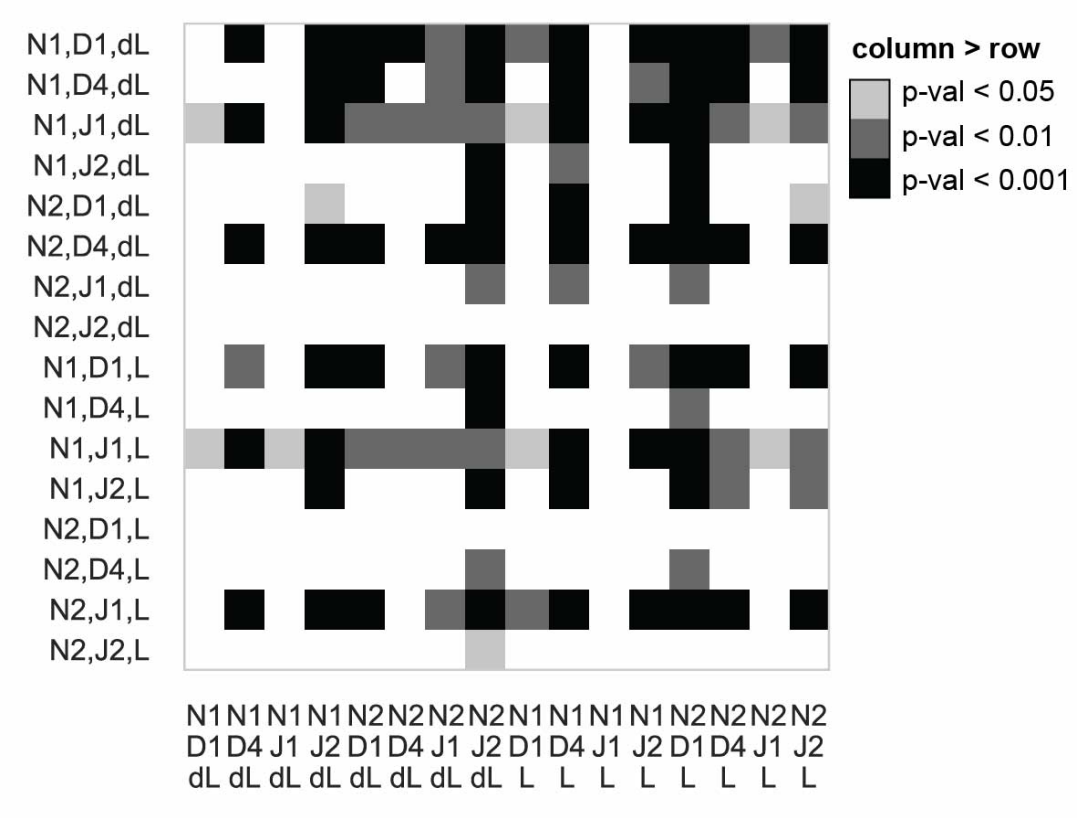

Figure 2—figure supplement 2: Statistical analysis of differences in trans-activation strength for all receptor-ligand-Fringe combinations

A matrix of p-values computed by comparing the relative strengths of 64 receptor-ligand-Fringe combinations from data in Figure 2B-D. For each matrix entry (row, column), the p-value was computed from testing the alternative hypothesis that the Notch combination in the column came from a distribution with a lower mean than the Notch combination in the corresponding row. Thus, dark squares indicate that the Notch combination labeling its column is likely to signal more strongly than the Notch combination labeling its row. P-values were computed via permutation testing with 10k bootstrap replicates (Methods).

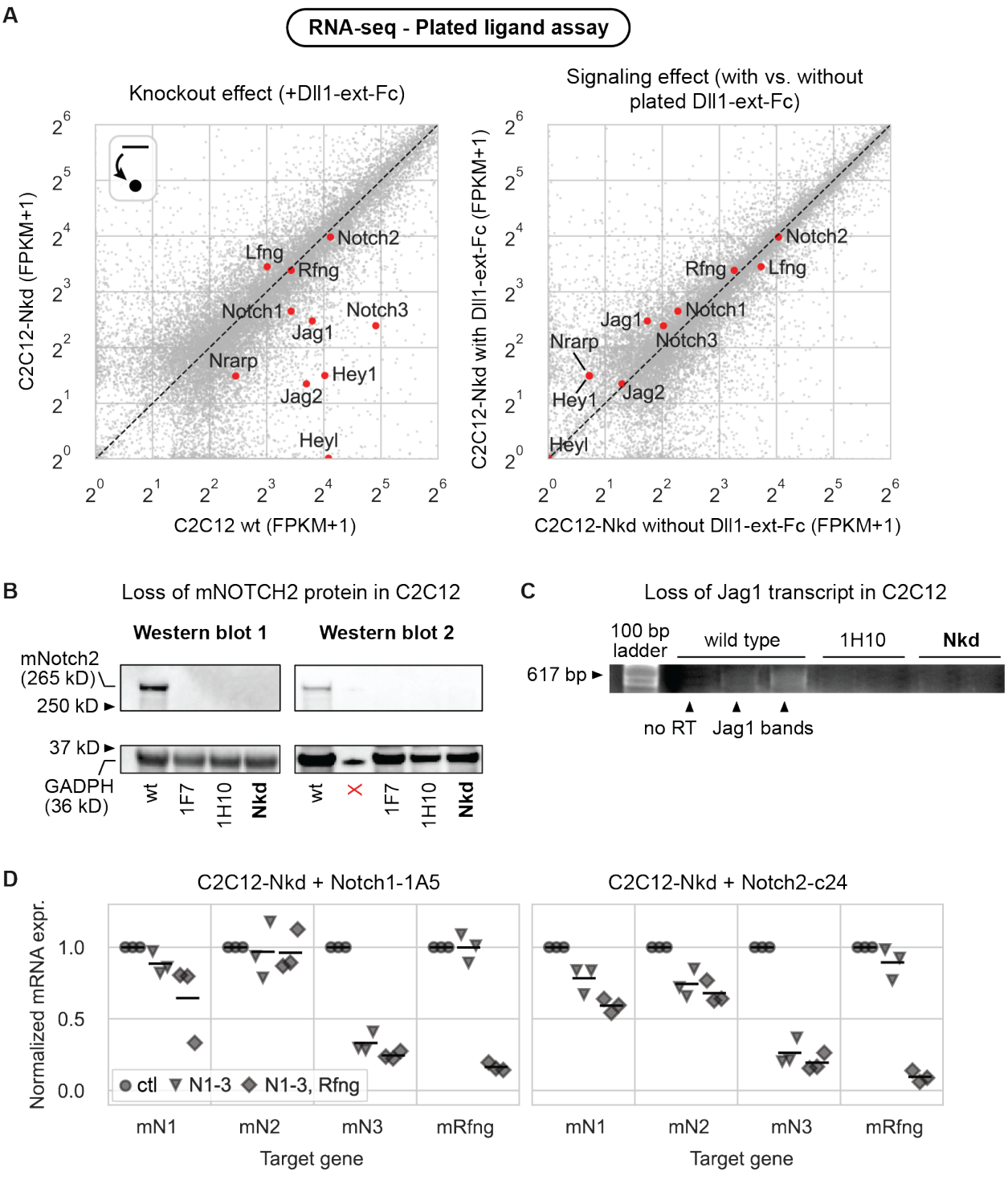

Figure 2—figure supplement 3: CRISPR/Cas9 editing of C2C12 cells yields Notch-depleted clone C2C12-Nkd *(caption on following page)*

(**A**) Scatterplots of RNA transcript levels in RNA-seq data from wild-type C2C12 cells or the C2C12-Nkd ("Notch-depleted") clone generated in this study using CRISPR/Cas9 targeting deletion of mNotch2 and

mJag1. Each data point is a transcript with a Fragments Per Kilobase of transcript per Million mapped reads (FPKM) value of ≥ 3 in at least one of the experimental conditions. The left scatterplot shows differences in expression between wild-type cells and the C2C12-Nkd clone with Notch signaling stimulated by plated recombinant Dll1-ext-Fc in a plated ligand assay. The right scatterplot shows the effect of Notch ligand stimulation of C2C12-Nkd by comparing expression in the + vs. - plated Dll1 conditions. Transcripts corresponding to key Notch pathway and target genes are colored red and labeled. The dot-and-arrow icon indicates the assay type used to generate the data (plated ligand assay), as described in Figure 1B.

(**B**) Western blot showing loss of endogenous Notch2 expression in CRISPR-treated C2C12 cell lines. Whole cell protein from C2C12 wild-type (wt) vs. CRISPR-treated C2C12 cell lines (1F7, 1H10, and Nkd) was separated by SDS-PAGE (4-12%) and analyzed by immunoblotting with antibodies against mouse Notch2 (265 kD) and mouse GAPDH (36 kD). (Left) First Western blot performed. (Right) Repeat Western blot to confirm the original results. The red X marks a well with no sample (signal is spillover from leftmost well).

(**C**) RT-PCR analysis showing loss of endogenous Jag1 in CRISPR-treated C2C12 cell lines. Agarose gel electrophoresis of Jag1 RT-PCR product from C2C12 wt cells and 2 CRISPR treated cells lines, 1H10 and Nkd, showing loss of Jag1 transcript (617 bp band). No RT = "no reverse transcription" control.

(**D**) qRT-PCR of mouse Notch transcripts (labeled on x-axis) in Notch1 and Notch2 receiver cells derived from the C2C12-Nkd clone. Cells were treated with either a negative control siRNA; siRNAs against mNotch1, mNotch2, and mNotch3 ("N1-3"); or siRNAs against all three endogenous mouse receptors and mRfng ("N1-3, Rfng"). Y-axis values are $2^{-\Delta Cq}$ values (computed using mSdhA as a housekeeping gene) normalized to the expression level in the negative control knockdown for each gene within each bioreplicate. Black bars are the mean of three biological replicates.

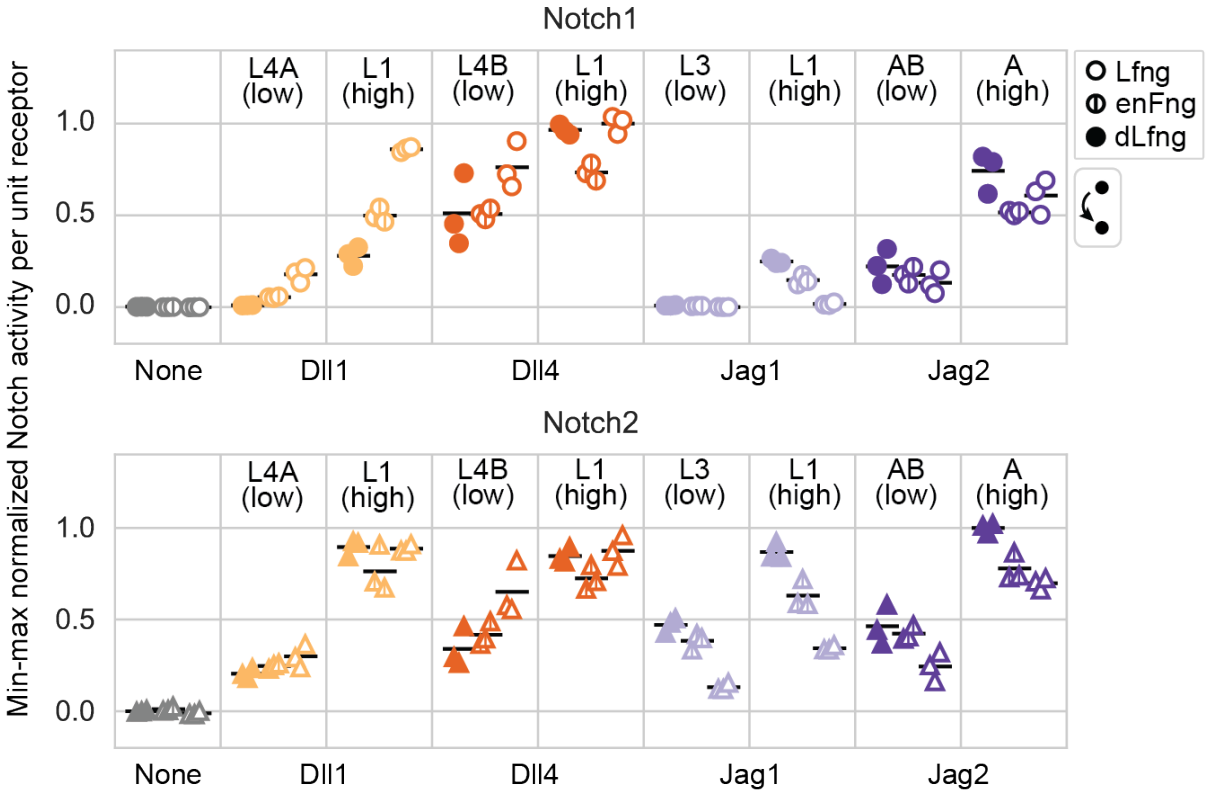

Figure 2—figure supplement 4: Endogenous Lfng activity dominates over Rfng in CHO-K1 cells

A comparison of signaling strengths for all receptor-ligand pairs in a trans-activation assay with CHO-K1 Notch1 and Notch2 receivers expressing endogenous CHO-K1 Fringes ("enFng"), dLfng, or Lfng (see Methods). Fringe treatment is denoted by marker fill. Sender populations used in each coculture are labeled at the top of each plot; see their ligand expression distributions in Figure 2A. Y-axis values are reporter activity (mCitrine, A.U.) divided by cotranslational receptor expression (mTurq2, A.U.), background subtracted and normalized to the strongest signaling activity measured for each receiver clone in this experiment. Black bars are the mean of three biological replicates. The dot-and-arrow icon indicates the assay type used to generate the data (trans-activation assay), as described in Figure 1B.

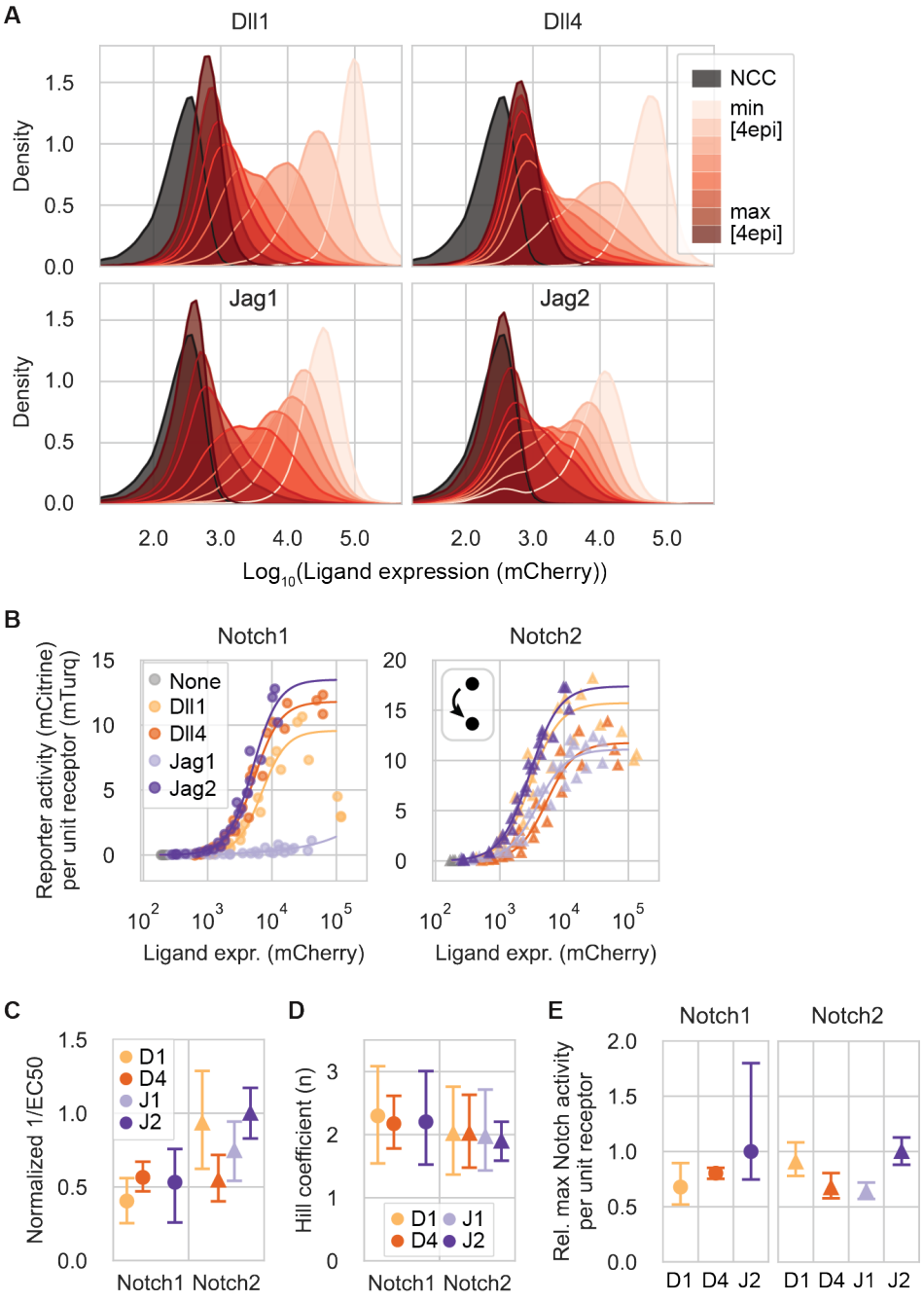

Figure 2—figure supplement 5: Relative activation strengths with endogenous CHO-K1 Fringes reflect an intermediate state between dLfng and Lfng

(**A**) Distributions of cotranslational ligand expression (mCherry, A.U.) in Tet-OFF senders expressing each of the four activating Notch ligands, tuned to different levels via titration of 4-epi-Tc concentration. Each histogram contains data from three biological replicates. Black histograms are wild-type CHO-K1 (NCC = no color control).

(**B**) Results of trans-activation assays for CHO-K1 Notch1 (left) and Notch2 (right) receivers cultured with excess sender cells expressing ligands at a range of levels corresponding to the cotranslational mCherry

expression distributions in (A). X-axis values are the mean of the mCherry fluorescence in senders used for each coculture sample data point. Y-axis values are the mean of the distribution in mCitrine (reporter activity, A.U.) divided by mTurq2 (cotranslational receptor expression, A.U.). Each set of receptor-ligand data points was fit to a Hill function via least-squares. The highest Dll1 expression level was excluded from the fits due to its nonmonotonicity. The dot-and-arrow icon indicates the assay type used to generate the data (trans-activation assay), as described in Figure 1B.

(**C-E**) Mean fit parameters computed from least-squares fits of 10k bootstrap replicates of the curves in (B) to Hill functions (Methods): inverse EC50 (C), Hill coefficient *n* (D), and max signaling activity (E). Error bars are 95% confidence intervals. Trans-activation strengths (1/EC50) for each receptor-ligand pair were normalized to the 1/EC50 value computed from the Jag2-Notch2 curve (C), and max signaling activities were normalized to the value from Jag2 coculture for each receptor separately (E). Colors indicate ligand identity; in the legend, ‘D’ stands for ‘Dll’ and ‘J’ stands for ‘Jag.’

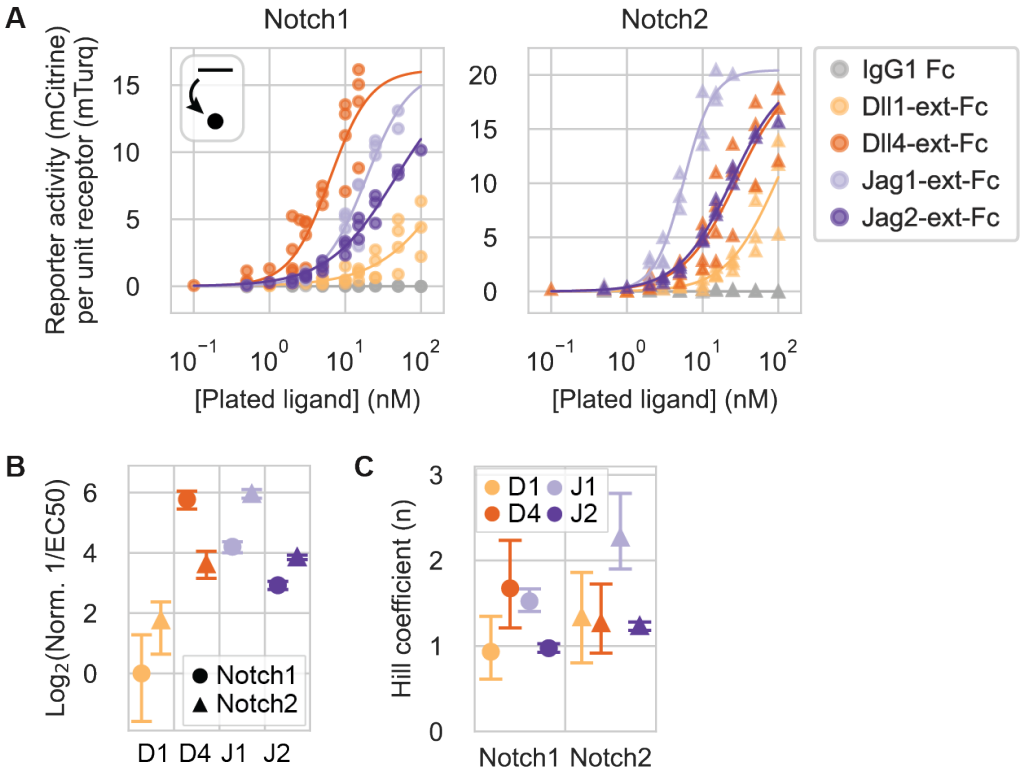

Figure 2—figure supplement 6: Receptor preferences in the plated ligand assay agree with coculture assays

(**A**) Results of plated ligand assays for CHO-K1 Notch1 (left) and Notch2 (right) receivers cultured on plated recombinant ligand-ext-Fc proteins at the concentrations indicated on the x-axis. Y-axis values are the mean of the distribution in mCitrine (reporter activity, A.U.) divided by mTurq2 (cotranslational receptor expression, A.U.). Each set of receptor-ligand data points was fit to a Hill function via least-squares, with the max activity set to the average signaling activity for the three biological replicates corresponding to the highest signaling activity for each receiver. The dot-and-arrow icon indicates the assay type used to generate the data (plated ligand assay), as described in Figure 1B.

(**B-C**) Mean fit parameters computed from least-squares fits of 10k bootstrap replicates of the curves in (A) to Hill functions (Methods): Log2 of the inverse EC50 (B) and Hill coefficient *n* (C). Error bars are 95% confidence intervals. Trans-activation strengths (computed as Log2 of the 1/EC50) for each receptor-ligand pair are relative to that of the Notch1-Dll1 curve (B). Colors indicate ligand identity; in the legend, 'D' stands for 'Dll' and 'J' stands for 'Jag.'

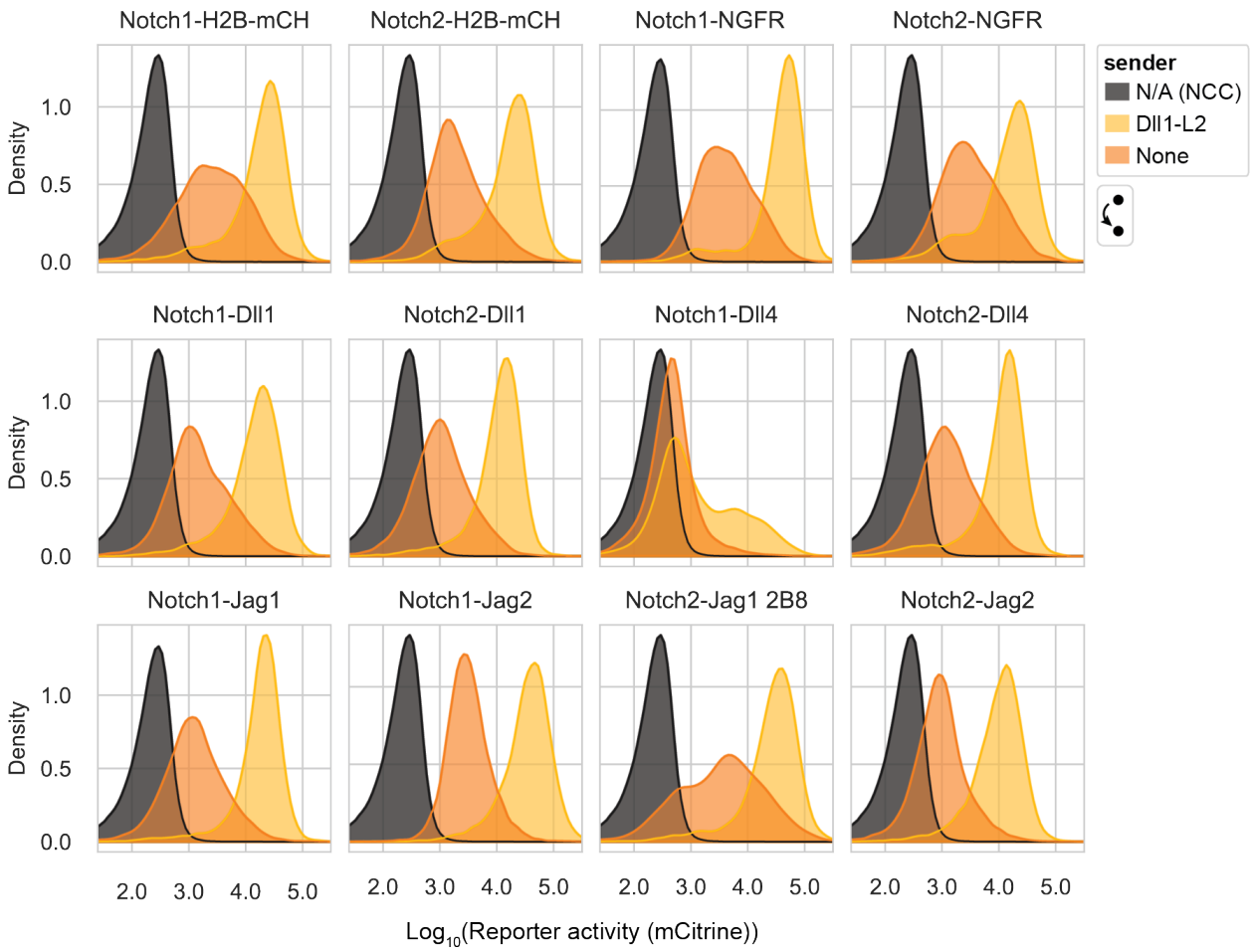

Figure 4—figure supplement 1: CHO-K1 receiver clones' reporter dynamic ranges with minimum cis-ligand expression

Histograms of reporter activity (mCitrine, A.U.) in the indicated receiver cells with minimum cis-ligand (max [4-epi-Tc]), cultured with wild-type CHO-K1 cells (sender = "None") or high-Dll1 CHO-K1 senders. Each receiver histogram includes data from three biological replicates. The dot-and-arrow icon below the legend indicates the assay type (trans-activation) used to generate the data, as described in Figure 1B.

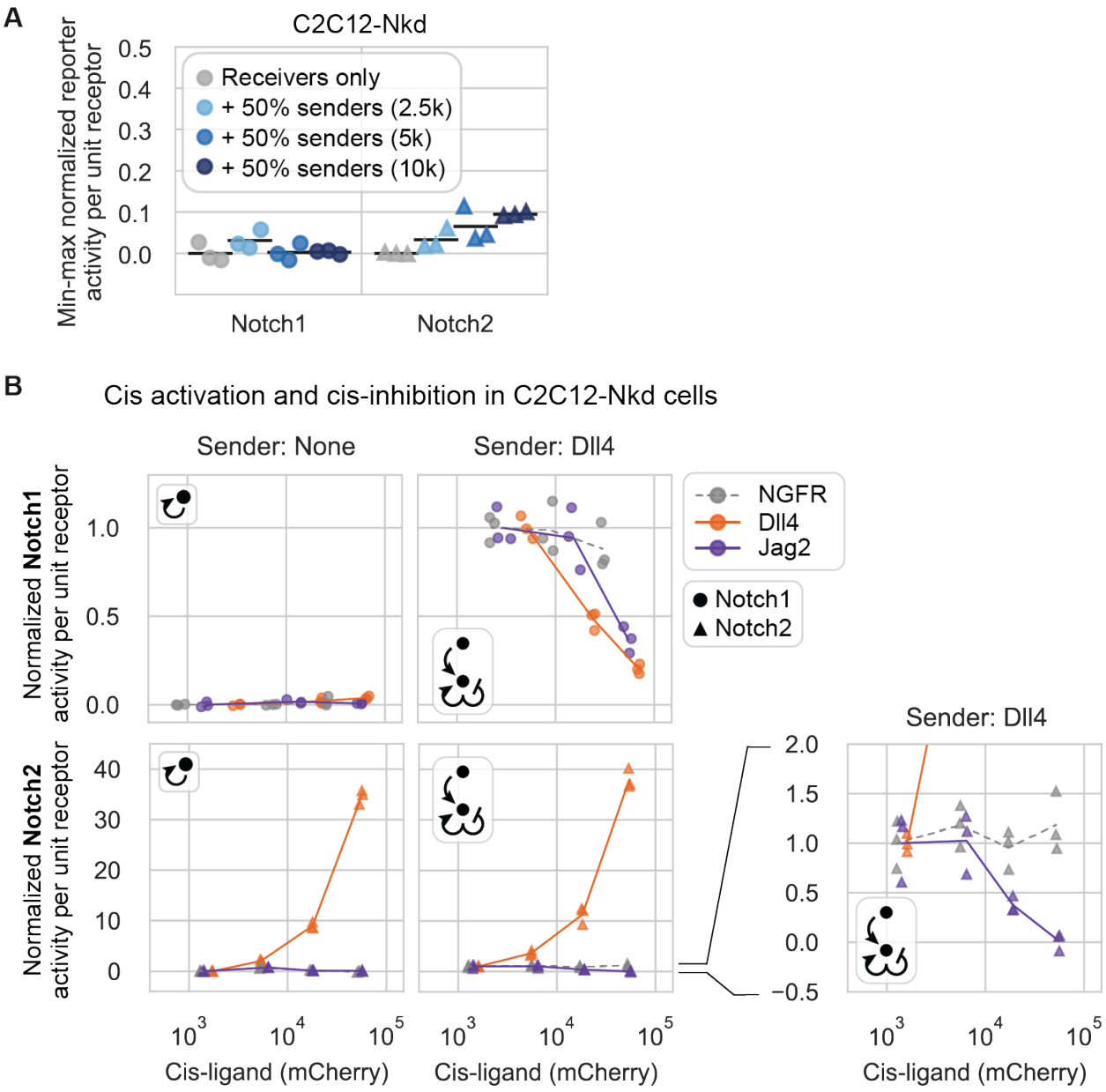

Figure 4—figure supplement 2: The Notch-depleted C2C12-Nkd cell line enables independent validation of key results from CHO-K1 experiments

(**A**) The cell density used in the C2C12 cis-activation assay prevents intercellular signaling. After siRNA treatment to knock down residual endogenous Notch components (Methods), C2C12-Nkd Notch1 or Notch2 receiver cells were plated sparsely at 2.5k, 5k, or 10k in a 12-well plate (not a 24-well plate as used for CHO-K1) along with an equal number of high-Dll1 C2C12-Nkd sender cells, and surrounded by 150k C2C12-Nkd parental cells expressing no ectopic ligands or receptors. Notch signaling activity is defined as the reporter activity (mCitrine, A.U.) divided by the cotranslational receptor expression (mTurq2, A.U.) in each cell, averaged across all cells in a given sample. Y-axis values are signaling activity minus signaling

in absence of ligand and divided by “max” signal (signaling level when receivers are cultured with a confluent excess of high-Dll1 senders). The 2.5k receiver + 2.5k sender condition (lightest blue), matching the 5k total receivers used in the cis-activation assay (in a 12-well plate for C2C12-Nkd cells), activated receivers to less than 5% of the maximal signal. Black bars are the mean of three biological repeats.

(**B**) Results of cis-activation (left column) and cis-modulation (right column) assays for C2C12-Nkd Notch1 (top row) and Notch2 (bottom row) receivers coexpressing a Notch ligand or control protein. For Notch2, individual receivers were sorted into discrete bins of mCherry (A.U.) and the mCitrine/mTurq2 (signaling activity) and mCherry (cotranslational cis-ligand expression) fluorescence values were averaged across all cells in that bin. For Notch1, single-cell data were not sorted into mCherry bins, but averaged by 4-epi-Tc concentration, because mCherry binning yielded anomalous reporter activities with the NGFR control, possibly due to selection of abnormally large cells when sorting into the high mCherry bins. For both receptors, signaling activity on the y-axis was normalized as in (A), except that the “max” signal (y = 1) is the signaling activity of receivers with no cis-ligand (max [4-epi-Tc]) cultured with the high-Dll4 senders (Dll4-2H10) used in the cis-modulation assay. Lines are interpolated through the mean of three biological replicates (individual data points) in each mCherry bin. The right-most bottom plot is a zoomed-in view of the data for Notch2 receivers cultured with high-Dll4 senders, showing Jag2 cis-inhibition of Notch2 activation by Dll4 senders. Dot-and-arrow icons indicate the assay type used to generate the data, as described in Figure 1B.

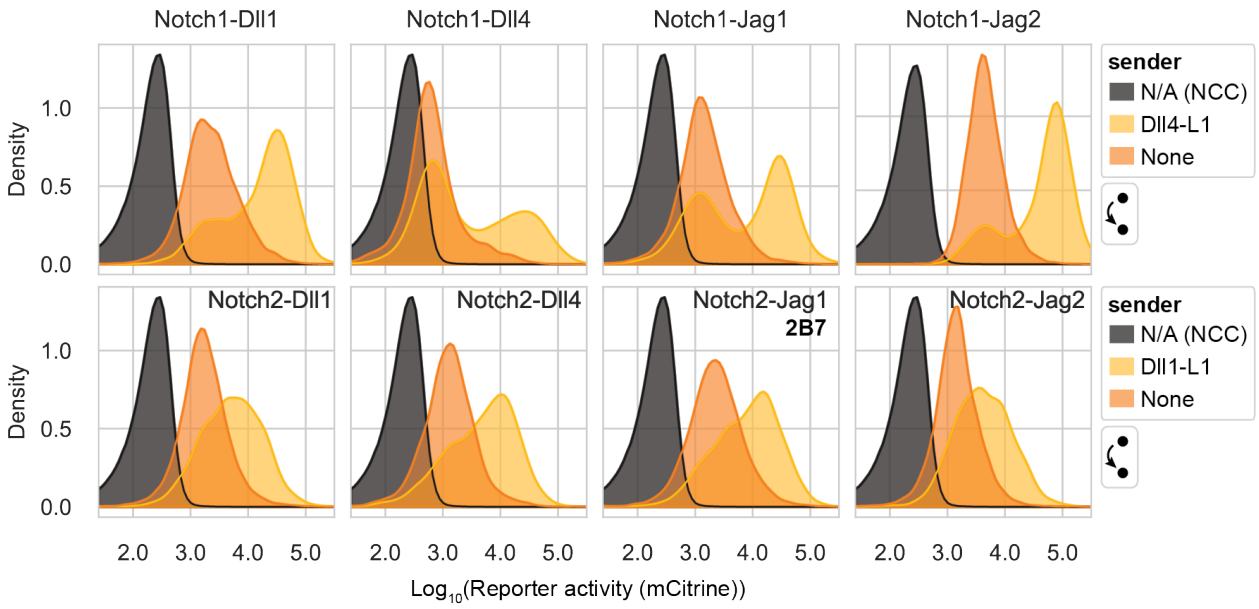

Figure 5—figure supplement 1: CHO-K1 receiver clones' reporter dynamic ranges with minimum cis-ligand expression

Histograms of reporter activity (mCitrine, A.U.) in the indicated receiver cells with minimum cis-ligand (max [4-epi-Tc]), transfected with Lfng and cultured with wild-type CHO-K1 cells (sender = "None"; n = 7 biological replicates per receiver) or high-Dll1 or -Dll4 senders (for Notch2 and Notch1, respectively; n = 4 biological replicates per receiver). Each receiver histogram includes pooled data from the described number of biological replicates. The averages of these distributions with CHO-K1 or Delta senders were used for background subtraction or y-axis normalization, respectively, in Figure 5A,B. Black histograms are CHO-K1 wild-type cells only (NCC = no color control). The dot-and-arrow icon indicates the assay type used to generate the data (trans-activation assay), as described in Figure 1B.

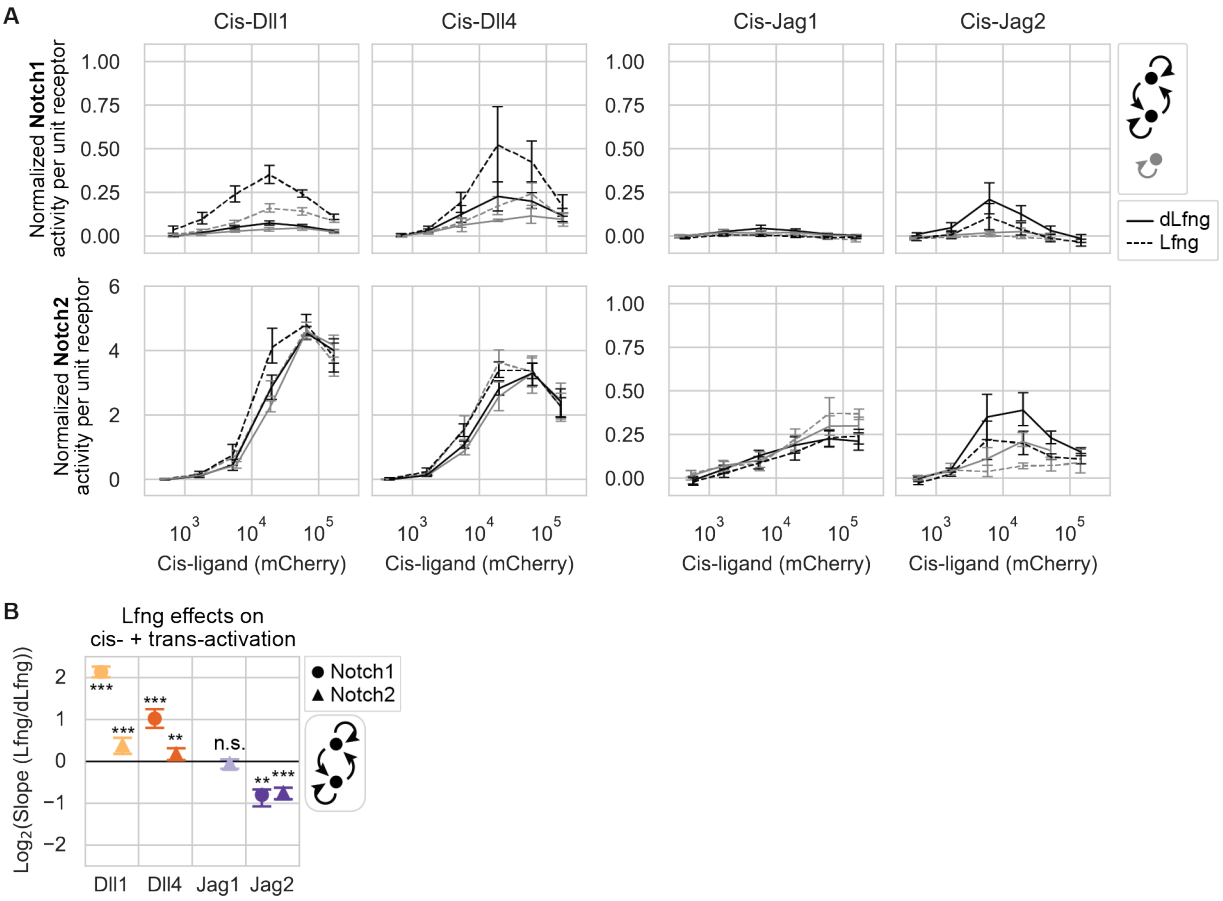

Figure 5—figure supplement 2: Allowing intercellular contacts increases Notch signaling relative to cis-activation alone

(**A**) Results of cis-activation (grey) and cis- + trans-activation (black) assays for CHO-K1 Notch1 (top row) and Notch2 (bottom row) receivers coexpressing a Notch ligand at different levels corresponding to a range of 4-epi-Tc concentrations; see distributions in Figure 5—figure supplement 3. (Cis-activation data are the same as in Figure 5A.) During ligand preinduction, endogenous Fringes were knocked down and cells were transfected with dLfng or Lfng (solid and dashed lines, respectively). X- and y-axis values are cis-ligand expression (mCherry, A.U.) and normalized Notch signaling activity (reporter activity (mCitrine, A.U.) divided by the cotranslational receptor expression (mTurq2, A.U.) in each cell), respectively, averaged across all cells in a given mCherry bin. Signaling activity on the y-axis was background subtracted and normalized to the "max" signaling in receivers with no cis-ligand (max [4-epi-Tc]) cultured with high-Dll1 or -Dll4 senders (for Notch2 and Notch1, respectively); see also Supplementary Table 4. Lines are interpolated through the mean of seven biological replicates in each mCherry bin. Error bars are 95% confidence intervals on the mean value across 10k bootstrap replicates.

(**B**) Lfng effects on cis- + trans-activation. Values are the log2 fold difference in the slope of the best-fit line to signaling activity (from A) in a scatterplot of Lfng vs dLfng; error bars are 95% confidence intervals on best-fit slopes computed for each of 10k bootstrap replicates. Asterisks denote the p-value from a Wilcoxon signed-rank test (one-sided) evaluating whether the slope of Lfng vs. dLfng is significantly greater than or less than 1 (* p-val < 0.05; ** p-val < 0.01; *** p-val < 0.001). Receptor-ligand combinations that did not activate above background levels were excluded.

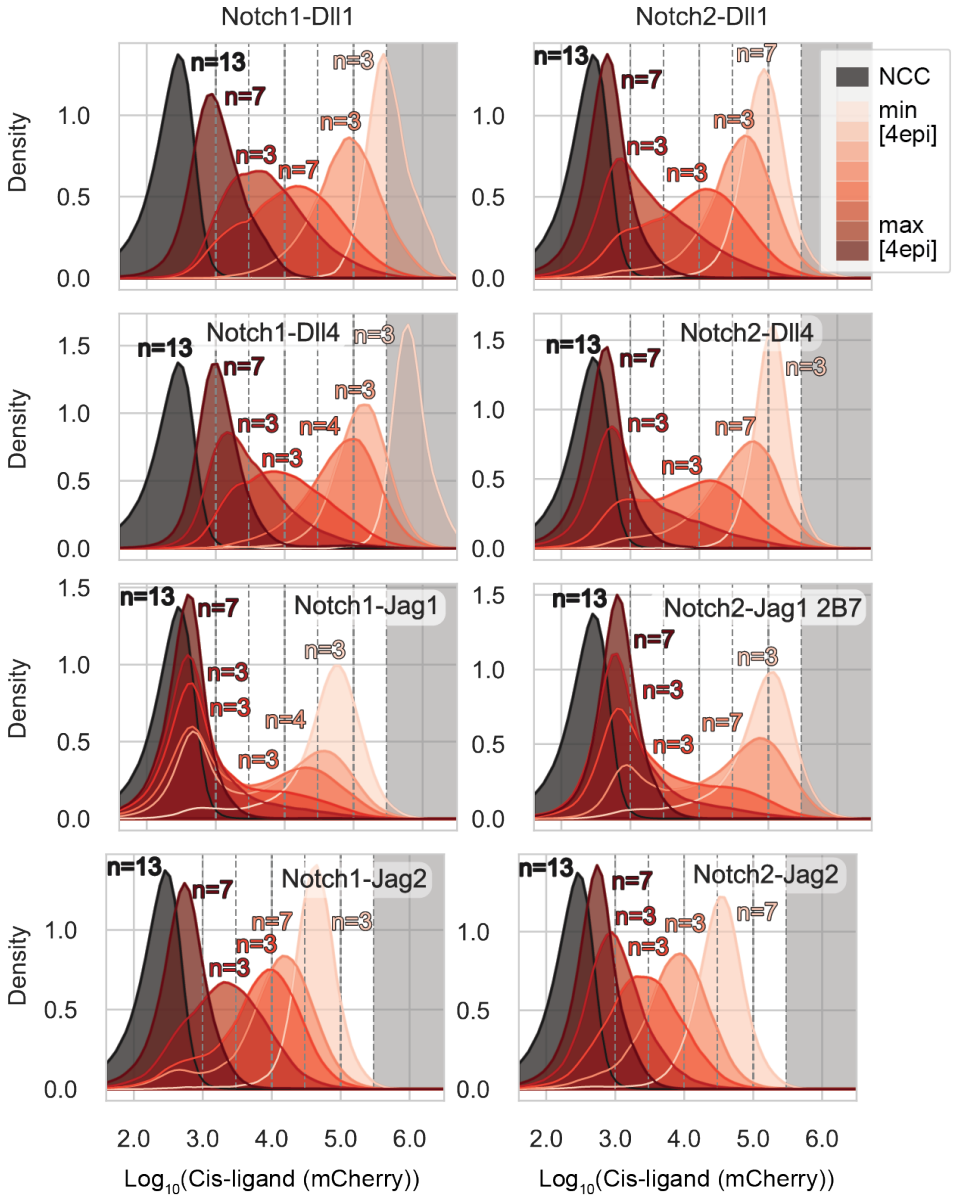

Figure 5—figure supplement 3: CHO-K1 receiver clones' cis-ligand expression distributions for the cis-activation assay and cis- + trans-activation assay

Distributions of cotranslational cis-ligand expression (mCherry, A.U.) corresponding to receivers used to generate data in Figure 5A. Each histogram corresponds to a specific 4-epi-Tc concentration ranging from 0-500 ng/mL, and includes data from the indicated number of biological replicates (*n*). Black histograms are CHO-K1 wild-type cells (NCC = no color control). To generate Figure 5A curves, receiver cells were binned into discrete intervals of mCherry expression indicated by the vertical dashed lines. Datapoints in the grey-shaded region were discarded.

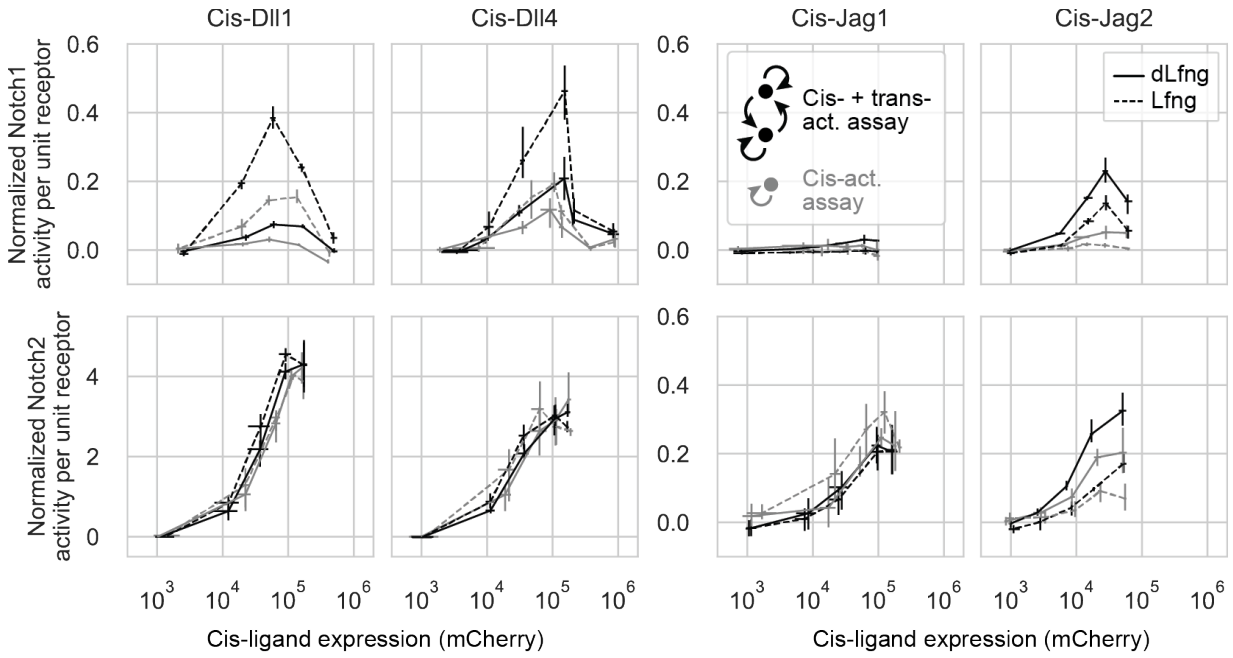

Figure 5—figure supplement 4: Flow cytometry data analysis pipeline without mCherry binning yields similar results

Results of cis-activation (grey) and cis- + trans-activation (black) assays for CHO-K1 Notch1 (top row) and Notch2 (bottom row) receivers coexpressing a Notch ligand at different levels corresponding to a range of 4-epi-Tc concentrations. These are the same data shown in Figure 5A, but instead of averaging fluorescence distributions across cells binned into different mCherry levels, distributions were averaged across all cells corresponding to the same 4-epi-Tc concentration. Line type denotes expression of dLfng (solid) or Lfng (dashed). Signaling activity on the y-axis was background subtracted and normalized to the "max" signaling in receivers with no cis-ligand (max [4-epi-Tc]) cultured with high-Dll1 or -Dll4 senders (for Notch2 and Notch1, respectively). Lines are interpolated through the mean of seven biological replicates in each mCherry bin. Error bars are 95% confidence intervals on the mean value across 10k bootstrap replicates. The dot-and-arrow icons indicate the assay type used to generate the data (grey = "Cis-activation assay"; black = "Cis- + trans-activation assay"), as described in Figure 1B.

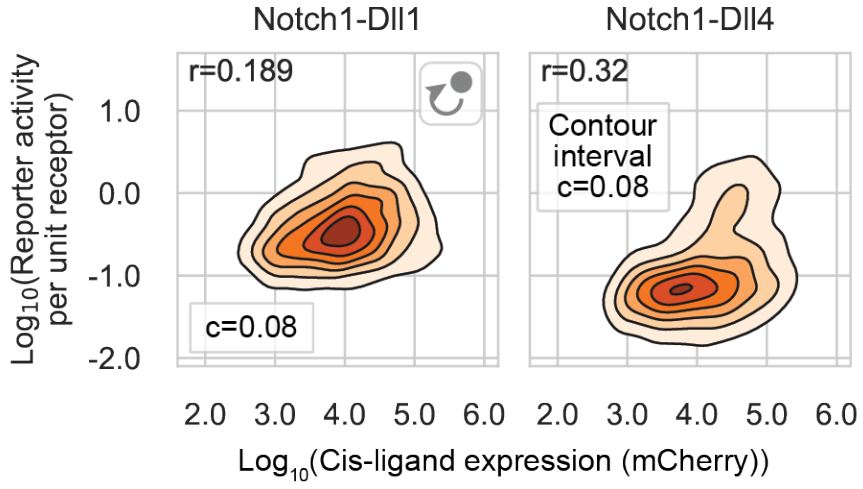

Figure 5—figure supplement 5: Delta-Notch1 cis-activation shows positive dependence on cis-ligand expression at the single-cell level

2D fluorescence distributions of signaling activity (mCitrine/mTurq2) versus cis-ligand expression (mCherry, A.U.) in single-cell fluorescence distributions from the cis-activation assays described in Figure 5A, with Lfng expression. Each plot shows data from a single biological replicate at a single 4-epi-Tc concentration with both a broad ligand expression distribution and substantial cis-activation signal (50 and 120 ng/mL for Dll1-Notch1 and Dll4-Notch1, respectively). Cell density in each discrete contour interval is indicated by color, and each contour level has a cell density range of n*c to (n+1)*c, where n is the contour level. The density interval below c is not shown. The Pearson's correlation coefficient *r* is shown in the top left of each plot, and all corresponding p-values were << 0.001. The dot-and-arrow icon indicates the assay type used to generate the data (cis-activation assay), as described in Figure 1B.

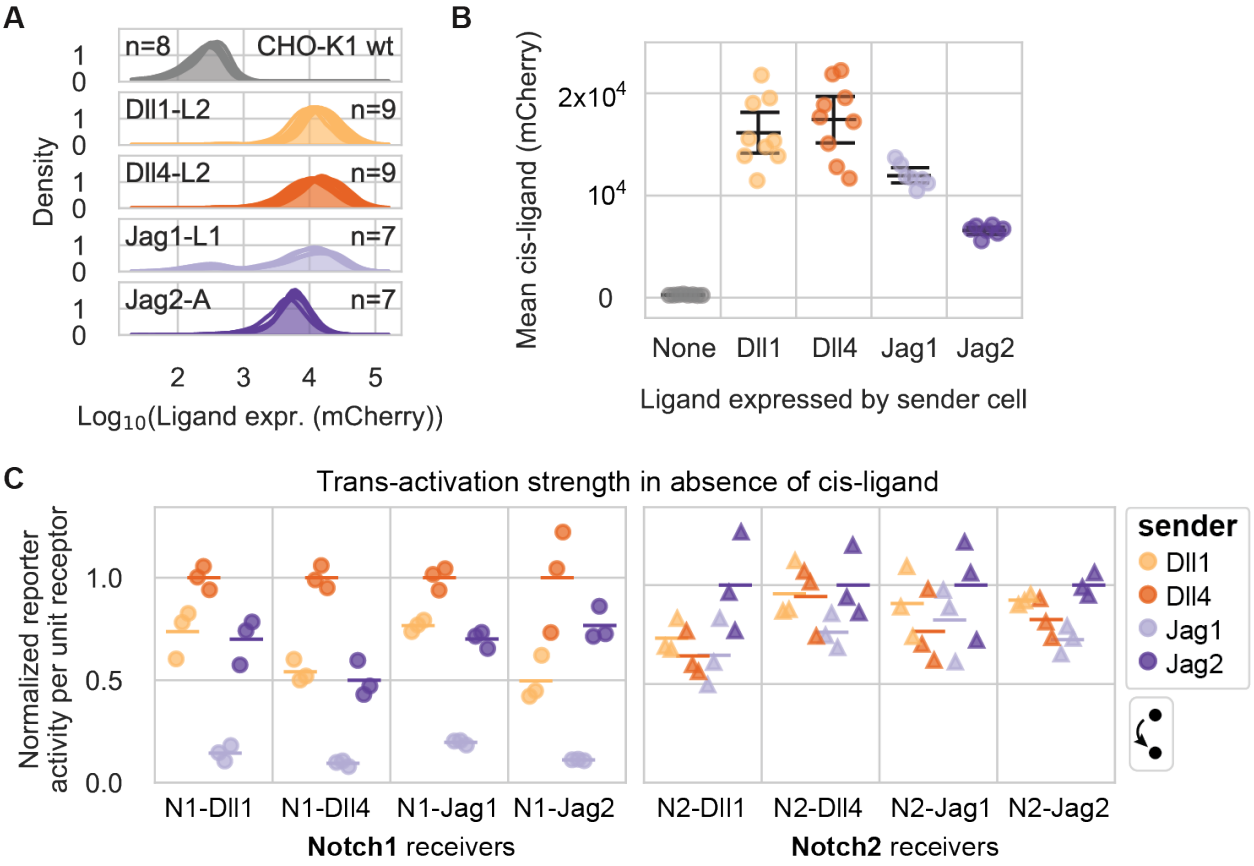

Figure 6—figure supplement 1: Ligands' trans-activation strengths show greater diversity for Notch1 than Notch2

(**A**) Histograms of single-cell distributions of cotranslational ligand expression (mCherry, A.U.) in the CHO-K1 sender populations used for this figure. Each histogram is a biological replicate, with a total of *n* replicates per plot.

(**B**) Mean cotranslational ligand expression (mCherry, A.U.) computed from histograms in (A). Error bars (top and bottom) are 95% confidence intervals on the mean value of the data points across 10k bootstrap replicates, and the middle bar is the mean of all the points.

(**C**) Normalized signaling activity in receiver cells (indicated on x-axis) cultured with excess senders (A, B) in a trans-activation assay (as indicated by the dot-and-arrow icon) in the absence of cis-ligand expression (at maximum 4-epi-Tc). Colors indicate the ligand expressed by the sender cells cultured in excess with a minority of receivers for a given datapoint. Normalized signaling activity is defined as reporter activity (mCitrine, A.U.) divided by cotranslational receptor expression (mTurq2, A.U.), normalized to the strongest signaling activity measured for each receiver clone in this experiment (average of three bioreplicates).

2.8 Supplementary Tables

Supplementary Table 1: Key resources

Reagent type (species) or resource	Designation	Source or reference	Identifiers	Additional information
Gene (Homo sapiens)	Notch1	NCBI ID: 4851		
Gene (Homo sapiens)	Notch2	NCBI ID: 4853		
Gene (Homo sapiens)	Dll1	NCBI ID: 28514		
Gene (Homo sapiens)	Dll4	NCBI ID: 54567		
Gene (Homo sapiens)	Jag1	NCBI ID: 182		
Gene (Homo sapiens)	Jag2	NCBI ID: 3714		

Gene (Homo sapiens)	NGFR	NCBI ID: 4804		
Gene (Mus musculus)	Rfng	NCBI ID: 19719		
Gene (Mus musculus)	Lfng	NCBI ID: 16848		
Cell line (Cricetulus griseus)	CHO-K1	ATCC	Cat# CCL-61	Figure 4; Figure 2; Figure 5; Figure 1—figure supplement 1; Figure 4—figure supplement 1; Figure 6; Figure 2—figure supplement 1; Figure 2—figure supplement 5; Figure 5—figure supplement 1; Figure 5—figure supplement 1; Figure 5—figure supplement 3; Figure 5—figure supplement 4.
Cell line (Cricetulus griseus)	CHO Dll1 sender L1	Derived from CHO-K1	CHO-K1+CBh-Dll1-2xFLAG- T2A-H2B-mCherry - Sort level 1 (high mCherry)	Figure 4; Figure 2; Figure 5; Figure 6; Figure 2—figure supplement 1; Figure 5—figure supplement 1; Figure 5—figure supplement 1; Figure 5—figure supplement 3.

Cell line (Cricetulus griseus)	CHO Dll1 sender L4B	Derived from CHO-K1	CHO-K1+CBh-Dll1-2xFLAG- T2A-H2B-mCherry - Sort level 4B (low mCherry)	Figure 2; Figure 2—figure supplement 1; Figure 2—figure supplement 2.
Cell line (Cricetulus griseus)	CHO Dll1 sender L4A	Derived from CHO-K1	CHO-K1+CBh-Dll1-2xFLAG- T2A-H2B-mCherry - Sort level 4A (low mCherry)	Figure 2; Figure 2—figure supplement 1; Figure 2—figure supplement 2.
Cell line (Cricetulus griseus)	CHO Dll1 sender L4	Derived from CHO-K1	CHO-K1+CBh-Dll1-2xFLAG- T2A-H2B-mCherry - Sort level 4 (medium mCherry)	Figure 2; Figure 2—figure supplement 1; Figure 2—figure supplement 2.
Cell line (Cricetulus griseus)	CHO Dll1 sender L2	Derived from CHO-K1	CHO-K1+CBh-Dll1-2xFLAG- T2A-H2B-mCherry - Sort level L2 (high mCherry)	Figure 4; Figure 2; Figure 4—figure supplement 1; Figure 6; Figure 2—figure supplement 2.
Cell line (Cricetulus griseus)	CHO Dll4 sender L1	Derived from CHO-K1	CHO-K1+CBh-Dll4-2xFLAG- T2A-H2B-mCherry - Sort level 1 (high mCherry)	Figure 4; Figure 2; Figure 5; Figure 6; Figure 2—figure supplement 1; Figure 5—figure supplement 1; Figure 5—figure supplement 1; Figure 5—figure supplement 3.
Cell line (Cricetulus griseus)	CHO Dll4 sender L4B	Derived from CHO-K1	CHO-K1+CBh-Dll4-2xFLAG- T2A-H2B-mCherry - Sort level 4B (medium mCherry)	Figure 2; Figure 2—figure supplement 1; Figure 2—figure supplement 2.

Cell line (Cricetulus griseus)	CHO Dll4 sender L4	Derived from CHO-K1	CHO-K1+CBh-Dll4-2xFLAG- T2A-H2B-mCherry - Sort level 4 (medium mCherry)	Figure 2; Figure 2—figure supplement 1; Figure 2—figure supplement 2.
Cell line (Cricetulus griseus)	CHO Dll4 sender L2	Derived from CHO-K1	CHO-K1+CBh-Dll4-2xFLAG- T2A-H2B-mCherry - Sort level 2 (medium mCherry)	Figure 6.
Cell line (Cricetulus griseus)	CHO Jag1 sender L1	Derived from CHO-K1	CHO-K1+CBh-Jag1-2xFLAG-T2A-H2B-mCherry - Sort level 1 (high mCherry)	Figure 2; Figure 6; Figure 2—figure supplement 1; Figure 2—figure supplement 2.
Cell line (Cricetulus griseus)	CHO Jag1 sender L2	Derived from CHO-K1	CHO-K1+CBh-Jag1-2xFLAG-T2A-H2B-mCherry - Sort level 2 (medium mCherry)	Figure 2; Figure 2—figure supplement 2.
Cell line (Cricetulus griseus)	CHO Jag1 sender L3	Derived from CHO-K1	CHO-K1+CBh-Jag1-2xFLAG-T2A-H2B-mCherry - Sort level 3 (low mCherry)	Figure 2; Figure 2—figure supplement 1; Figure 2—figure supplement 2.
Cell line (Cricetulus griseus)	CHO Jag2 sender A	Derived from CHO-K1	CHO-K1+CBh-Jag2-2xFLAG-T2A-H2B-mCherry - Sort level A (high mCherry)	Figure 2; Figure 6; Figure 2—figure supplement 1; Figure 2—figure supplement 2.
Cell line (Cricetulus griseus)	CHO Jag2 sender AB	Derived from CHO-K1	CHO-K1+CBh-Jag2-2xFLAG-T2A-H2B-mCherry - Sort level AB (medium mCherry)	Figure 2; Figure 2—figure supplement 1; Figure 2—figure supplement 2.
Cell line (Cricetulus griseus)	CHO Jag2 sender AA	Derived from CHO-K1	CHO-K1+CBh-Jag2-2xFLAG-T2A-H2B-mCherry - Sort level AA (high mCherry)	Figure 2; Figure 2—figure supplement 2.

Cell line (Cricetulus griseus)	CHO Jag2 sender B	Derived from CHO-K1	CHO-K1+CBh-Jag2-2xFLAG-T2A-H2B-mCherry - Sort level B (low mCherry)	Figure 2; Figure 2—figure supplement 2.
Cell line (Cricetulus griseus)	CHO TetOff Dll1 sender G1	Derived from CHO-K1	CHO-K1+Tet-Off Dll1-2xFLAG-T2A-H2B-mCherry G1	Figure 1—figure supplement 2; Figure 2—figure supplement 5.
Cell line (Cricetulus griseus)	CHO TetOff Dll4 sender Nkd	Derived from CHO-K1	CHO-K1+Tet-Off Dll4-2xFLAG-T2A-H2B-mCherry Nkd	Figure 1—figure supplement 2; Figure 2—figure supplement 5.
Cell line (Cricetulus griseus)	CHO TetOff Jag1 sender 1G3	Derived from CHO-K1	CHO-K1+Tet-Off Jag1-2xFLAG-T2A-H2B-mCherry 1G3	Figure 2—figure supplement 5.
Cell line (Cricetulus griseus)	CHO TetOff Jag2 sender 1H6	Derived from CHO-K1	CHO-K1+Tet-Off Jag2-2xFLAG-T2A-H2B-mCherry 1H6	Figure 2—figure supplement 5.
Cell line (Cricetulus griseus)	CHO reporter	Derived from CHO-K1	CHO-K1+ 2xHS4-UAS-H2B-Citrine-2xHS4 H1	Figure 3.
Cell line (Cricetulus griseus)	CHO N1 receiver 2D1	Derived from CHO reporter	CHO-K1+ 2xHS4-UAS-H2B-Citrine-2xHS4+ PB-PGK-N1ECD-Gal4esn- T2A-H2B-mTurq2 2-D1	Figure 4; Figure 2; Figure 3; Figure 2—figure supplement 1; Figure 2—figure supplement 5; Figure 2—figure supplement 6.
Cell line (Cricetulus griseus)	CHO N2 receiver 2A4	Derived from CHO reporter	CHO-K1+ 2xHS4-UAS-H2B-Citrine-2xHS4+ PB-PGK-N2ECD-Gal4esn-T2A-H2B-mTurq2 2-A4	Figure 4; Figure 2; Figure 3; Figure 2—figure supplement 1; Figure 2—figure supplement 5; Figure 2—figure supplement 6.

Cell line (Cricetulus griseus	CHO N1-TetOff Dll1 2G5	Derived from CHO reporter	CHO-K1+ 2xHS4-UAS-H2B-Citrine- 2xHS4+Tet-Off Dll1-2xFLAG-T2A-H2B- mCherry+ PB-CAG-N1ECD-Gal4esn- T2A-H2B-mTurq2 2-G5	Figure 4; Figure 2; Figure 5; Figure 1—figure supplement 1; Figure 4—figure supplement 1; Figure 6; Figure 2—figure supplement 2; Figure 5—figure supplement 1; Figure 5—figure supplement 1; Figure 5—figure supplement 3; Figure 5—figure supplement 4; Figure 5—figure supplement 5.
Cell line (Cricetulus griseus	CHO N1-TetOff Dll4 1G11	Derived from CHO reporter	CHO-K1+ 2xHS4-UAS-H2B-Citrine- 2xHS4+Tet-Off Dll4-2xFLAG-T2A-H2B- mCherry+ PB-CAG-N1ECD-Gal4esn- T2A-H2B-mTurq2 1-G11	Figure 4; Figure 2; Figure 5; Figure 1—figure supplement 1; Figure 4—figure supplement 1; Figure 6; Figure 2—figure supplement 2; Figure 5—figure supplement 1; Figure 5—figure supplement 1; Figure 5—figure supplement 3; Figure 5—figure supplement 4; Figure 5—figure supplement 5.

Cell line (Cricetulus griseus	CHO N1-TetOff Jag1 1E2	Derived from CHO reporter	CHO-K1+ 2xHS4-UAS-H2B-Citrine- 2xHS4+Tet-Off Jag1-2xFLAG-T2A-H2B- mCherry+ PB-CAG-N1ECD-Gal4esn-T2A-H2B-mTurq2 1-E2	Figure 4; Figure 2; Figure 5; Figure 1—figure supplement 1; Figure 4—figure supplement 1; Figure 6; Figure 2—figure supplement 2; Figure 5—figure supplement 1; Figure 5—figure supplement 1; Figure 5—figure supplement 3; Figure 5—figure supplement 4.
Cell line (Cricetulus griseus	CHO N1-TetOff Jag2 2E10	Derived from CHO reporter	CHO-K1+ 2xHS4-UAS-H2B-Citrine- 2xHS4+Tet-Off Jag2-2xFLAG-T2A-H2B- mCherry+ PB-CAG-N1ECD-Gal4esn- T2A-H2B-mTurq2 2-E10	Figure 4; Figure 2; Figure 5; Figure 1—figure supplement 1; Figure 4—figure supplement 1; Figure 6; Figure 2—figure supplement 2; Figure 5—figure supplement 1; Figure 5—figure supplement 1; Figure 5—figure supplement 3; Figure 5—figure supplement 4.

Cell line (Cricetulus griseus	CHO N2-TetOff Dll1 1C4	Derived from CHO reporter	CHO-K1+ 2xHS4-UAS-H2B-Citrine- 2xHS4+Tet-Off Dll1-2xFLAG-T2A-H2B- mCherry+ PB-CAG-N2ECD-Gal4esn- T2A-H2B-mTurq2 1-C4	Figure 4; Figure 5; Figure 1—figure supplement 1; Figure 4—figure supplement 1; Figure 6; Figure 5—figure supplement 1; Figure 5—figure supplement 1; Figure 5—figure supplement 3; Figure 5—figure supplement 4.
Cell line (Cricetulus griseus	CHO N2-TetOff Dll4 1B8	Derived from CHO reporter	CHO-K1+ 2xHS4-UAS-H2B-Citrine- 2xHS4+Tet-Off Dll4-2xFLAG-T2A-H2B- mCherry+ PB-CAG-N2ECD-Gal4esn- T2A-H2B-mTurq2 1-B8	Figure 4; Figure 5; Figure 1—figure supplement 1; Figure 4—figure supplement 1; Figure 6; Figure 5—figure supplement 1; Figure 5—figure supplement 1; Figure 5—figure supplement 3; Figure 5—figure supplement 4.
Cell line (Cricetulus griseus	CHO N2-TetOff Jag1 2B8	Derived from CHO reporter	CHO-K1+ 2xHS4-UAS-H2B-Citrine- 2xHS4+Tet-Off Jag1-2xFLAG-T2A-H2B- mCherry+ PB-CAG-N2ECD-Gal4esn- T2A-H2B-mTurq2 2-B8	Figure 4; Figure 1—figure supplement 1; Figure 4—figure supplement 1; Figure 6.

Cell line (Cricetulus griseus	CHO N2-TetOff Jag1 2B7	Derived from CHO reporter	CHO-K1+ 2xHS4-UAS-H2B-Citrine- 2xHS4+Tet-Off Jag1-2xFLAG-T2A-H2B- mCherry+ PB-CAG-N2ECD-Gal4esn- T2A-H2B-mTurq2 2-B7	Figure 2; Figure 5; Figure 2—figure supplement 2; Figure 5—figure supplement 1; Figure 5—figure supplement 1; Figure 5—figure supplement 3; Figure 5—figure supplement 4.
Cell line (Cricetulus griseus	CHO N2-TetOff Jag2 1A1	Derived from CHO reporter	CHO-K1+ 2xHS4-UAS-H2B-Citrine- 2xHS4+Tet-Off Jag2-2xFLAG-T2A-H2B- mCherry+ PB-CAG-N2ECD-Gal4esn- T2A-H2B-mTurq2 1-A1	Figure 4; Figure 2; Figure 5; Figure 1—figure supplement 1; Figure 4—figure supplement 1; Figure 6; Figure 2—figure supplement 2; Figure 5—figure supplement 1; Figure 5—figure supplement 1; Figure 5—figure supplement 3; Figure 5—figure supplement 4.
Cell line (Cricetulus griseus	CHO N1-TetOff H2B-mCherry	Derived from CHO reporter	CHO-K1+ 2xHS4-UAS-H2B-Citrine- 2xHS4+Tet-Off H2B-mCherry+ PB-CAG-N1ECD-Gal4esn-T2A-H2B-mTurq2 F4	Figure 4; Figure 1—figure supplement 1; Figure 4—figure supplement 1.
Cell line (Cricetulus griseus	CHO N2-TetOff H2B-mCherry	Derived from CHO reporter	CHO-K1+ 2xHS4-UAS-H2B-Citrine- 2xHS4+Tet-Off H2B-mCherry+ PB-CAG-N2ECD-Gal4esn-T2A-H2B-mTurq2 G2	Figure 4; Figure 1—figure supplement 1; Figure 4—figure supplement 1.

Cell line (Cricetulus griseus	CHO N1-TetOff NGFR-T2A- H2B-mCherry	Derived from CHO reporter	CHO-K1+ 2xHS4-UAS-H2B-Citrine- 2xHS4+Tet-Off NGFR-T2A-H2B-mCherry+ PB-CAG-N1ECD-Gal4esn- T2A-H2B-mTurq2 2-A6	Figure 4; Figure 1—figure supplement 1; Figure 4—figure supplement 1.
Cell line (Cricetulus griseus	CHO N2-TetOff NGFR-T2A- H2B-mCherry	Derived from CHO reporter	CHO-K1+ 2xHS4-UAS-H2B-Citrine- 2xHS4+Tet-Off NGFR-T2A-H2B-mCherry+ PB-CAG-N2ECD-Gal4esn- T2A-H2B-mTurq2 1-H4	Figure 4; Figure 1—figure supplement 1; Figure 4—figure supplement 1.
Cell line (*Mus musculus*)	C2C12	Cat# CRL-1772	ATCC	Figure 2—figure supplement 3.
Cell line (*Mus musculus*)	C2C12-Nkd	Derived from C2C12	C2C12 with N2 and Jag1 CRISPR knockout	Figure 2; Figure 2—figure supplement 3; Figure 4—figure supplement 2.
Cell line (*Mus musculus*)	C2C12 reporter	Derived from C2C12-Nkd	C2C12-Nkd + 2xHS4-UAS-H2B-Citrine- 2xHS4 B5	
Cell line (*Mus musculus*)	C2C12 N1 receiver	Derived from C2C12 reporter	C2C12-Nkd + 2xHS4-UAS-H2B-Citrine - 2xHS4+ PB-CAG-N1ECD-Gal4esn- T2A-H2B-mTurq2 1-A5	Figure 2; Figure 4—figure supplement 2; Figure 2—figure supplement 2.
Cell line (*Mus musculus*)	C2C12 N2 receiver	Derived from C2C12 reporter	C2C12-Nkd + 2xHS4-UAS-H2B-Citrine - 2xHS4+ PB-CAG-N2ECD-Gal4esn- T2A-H2B-mTurq2 c24	Figure 2; Figure 4—figure supplement 2; Figure 2—figure supplement 2.
Cell line (*Mus musculus*)	C2C12 Dll1 sender c19	Derived from C2C12-Nkd	C2C12-Nkd+ CBh-Dll1-2xFLAG-T2A- H2B-mCherry c19 (high mCherry)	Figure 2; Figure 4—figure supplement 2.

Cell line (*Mus musculus*)	C2C12 Dll4 sender 2-H10	Derived from C2C12-Nkd	C2C12-Nkd+ CBh-Dll4-2xFLAG-T2A- H2B-mCherry 2-H10 (high mCherry)	Figure 4—figure supplement 2.
Cell line (*Mus musculus*)	C2C12 Jag1 sender c11	Derived from C2C12-Nkd	C2C12-Nkd+ CBh-Jag1-2xFLAG-T2A- H2B-mCherry c11 (high mCherry)	Figure 2.
Cell line (*Mus musculus*)	C2C12 N1-TetOff NGFR	Derived from C2C12 reporter	C2C12+ 2xHS4-UAS-H2B-Citrine- 2xHS4+Tet-Off NGFR-2xFLAG-T2A-H2B- mCherry+ PB-CAG-N1ECD-Gal4esn- T2A-H2B-mTurq2 1-H6	Figure 4—figure supplement 2.
Cell line (*Mus musculus*)	C2C12 N2-TetOff NGFR	Derived from C2C12 reporter	C2C12+ 2xHS4-UAS-H2B-Citrine- 2xHS4+Tet-Off NGFR-2xFLAG-T2A-H2B- mCherry+ PB-CAG-N2ECD-Gal4esn- T2A-H2B-mTurq2 1-E9	Figure 4—figure supplement 2.
Cell line (*Mus musculus*)	C2C12 N1-TetOff Dll4	Derived from C2C12 reporter	C2C12+ 2xHS4-UAS-H2B-Citrine- 2xHS4+Tet-Off Dll4-2xFLAG-T2A-H2B- mCherry+ PB-CAG-N1ECD-Gal4esn- T2A-H2B-mTurq2 2-D1	Figure 4—figure supplement 2.
Cell line (*Mus musculus*)	C2C12 N2-TetOff Dll4	Derived from C2C12 reporter	C2C12+ 2xHS4-UAS-H2B-Citrine- 2xHS4+Tet-Off Dll4-2xFLAG-T2A-H2B- mCherry+ PB-CAG-N2ECD-Gal4esn- T2A-H2B-mTurq2 3-B12	Figure 4—figure supplement 2.

Cell line (*Mus musculus*)	C2C12 N1-TetOff Jag2	Derived from C2C12 reporter	C2C12+ 2xHS4-UAS-H2B-Citrine- 2xHS4+Tet-Off Jag2-2xFLAG-T2A-H2B- mCherry+ PB-CAG-N1ECD-Gal4esn- T2A-H2B-mTurq2 1-E7	Figure 4—figure supplement 2.
Cell line (*Mus musculus*)	C2C12 N2-TetOff Jag2	Derived from C2C12 reporter	C2C12+ 2xHS4-UAS-H2B-Citrine- 2xHS4+Tet-Off Jag2-2xFLAG-T2A-H2B- mCherry+ PB-CAG-N2ECD-Gal4esn- T2A-H2B-mTurq2 1-B12	Figure 4—figure supplement 2.
Transfected construct (recombinant DNA)	Super PiggyBac Transposase Expression Vector	System Biosciences	Cat# PB210PA-1	Transposase used in all transfections with PiggyBac vectors
Transfected construct (recombinant DNA)	pEV-2xHS4-UAS-H2B-Citrine-2xHS4	This paper		Reporter for hNotch-Gal4 receptors in cell lines
Transfected construct (recombinant DNA)	PB-CMV-MCS-EF1-Puro (PiggyBac vector)	System Biosciences	Cat# PB510B-1	Base vector used to derive all PiggyBac constructs
Transfected construct (recombinant DNA)	PB-PGK-N1ECD-Gal4esn-T2A-H2B-mTurq2	This paper		Notch1ECD- Gal4 synthetic receptor in CHO receiver cells
Transfected construct (recombinant DNA)	PB-PGK-N2ECD-Gal4esn-T2A-H2B-mTurq2	This paper		Notch2ECD- Gal4 synthetic receptor in CHO receiver cells

Transfected construct (recombinant DNA)	PB-CAG-N1ECD-Gal4esn-T2A-H2B-mTurq2	This paper		Notch1ECD- Gal4 synthetic receptor in Tet-Off cell lines and C2C12 receiver cells
Transfected construct (recombinant DNA)	PB-CAG-N2ECD-Gal4esn-T2A-H2B-mTurq2	This paper		Notch2ECD- Gal4 synthetic receptor in Tet-Off cell lines and C2C12 receiver cells
Transfected construct (recombinant DNA)	pCW57.1-MAT2A	Addgene	Cat# 100521	Base vector used to derive all Tet-Off constructs and constitutive ligand constructs
Transfected construct (recombinant DNA)	pCW57.1 Tet-Off Dll1-2xFLAG-T2A-H2B-mCherry	This paper		Repressible Dll1 ligand in cell lines. Used to make lentivirus.
Transfected construct (recombinant DNA)	pCW57.1 Tet-Off Dll4-2xFLAG-T2A-H2B-mCherry	This paper		Repressible Dll4 ligand in cell lines. Used to make lentivirus.
Transfected construct (recombinant DNA)	pCW57.1 Tet-Off Jag1-2xFLAG-T2A-H2B-mCherry	This paper		Repressible Jag1 ligand in cell lines. Used to make lentivirus.
Transfected construct (recombinant DNA)	pCW57.1 Tet-Off Jag2-2xFLAG-T2A-H2B-mCherry	This paper		Repressible Jag2 ligand in cell lines. Used to make lentivirus.

Transfected construct (recombinant DNA)	pCW57.1 Tet-Off H2B-mCherry	This paper		Repressible H2B-mCherry used as negative control in cell lines. Used to make lentivirus.
Transfected construct (recombinant DNA)	pCW57.1 Tet-Off NGFR-T2A-H2B-mCherry	This paper		Repressible NGFR ligand used as negative control in cell lines. Used to make lentivirus.
Transfected construct (recombinant DNA)	pCW57.1 CBh-Dll1-2xFLAG-T2A-H2B-mCherry	This paper		Constitutively expressed Dll1 ligand in cell lines. Used to make lentivirus.
Transfected construct (recombinant DNA)	pCW57.1 CBh-Dll4-2xFLAG-T2A-H2B-mCherry	This paper		Constitutively expressed Dll4 ligand in cell lines. Used to make lentivirus.
Transfected construct (recombinant DNA)	pCW57.1 CBh-Jag1-2xFLAG-T2A-H2B-mCherry	This paper		Constitutively expressed Jag1 ligand in cell lines. Used to make lentivirus.
Transfected construct (recombinant DNA)	pCW57.1 CBh-Jag2-2xFLAG-T2A-H2B-mCherry	This paper		Constitutively expressed Jag2 ligand in cell lines. Used to make lentivirus.
Transfected construct (recombinant DNA)	PB-CMV-Lfng-BGHpA-EF1-Puro	Lebon et al. 2014		Constitutively expressed Lfng in cell lines treated with siRNA

Transfected construct (recombinant DNA)	PB-CMV-Lfng(D289E)-BGHpA-EF1-Puro	This paper		Constitutively expressed dLfng (D289E) in cell lines treated with siRNA. Sequence from (Luther, Schindelin, and Haltiwanger 2009)
Transfected construct (recombinant DNA)	PB-CMV7-IFP2.0-BGHpA-SV40-Neo			Vector co-transfected with fringe plasmids
Transfected construct (recombinant DNA)	pX330 (CRISPR-Cas9 plasmid system)	Nandagopal et al. 2019 Cong et al. 2013		Plasmid used to insert RNA guide sequences for use in CRISPR knockdown in C2C12 cells
Antibody	PE anti-human Notch1 antibody MHN1-519	BioLegend	Cat# 352105	Used in soluble ligand binding assay
Antibody	PE anti-human Notch2 antibody MHN2-25	BioLegend	Cat# 348303	Used in soluble ligand binding assay
Antibody	goat anti-human IgG Alexa Fluor 594	Thermo Fisher Scientific	Cat# A-11014	Secondary antibody used to precluster ligands in soluble ligand binding assay
Antibody	Rabbit anti-Notch2	Cell Signaling Technology	Cat# 5732	For Westerns

Antibody	Rabbit anti-GAPDH	Cell Signaling Technology	Cat# 2118	For Westerns
Antibody	Amersham ECL Rabbit IgG, HRP-linked whole Ab	Cytiva	Cat# NA934	For Westerns
siRNA	AllStars Neg. Control siRNA	Qiagen	Cat# 1027281	
siRNA	Custom Select siRNA hamster Rfng	Thermo Fisher Scientific	Cat# 4399666 ID# s553138	Sequence (5' to 3') GCUGUAAAAUG UCAGUGGAtt
siRNA	Custom Select siRNA hamster Lfng	Thermo Fisher Scientific	Cat# 4399665 ID# 555728	Sequence (5' to 3') AGCUAAUGAUG AUAAGGGAtt
siRNA	Silencer Select siRNA mouse N1	Thermo Fisher Scientific	Cat # 4390771 ID# s70699	
siRNA	Custom Stealth siRNA mouse N2	Thermo Fisher Scientific	Cat # 10620312 ID# 359602D12	Sequence (5' to 3') GACCUUCACCC AUCCUGCAAGU UCA
siRNA	Stealth siRNA mouse N3	Thermo Fisher Scientific	Cat# 1320001 ID# mss207111	
siRNA	Silencer Select siRNA mouse Rfng	Thermo Fisher Scientific	Cat# 4390771 ID# s72908	
Reagent	Zeocin	Thermo Fisher Scientific	Cat# R25001	

Reagent	Geneticin	Thermo Fisher Scientific	Cat# 10131-035	
Reagent	Blasticidin	Invivogen	Cat# ANT-BL-1	
Reagent	HBSS, no calcium, no magnesium, no phenol red	Thermo Fisher Scientific	Cat# 14175-095	
Reagent	Alpha MEM Earle's Salts	FUJIFILM Irvine Scientifc	Cat #9144-500	
Reagent	DMEM high glucose, no glutamine	Thermo Fisher Scientific	Cat# 11960069	
Reagent	Fetal Bovine Serum (FBS)	Avantor VWR	Cat# 97068-085 Lot# 323K20	
Reagent	100X Sodium Pyruvate	Thermo Fisher Scientific	Cat# 11360-070	
Reagent	100X Penicillin, Streptomysin, Glutamine	Thermo Fisher Scientific	Cat# 10378-016	
Reagent	Lipfectamine RNAiMAX Transfection Reagent	Thermo Fisher Scientific	Cat# 13778075	
Reagent	Trypsin (0.25%), phenol red	Thermo Fisher Scientific	Cat# 15050065	No EDTA

Reagent	Polyplus-transfection jetOPTIMUS DNA Transfection Reagent	Genesee Scientific	Cat# 55-250	
Protein	Bovine Serum Albumin	Sigma Aldrich	Cat# A4503	
Protein	Cas9 Protein	PNA Bio Inc	Cat# CP01	
Peptide, recombinant protein	Recombinant Human Dll1ext-Fc fusion proteins	(Sprinzak et al. 2010)	Kindly provided by Irwin Bernstein, MD at Fred Hutchinson Cancer Reserch Center	
Peptide, recombinant protein	Recombinant Human IgG1 Fc Protein	Bio-Techne/R&D Systems	Cat# 110-HG-100	
Peptide, recombinant protein	Recombinant Human DLL1 Fc Chimera Protein	Bio-Techne/R&D Systems	Cat# 10184-DL-050	
Peptide, recombinant protein	Recombinant Human DLL4 Fc Chimera Protein	Bio-Techne/R&D Systems	Cat# 10185-D4-050	
Peptide, recombinant protein	Recombinant Human Jag1 Fc Chimera Protein	Bio-Techne/R&D Systems	Cat# 1277-JG-050	
Peptide, recombinant protein	Recombinant Human Jag2 Fc Chimera Protein	Bio-Techne/R&D Systems	Cat# 1726-JG-050	

Chemical compound, drug	DAPT	Sigma Aldrich	Cat# D5942	
Chemical compound, drug	4-epi tetracycline hydrochloride	Sigma Aldrich	Cat# 37918	
Commercial assay or kit	Megashortscript T7 transcription kit	Thermo Fisher Scientific	Cat# AM1354	
Commercial assay or kit	RNeasy Mini Kit	Qiagen	Cat# 74104	
Commercial assay or kit	QIAshredder	Qiagen	Cat# 79656	
Commercial assay or kit	iScript cDNA Sythesis Kit	Bio-Rad	Cat# 1708890	
Commercial assay or kit	MycoStrip	InvivoGen	Cat# rep-mys-100	
CHO-K1 RNA-seq database	https://anksi.shinyapps.io/biosciences/		(Singh, Kildegaard, and Andersen 2018)	
Software, algorithm	RNA-sequencing read trimming and quality control	TrimGalore	https://www.bioinformatics.babraham.ac.uk/projects/trim_galore/	
Software, algorithm	RNA-sequencing read alignment	HISAT2 v2.1.0 (via Galaxy)	http://daehwankimlab.github.io/hisat2/; https://usegalaxy.org/	

Software, algorithm	RNA-sequencing transcript abundance calculation	StringTie v1.3.4 (via Galaxy)	http://ccb.jhu.edu/software/stringtie/; https://usegalaxy.org/	
Software, algorithm	Import of flow cytometry .fcs files for data processing in Python3	FlowCal	https://flowcal.readthedocs.io/en/latest/; (Castillo-Hair et al. 2016)	

Supplementary Table 2: Notch gene expression in wild-type CHO-K1 cells

Gene	Expression (CPM)
Notch1	6.66
Notch2	192.67
Notch3	8.14
Notch4	0.43
Jag1	9.58
Lfng	3.97
Rfng	71.51

These expression values in counts per million reads mapped (CPM) were obtained from the CHO gene expression visualization application (CGEVA) database of CHO RNA-seq data, including from wild-type CHO-K1 cells, located at https://anksi.shinyapps.io/biosciences/ (Singh, Kildegaard, and Andersen 2018). Dll1, Dll4, Jag2, and Mfng were not available in the database. See also Methods.

Supplementary Table 3: 4-epi-Tc concentrations used to induce ligand expression

Where Tet-Off inducible sender or receiver cells were used but don't appear in the table below, 4-epi-Tc was used at a concentration of 500-800 ng/mL to fully suppress expression.

Experiment	Cell type	Cell line (clone)	[4-epi-Tc] (ng/mL)
Figure 4B; Figure 1-S1; Figure 4-S1	CHO-K1	Notch1-H2B-mCh (F4)	0, 5, 10, 15, 20, 50, 500
Figure 4B; Figure 1-S1; Figure 4-S1	CHO-K1	Notch1-NGFR (2A6)	0, 5, 10, 15, 20, 50, 500
Figure 4B; Figure 1-S1; Figure 4-S1	CHO-K1	Notch1-Dll1 (2G5)	0, 20, 50, 100, 200, 300, 500
Figure 4B; Figure 1-S1; Figure 4-S1	CHO-K1	Notch1-Dll4 (1G11)	0, 40, 70, 100, 150, 200, 500
Figure 4B; Figure 1-S1; Figure 4-S1	CHO-K1	Notch1-Jag1 (1E2)	0, 20, 50, 100, 200, 300, 500
Figure 4B; Figure 1-S1; Figure 4-S1	CHO-K1	Notch1-Jag2 (2E10)	0, 40, 70, 100, 150, 200, 800
Figure 4B; Figure 1-S1; Figure 4-S1	CHO-K1	Notch2-H2B-mCh (G2)	0, 5, 10, 15, 20, 50, 500
Figure 4B; Figure 1-S1; Figure 4-S1	CHO-K1	Notch2-NGFR (1H4)	0, 5, 10, 15, 20, 50, 500
Figure 4B; Figure 1-S1; Figure 4-S1	CHO-K1	Notch2-Dll1 (1C4)	0, 10, 20, 40, 100, 200, 500
Figure 4B; Figure 1-S1; Figure 4-S1	CHO-K1	Notch2-Dll4 (1B8)	0, 10, 20, 40, 100, 200, 500
Figure 4B; Figure 1-S1; Figure 4-S1	CHO-K1	Notch2-Jag1 (2B8)	0, 10, 20, 40, 100, 200, 500
Figure 4B; Figure 1-S1; Figure 4-S1	CHO-K1	Notch2-Jag2 (1A1)	0, 10, 20, 40, 100, 200, 500

Figure 4D	CHO-K1	Notch2-Dll1 (1C4)	10, 500
Figure 4D	CHO-K1	Notch2-Dll4 (1B8)	10, 500
Figure 6	CHO-K1	Notch1-Dll1 (2G5)	0, 20, 50, 100, 200, 300, 500
Figure 6	CHO-K1	Notch1-Dll4 (1G11)	0, 40, 70, 100, 150, 200, 500
Figure 6	CHO-K1	Notch1-Jag1 (1E2)	0, 20, 50, 100, 200, 300, 500
Figure 6	CHO-K1	Notch1-Jag2 (2E10)	0, 40, 70, 100, 150, 200, 800
Figure 6	CHO-K1	Notch2-Dll1 (1C4)	0, 10, 20, 40, 100, 200, 500
Figure 6	CHO-K1	Notch2-Dll4 (1B8)	0, 10, 20, 40, 100, 200, 500
Figure 6	CHO-K1	Notch2-Jag1 (2B8)	0, 10, 20, 40, 100, 200, 500
Figure 6	CHO-K1	Notch2-Jag2 (1A1)	0, 10, 20, 40, 100, 200, 500
Figure 4-S2B	C2C12-Nkd	Notch1-NGFR (1H6)	0, 10, 500
Figure 4-S2B	C2C12-Nkd	Notch1-Dll4 (2D1)	0, 15, 500
Figure 4-S2B	C2C12-Nkd	Notch1-Jag2 (1E7)	0, 25, 500
Figure 4-S2B	C2C12-Nkd	Notch2-NGFR (1E9)	0, 10, 500
Figure 4-S2B	C2C12-Nkd	Notch2-Dll4 (3B12)	0, 15, 500
Figure 4-S2B	C2C12-Nkd	Notch2-Jag2 (1B12)	0, 25, 500
Figure 1-S2A	CHO-K1	Tet-OFF Dll1 (G1)	10

Figure 1-S2A	CHO-K1	Tet-OFF Dll4 (2D6)	5
Figure 1-S2B	CHO-K1	Tet-OFF Dll1 (G1)	0
Figure 1-S2B	CHO-K1	Tet-OFF Dll4 (2D6)	0
Figure 2-S5	CHO-K1	Tet-OFF Dll1 (G1)	0, 20, 40, 60, 80, 100, 150, 500
Figure 2-S5	CHO-K1	Tet-OFF Dll4 (2D6)	0, 10, 20, 30, 40, 60, 80, 500
Figure 2-S5	CHO-K1	Tet-OFF Jag1 (1G3)	0, 5, 10, 15, 20, 35, 50, 500
Figure 2-S5	CHO-K1	Tet-OFF Jag2 (1H6)	0, 5, 10, 15, 20, 25, 40, 500
Figure 5A; Figure 5-S1; Figure 5-S2; Figure 5-S4	CHO-K1	Notch1-Dll1 (2G5)	0, 25, 50, 80, 500
Figure 5A; Figure 5-S1; Figure 5-S2; Figure 5-S4	CHO-K1	Notch1-Dll4 (1G11)	0, 30, 50, 80, 100, 120, 500
Figure 5A; Figure 5-S1; Figure 5-S2; Figure 5-S4	CHO-K1	Notch1-Jag1 (1E2)	0, 5, 10, 15, 20, 30, 500
Figure 5A; Figure 5-S1; Figure 5-S2; Figure 5-S4	CHO-K1	Notch1-Jag2 (2E10)	0, 10, 20, 25, 40, 50, 800
Figure 5A; Figure 5-S1; Figure 5-S2; Figure 5-S4	CHO-K1	Notch2-Dll1 (1C4)	0, 5, 15, 30, 500
Figure 5A; Figure 5-S1; Figure 5-S2; Figure 5-S4	CHO-K1	Notch2-Dll4 (1B8)	0, 5, 15, 30, 500

Figure 5A; Figure 5-S1; Figure 5-S2; Figure 5-S4	CHO-K1	Notch2-Jag1 (2B7)	0, 5, 10, 15, 20, 30, 500
Figure 5A; Figure 5-S1; Figure 5-S2; Figure 5-S4	CHO-K1	Notch2-Jag2 (1A1)	0, 5, 10, 15, 25, 30, 50, 500
Figure 5D	CHO-K1	Notch1-Dll1 (2G5)	50
Figure 5D	CHO-K1	Notch1-Dll4 (1G11)	50
Figure 5D	CHO-K1	Notch1-Jag1 (1E2)	5
Figure 5D	CHO-K1	Notch1-Jag2 (2E10)	10
Figure 5D	CHO-K1	Notch2-Dll1 (1C4)	15
Figure 5D	CHO-K1	Notch2-Dll4 (1B8)	30
Figure 5D	CHO-K1	Notch2-Jag1 (2B7)	5
Figure 5D	CHO-K1	Notch2-Jag2 (1A1)	0
Figure 5-S5	CHO-K1	Notch1-Dll1 (2G5)	50
Figure 5-S5	CHO-K1	Notch1-Dll4 (1G11)	120

Supplementary Table 4: Sender-receiver cell pairs used for coculture assays

Where multiple receivers are listed, they were cultured with the same senders but in separate wells (receivers were not mixed together). All experiments with CHO-K1 cells used wild-type cells as negative sending controls and experiments with C2C12-Nkd receivers used the blank C2C12-Nkd parental line as negative controls.

Experiment	Cell type	Receivers (clone)	Sender
Figure 4A	CHO-K1	Notch1 (2D1)	Dll4-L1
Figure 4A	CHO-K1	Notch2 (2A4)	Dll1-L1
Figure 4B; Figure 4-S1	CHO-K1	Notch1-H2B-mCh (F4)	Dll1-L2
Figure 4B; Figure 4-S1	CHO-K1	Notch1-NGFR (2A6)	Dll1-L2
Figure 4B; Figure 4-S1	CHO-K1	Notch1-Dll1 (2G5)	Dll1-L2
Figure 4B; Figure 4-S1	CHO-K1	Notch1-Dll4 (1G11)	Dll1-L2
Figure 4B; Figure 4-S1	CHO-K1	Notch1-Jag1 (1E2)	Dll1-L2
Figure 4B; Figure 4-S1	CHO-K1	Notch1-Jag2 (2E10)	Dll1-L2
Figure 4B; Figure 4-S1	CHO-K1	Notch2-H2B-mCh (G2)	Dll1-L2
Figure 4B; Figure 4-S1	CHO-K1	Notch2-NGFR (1H4)	Dll1-L2
Figure 4B; Figure 4-S1	CHO-K1	Notch2-Dll1 (1C4)	Dll1-L2
Figure 4B; Figure 4-S1	CHO-K1	Notch2-Dll4 (1B8)	Dll1-L2
Figure 4B; Figure 4-S1	CHO-K1	Notch2-Jag1 (2B8)	Dll1-L2

Figure 4B; Figure 4-S1	CHO-K1	Notch2-Jag2 (1A1)	Dll1-L2
Figure 6; Figure 6—figure supplement 1	CHO-K1	Notch1-Dll1 (2G5)	Dll1-L2, Dll4-L2, Jag1-L1, Jag2-A
Figure 6; Figure 6—figure supplement 1	CHO-K1	Notch1-Dll4 (1G11)	Dll1-L2, Dll4-L2, Jag1-L1, Jag2-A
Figure 6; Figure 6—figure supplement 1	CHO-K1	Notch1-Jag1 (1E2)	Dll1-L2, Dll4-L2, Jag1-L1, Jag2-A
Figure 6; Figure 6—figure supplement 1	CHO-K1	Notch1-Jag2 (2E10)	Dll1-L2, Dll4-L2, Jag1-L1, Jag2-A
Figure 6; Figure 6—figure supplement 1	CHO-K1	Notch2-Dll1 (1C4)	Dll1-L2, Dll4-L2, Jag1-L1, Jag2-A
Figure 6; Figure 6—figure supplement 1	CHO-K1	Notch2-Dll4 (1B8)	Dll1-L2, Dll4-L2, Jag1-L1, Jag2-A
Figure 6; Figure 6—figure supplement 1	CHO-K1	Notch2-Jag1 (2B8)	Dll1-L2, Dll4-L2, Jag1-L1, Jag2-A
Figure 6; Figure 6—figure supplement 1	CHO-K1	Notch2-Jag2 (1A1)	Dll1-L2, Dll4-L2, Jag1-L1, Jag2-A
Figure 4-S2A	C2C12-Nkd	Notch1 (1A5)	Dll1 (c19)
Figure 4-S2A	C2C12-Nkd	Notch2 (c24)	Dll1 (c19)
Figure 4-S2B	C2C12-Nkd	Notch1-NGFR (1H6)	Dll4 (2H10)
Figure 4-S2B	C2C12-Nkd	Notch1-Dll4 (2D1)	Dll4 (2H10)
Figure 4-S2B	C2C12-Nkd	Notch1-Jag2 (1E7)	Dll4 (2H10)
Figure 4-S2B	C2C12-Nkd	Notch2-NGFR (1E9)	Dll4 (2H10)
Figure 4-S2B	C2C12-Nkd	Notch2-Dll4 (3B12)	Dll4 (2H10)
Figure 4-S2B	C2C12-Nkd	Notch2-Jag2 (1B12)	Dll4 (2H10)
Figure 2B-D; Figure 2-S4; Figure 2-S2	CHO-K1	Notch1 (2D1); Notch2 (2A4)	Dll1-L4A

Figure 2B-D; Figure 2-S4; Figure 2-S2	CHO-K1	Notch1 (2D1); Notch2 (2A4)	Dll1-L1
Figure 2B-D; Figure 2-S4; Figure 2-S2	CHO-K1	Notch1 (2D1); Notch2 (2A4)	Dll4-L4B
Figure 2B-D; Figure 2-S4; Figure 2-S2	CHO-K1	Notch1 (2D1); Notch2 (2A4)	Dll4-L1
Figure 2B-D; Figure 2-S4; Figure 2-S2	CHO-K1	Notch1 (2D1); Notch2 (2A4)	Jag1-L3
Figure 2B-D; Figure 2-S4; Figure 2-S2	CHO-K1	Notch1 (2D1); Notch2 (2A4)	Jag1-L1
Figure 2B-D; Figure 2-S4; Figure 2-S2	CHO-K1	Notch1 (2D1); Notch2 (2A4)	Jag2-AB
Figure 2B-D; Figure 2-S4; Figure 2-S2	CHO-K1	Notch1 (2D1); Notch2 (2A4)	Jag2-A
Figure 2B-D only	CHO-K1	Notch1-Dll1 (2G5)	Dll4-L4B
Figure 2B-D only	CHO-K1	Notch1-Dll1 (2G5)	Jag2-A
Figure 2B-D only	CHO-K1	Notch1-Dll4 (1G11)	Dll4-L4B
Figure 2B-D only	CHO-K1	Notch1-Dll4 (1G11)	Jag2-A
Figure 2B-D only	CHO-K1	Notch1-Jag1 (1E2)	Dll4-L4B
Figure 2B-D only	CHO-K1	Notch1-Jag1 (1E2)	Jag2-A
Figure 2B-D only	CHO-K1	Notch1-Jag2 (2E10)	Dll4-L4B
Figure 2B-D only	CHO-K1	Notch1-Jag2 (2E10)	Jag2-A
Figure 2B-D only	CHO-K1	Notch2-Jag1 (2B7); Notch2-Jag2 (1A1)	Dll4-L4B
Figure 2B-D only	CHO-K1	Notch2-Jag1 (2B7); Notch2-Jag2 (1A1)	Dll1-L4A
Figure 2B-D only	CHO-K1	Notch2-Jag1 (2B7); Notch2-Jag2 (1A1)	Jag2-B

Figure 2B-D only	CHO-K1	Notch1 (2D1); Notch2 (2A4)	Dll4-L4
Figure 2B-D only	CHO-K1	Notch1 (2D1); Notch2 (2A4)	Jag1-L2
Figure 2B-D only	CHO-K1	Notch1 (2D1); Notch2 (2A4)	Jag2-AA
Figure 2E	C2C12-Nkd	Notch1 (1A5)	Dll1 (c19)
Figure 2E	C2C12-Nkd	Notch1 (1A5)	Jag1 (c11)
Figure 2E	C2C12-Nkd	Notch2 (c24)	Dll1 (c19)
Figure 2E	C2C12-Nkd	Notch2 (c24)	Jag1 (c11)
Figure 2-S5B	CHO-K1	Notch1 (2D1); Notch2 (2A4)	Tet-OFF Dll1 (G1)
Figure 2-S5B	CHO-K1	Notch1 (2D1); Notch2 (2A4)	Tet-OFF Dll4 (2D6)
Figure 2-S5B	CHO-K1	Notch1 (2D1); Notch2 (2A4)	Tet-OFF Jag1 (1G3)
Figure 2-S5B	CHO-K1	Notch1 (2D1); Notch2 (2A4)	Tet-OFF Jag2 (1H6)
Figure 5A; Figure 5-S1; Figure 5-S3; Figure 5-S4	CHO-K1	Notch1-Dll1 (2G5)	Dll4-L1
Figure 5A; Figure 5-S1; Figure 5-S3; Figure 5-S4	CHO-K1	Notch1-Dll4 (1G11)	Dll4-L1
Figure 5A; Figure 5-S1; Figure 5-S3; Figure 5-S4	CHO-K1	Notch1-Jag1 (1E2)	Dll4-L1
Figure 5A; Figure 5-S1; Figure 5-S3; Figure 5-S4	CHO-K1	Notch1-Jag2 (2E10)	Dll4-L1

Figure 5A; Figure 5-S1; Figure 5-S3; Figure 5-S4	CHO-K1	Notch2-Dll1 (1C4)	Dll1-L1
Figure 5A; Figure 5-S1; Figure 5-S3; Figure 5-S4	CHO-K1	Notch2-Dll4 (1B8)	Dll1-L1
Figure 5A; Figure 5-S1; Figure 5-S3; Figure 5-S4	CHO-K1	Notch2-Jag1 (2B7)	Dll1-L1
Figure 5A; Figure 5-S1; Figure 5-S3; Figure 5-S4	CHO-K1	Notch2-Jag2 (1A1)	Dll1-L1

Supplementary Table 5: Recombinant Notch ligands and concentrations

Experiment	Cell type	Receivers (clone)	Ligand (conc.)
Figure 2-S3A (plated ligand assay)	C2C12	C2C12 (wt)	Dll1-ext-Fc* (2 μg/mL)
Figure 2-S3A (plated ligand assay)	C2C12	C2C12 (Nkd)	Dll1-ext-Fc* (2 μg/mL)
Figure 3A,B (soluble ligand binding assay)	CHO-K1	Parental reporter (cH1); Notch1 (2D1); Notch2 (2A4)	Dll1-ext-Fc (1 nM)
Figure 3A,B (soluble ligand binding assay)	CHO-K1	Parental reporter (cH1); Notch1 (2D1); Notch2 (2A4)	Dll4-ext-Fc (1 nM)
Figure 3A,B (soluble ligand binding assay)	CHO-K1	Parental reporter (cH1); Notch1 (2D1); Notch2 (2A4)	Jag1-ext-Fc (0.5 nM)
Figure 3A,B (soluble ligand binding assay)	CHO-K1	Parental reporter (cH1); Notch1 (2D1); Notch2 (2A4)	Jag2-ext-Fc (1 nM)
Figure 3C (plated ligand assay)	CHO-K1	Notch1 (2D1)	Dll1-ext-Fc (75 and 150 nM)
Figure 3C (plated ligand assay)	CHO-K1	Notch1 (2D1)	Dll4-ext-Fc (50 nM)
Figure 3C (plated ligand assay)	CHO-K1	Notch1 (2D1)	Jag1-ext-Fc (20 and 50 nM)
Figure 3C (plated ligand assay)	CHO-K1	Notch1 (2D1)	IgG1 Fc (150 nM)
Figure 2-S6 (plated ligand assay)	CHO-K1	Notch1 (2D1); Notch2 (2A4)	Dll1-ext-Fc (0.5, 1, 2, 3, 5, 10, 15, 25, 50, and 100 nM)
Figure 2-S6 (plated ligand assay)	CHO-K1	Notch1 (2D1)	Dll4-ext-Fc (0.1, 0.5, 1, 2, 2.5, 3, 5, 10, and 15 nM)
Figure 2-S6 (plated ligand assay)	CHO-K1	Notch1 (2D1)	Jag1-ext-Fc (0.5, 2, 3, 5, 10, 15, 25 and 50 nM)

Figure 2-S6 (plated ligand assay)	CHO-K1	Notch1 (2D1); Notch2 (2A4)	Jag2-ext-Fc (0.5, 1, 2, 3, 5, 10, 15, 25, 50, and 100 nM)
Figure 2-S6 (plated ligand assay)	CHO-K1	Notch1 (2D1); Notch2 (2A4)	IgG1 Fc (0.5, 2, 3, 5, 10, 15, 25, 50, and 100 nM)
Figure 2-S6 (plated ligand assay)	CHO-K1	Notch2 (2A4)	Dll4-ext-Fc (0.1, 0.5, 1, 2, 5, 10, 15, 25, 50, and 100 nM)
Figure 2-S6 (plated ligand assay)	CHO-K1	Notch2 (2A4)	Jag1-ext-Fc (0.5, 2, 3, 5, 10, 15, and 25 nM)

*Dll1-ext-Fc provided by Irwin Bernstein; all other recombinant ligands are from Bio-Techne/R&D Systems (see Supplementary Table 1).

Supplementary Table 6: Primers for RT-PCR and qRT-PCR

PCR Method	Gene Target	Forward Primer	Reverse Primer
RT-PCR	Mouse Jag1	CCAAAGCCTCTCAACTTAGTGC	CTTAGTTTTCCCGCACTTGTGTTT
qRT-PCR	mCherry	CCTCAGTTCATGTACGGCTCC	TCGAAGTTCATCACGCGCTC
qRT-PCR	Mouse Notch1	ATGTCAATGTTCGAGGACCAG	TCACTGTTGCCTGTCTCAAG
qRT-PCR	Mouse Notch2	GGACTGTGAAGAGGACATCAAT	CACTGGCAGGAGAAGGTATTC
qRT-PCR	Mouse Notch3	TGCCAGGGAATTTCAGGTG	AGGCAAGAACAGGAAAAGGAG
qRT-PCR	Mouse SdhA (housekeeping)	AGTGGGCT GTCTTCCTTAAC	GGATTGCTTCT GTTTGCTTGG
qRT-PCR	CHO Lfng	GAGGAGCTGGCTTCTGTATTAG	AGCAGTGCTTCCACAATGTA
qRT-PCR	CHO or Mouse Rfng	GTCCTGAGAACCCACGTAATG	AGTGGGTGTCTGGGTAGAGAA
qRT-PCR	CHO Beta-actin (housekeeping)	ACTGGGACGATATGGAGAAG	GGTCATCTTTTCACGGTTGG

Chapter III: Conclusions and Future Work

3.1 A comparison of signaling activities with previously published results identifies priorities for follow-up research

The receptor-ligand activation strengths measured in Chapter 2, and their dependence on Lfng expression, largely agree with existing literature where previous records exist. However, some discrepancies identify Notch signaling behaviors that may be more sensitive to cell type or other contextual factors, which merit further investigation.

Our measurements of Notch1 and Notch2 activation by the Delta ligands show striking quantitative similarity with previous measurements in a different cell line. Tveriakhina et al. reported that Dll4 activated Notch1 and Notch2 with a ~10-fold stronger efficiency and ~2-fold weaker efficiency than Dll1 did in E14TG2a mouse embryonic stem cells, respectively (Tveriakhina et al. 2018). We found in CHO-K1 cells that, without Lfng expression, Dll4 activated Notch1 and Notch2 with a 9-fold stronger efficiency and ~2.5-fold weaker efficiency than Dll1 did, respectively. The ~10-fold preference of Notch1 for Dll4 over Dll1 may reflect the similar difference in Notch1 binding affinity of the recombinant Dll4 ligand extracellular domain compared with that of Dll1 (Andrawes et al. 2013). We found that Dll4 also cis-activated Notch1 more efficiently than Dll1 did, as reported previously (Nandagopal, Santat, and Elowitz 2019).

Likewise, our finding that Jag1 is the weakest Notch1 ligand, despite its ability to efficiently bind and cis-inhibit Notch1, is consistent with Jag1's unique inability to support T cell maturation (Van de Walle et al. 2011; Lehar et al. 2005) and with its essential biological role as a Notch1 inhibitor (Pedrosa et al. 2015; Benedito et al. 2009; Golson et al. 2009).

Our observations that Lfng potentiates all Delta-Notch signaling and attenuates all Jagged-Notch signaling, in a manner qualitatively independent of receptor identity, agrees with others' reports that Lfng potentiated Dll1-Notch1 signaling and attenuated Jag1- and Jag2-Notch1 signaling (Kakuda et al. 2020; Yang et al. 2005; Hicks et al. 2000). Likewise, there is existing evidence that Lfng potentiates Dll4-Notch1 signaling in T cell progenitors (Stanley and Guidos 2009; Song et al. 2016) and in angiogenesis (Benedito et al. 2009). One prior report suggested that Lfng did not affect Notch1 activation by plated Dll4-ext-Fc (Kakuda et al. 2020); however, this discrepancy might be explained by the ligand supply level. Specifically, if the plated Dll4 concentration in

Kakuda et al.'s experiment maximally activated Notch1 even without Lfng, Lfng would not be able to further boost Dll4-Notch1 signaling, just as we saw that Lfng was not able to further boost signaling in our "high" Dll4-Notch1 coculture assay (Figure 2—figure supplement 4).

The literature provides conflicting reports of Lfng effects on Notch2 signaling. Hicks et al. reported that Lfng strengthens Notch2 transactivation by Jag1 as well as by Dll1 in C2C12 cells, in contrast with its effects on Jag1-Notch1 signaling measured in the same study (Hicks et al. 2000), and in contrast with our observations that Lfng weakened Jag1-Notch2 signaling. Kakuda et al. reported no Lfng effect on Notch2 trans-activation by either Jag1 or Jag2, although trans-activation by both was attenuated by Mfng, and Mfng effects qualitatively matched those of Lfng for Notch1 (Kakuda et al. 2020). Others observed in CHO-K1 cells that Lfng (and to a greater extent, Mfng) weakened Jag1-Notch2 signaling, in agreement with our results (Shimizu et al. 2001); however, in the same study, they detected no Fringe-mediated potentiation of Dll1-Notch2 signaling, in contrast with our results and others (Hicks et al. 2000; Kakuda et al. 2020). It is possible that Lfng effects on Notch2 depend qualitatively on cell-specific factors, although previous failures to detect Fringe effects might be explained by saturating ligand levels.

Our analysis of Lfng effects on Notch-ligand binding was consistent with previous results, with one exception. Others previously reported that Lfng increased Jag1's Notch1 binding affinity, despite reducing its Notch1 activation potential (Hicks et al. 2000; Kakuda and Haltiwanger 2017; Taylor et al. 2014; Yang et al. 2005). These reports also found that Lfng strengthened Dll1-Notch1 binding, in tandem with its activation potential. Likewise, we saw that Lfng strengthened and weakened Dll1- and Jag1-Notch1 trans-activation, respectively, both in the coculture-based trans-activation assay and the plated ligand assay. In contrast with Notch1, our analysis of Notch2 binding conflicted with one previous report. Specifically, we failed to detect a change in Jag1-Notch2 binding with Lfng vs. dLfng expression, in contrast with one previous study suggesting that Lfng reduced Jag1-Notch2 binding strength (Shimizu et al. 2001). It is possible that the ligand concentrations we used were saturating for binding to surface receptors, preventing detection of a real effect. We similarly failed to detect significant Lfng effects on binding strengths for all other receptor-ligand combinations except Jag2-Notch1, whose interaction was strengthened by Lfng. Future work is needed to assess Lfng effects on the binding strength of Dll4-Notch1 and all Notch2-ligand interactions.

Previous studies provide limited data comparing cis-inhibition strengths for receptor-ligand pairs. One comparison of Delta-mediated cis-inhibition in CHO cells found that Dll4 cis-inhibited Notch1 more efficiently than Dll1 did (Preuße et al. 2015). Our results agree, but only in the case where the trans-activating ligand is Dll4 (Figure 6B). By contrast, we found that Dll1 was a more effective Notch1 cis-inhibitor than Dll4 was when the trans-activating ligand was Dll1 or Jag2. This is consistent with the larger trend that emerged from our data, showing that cis-ligands have a comparative inhibitory advantage when competing with a trans-ligand of the same identity compared with other trans-ligands.

We did not analyze Fringe effects on cis- or trans-inhibition in this paper. However, our analyses support predictions of Fringe effects on cis- and trans-inhibition that are consistent with some previous studies and at odds with others. For example, the finding that Lfng strengthens Jag1-Notch1 binding while decreasing its activation suggests that Lfng could strengthen competitive trans-inhibition of Notch1 by Jag1, in agreement with reports that Jag1's ability to trans-inhibit Dll4-Notch1 signaling in angiogenesis (Pedrosa et al. 2015; Benedito et al. 2009), and Dll1-Notch1 signaling in the embryonic pancreas (Golson et al. 2009), is dependent on Lfng expression. Our data predict that Lfng strengthens Notch1 cis-inhibition by Jag1, for the same reasons. However, one previous report suggested that Lfng weakened Notch1 cis-inhibition by Jag1 (LeBon et al. 2014). Future experiments will be needed to resolve this theoretical discrepancy.

The largest contradiction between our results and existing literature concerns the strong cis-activation we observed for the Notch2-Dll4 combination. In our hands, the Delta ligands cis-activated and did not cis-inhibit Notch2, both in CHO-K1 and C2C12 cells, in contrast with a recent report that wild-type Dll4 cis-inhibited Notch2 in U2OS osteosarcoma cells (D. Chen et al. 2023). Obvious differences between these two assays include cell type, method of ligand expression, and receptor intracellular domain composition (a minimal Gal4, in our case). In vivo investigation of Notch2 cis-activation is critically needed to determine whether cis-activation occurs in natural contexts and is a physiologically important signaling process.

In summary, our results largely agree with existing analyses of cis and trans Notch1-ligand interactions, and their dependence on Lfng. Our data help resolve contradictory observations of Lfng effects on Notch2 signaling by showing that Delta- and Jagged-mediated Notch2 signaling are strengthened and weakened by Lfng, respectively, in a manner qualitatively consistent with

Lfng effects on Notch1 signaling. We also provide new data characterizing relative activation strengths, cis-inhibition strengths, and Lfng effects on activation and binding, for receptor-ligand combinations previously uninvestigated. Future work is needed to comprehensively assess Lfng effects on both ligand-receptor binding and inhibition strengths, and to determine whether the discrepancies in Notch2-Dll4 cis-activation and cis-inhibition behaviors observed in Chapter 2 compared with a previous report (D. Chen et al. 2023) can be explained by cell type differences, artifacts of chimeric Notch2-Gal4 signaling, or other factors.

3.2 Future work: A comprehensive model of Notch signaling

The work in Chapter 2 identifies ways to build on existing mathematical descriptions of the Notch signaling architecture to enable parameterization and modeling of receptor-ligand-Fringe interactions occurring in natural cell types. To our knowledge, a combinatorial model of Notch signaling allowing for competition between more than one receptor and two ligands does not yet exist. Our results suggest that a sufficiently complex model architecture should include competitive receptor-ligand binding (in cis and trans), for an arbitrarily complex set of receptors and ligands, and should allow trans-activation efficiencies to be stronger or weaker than cis-activation efficiencies. Orientation-dependent (cis vs. trans) binding strength parameters should have third-order dependence on the identities of the receptor and both competing ligands, which would enable recapitulation of our observations that ligands have a comparative cis-inhibitory advantage when competing against a trans-ligand of the same identity, rather than against a different ligand (Chapter 2.3.13). Fringes should be able to independently modulate trans-activation efficiencies, cis-activation efficiencies, and binding efficiencies to different extents and even in different directions, for any given receptor-ligand pair. This will allow Fringe to enhance trans-inhibition of Notch1 by Jag1, for example, by strengthening binding and weakening activation (Chapter 2.3.7) (Hicks et al. 2000; Kakuda and Haltiwanger 2017; Taylor et al. 2014; Yang et al. 2005; Pedrosa et al. 2015; Benedito et al. 2009; Golson et al. 2009). It remains to be determined whether Fringe effects on cis-binding vs. trans-binding may differ for the same receptor-ligand pair.

A unifying Notch model should also recapitulate the nonmonotonic dose-response trends observed at high ligand levels for Notch1 cis-activation (Nandagopal, Santat, and Elowitz 2019) and, to a lesser extent, for Notch2 cis-activation and trans-activation of both receptors (Chapter 2), as well

as for trans-activation of Notch by Delta in *Drosophila* (Yatsenko and Shcherbata 2021; Zamfirescu, Yatsenko, and Shcherbata 2022). In the case of cis-activation, non-monotonic curves have been simulated by allowing ligand:receptor complexes to form with a 1:1 (activating) or 2:1 (non-activating) stoichiometry (Nandagopal, Santat, and Elowitz 2019; D. Chen et al. 2023). This model is supported by experimental data showing that a dimerization-deficient Dll4 mutant cannot cis-inhibit Notch2, but wild-type Dll4 can cis-inhibit Notch2 (D. Chen et al. 2023). (The latter result conflicts with our observation that Dll4 cannot cis-inhibit Notch2 because it cis-activates strongly, as discussed in Chapter 3.1.) However, it is unclear whether the non-monotonicity we observed in trans-activation curves at high ligand levels also requires ligand dimerization (ligand:receptor stiochiometries > 1:1) or whether high ligand expression reduces signaling activity by other means in trans-activation. Further experimental investigation will be needed to determine the best way to model nonmonotonic trans-activation curves.

Finally, a complete model of Notch signaling should include the purely cis-inhibitory ligand Dll3. Dll3 is an Lfng-dependent Notch inhibitor, plays a critical role during somitogenesis, and can both enhance sending potential of coexpressed ligands or reduce receiving potential of coexpressed Notch1 (Bochter et al. 2022; Ladi et al. 2005; Zhang, Norton, and Gridley 2002). The mechanism of Dll3-mediated cis-inhibition is thought to differ from that of the activating ligands, and likely involves receptor sequestration away from the membrane (Chapman et al. 2011; Serth et al. 2015), but is incompletely understood. Further work is needed to determine the appropriate way to incorporate Dll3-mediated cis-inhibition into a comprehensive mathematical model of Notch signaling.

Some open questions about Notch model architecture design relate to our present lack of data analyzing combinations with more than one ligand or more than one receptor in the same cell. For example, it is possible that biophysical synergies alter the binding activity or cis-activation strength of Dll4-Notch1 (weak cis-activation) or Dll4-Notch2 (strong cis-activation) when Dll4 is coexpressed with both receptors, compared to when Dll4 is coexpressed with only Notch1 or only Notch2. Experiments with engineered receiver cells that allow orthogonal readout of signaling activity through two different receptors in the same cell would shed light on this question.

Our investigation in Chapter 2 ignored the role of interactions between Notch ligand or receptor intracellular domains, but these interactions provide additional mechanisms for competitive

inhibition, which could be integrated into a mathematical model. For example, cis-inhibition of Notch1 by Jag1 could reduce signaling activity with greater efficiency than we observed if bidirectional signaling occurs, since others have reported that the Jag1 intracellular domain (JICD), proteolytically cleaved in response to receptor binding, can bind the Notch intracellular domain (NICD) and destabilize it in addition to preventing NICD from associating with its transcriptional cofactors (Kim et al., 2011; Sánchez-Iranzo et al., 2022). Other studies suggested that the intracellular domain of Notch3 (Beatus et al. 1999) is a poor transcription factor and may function primarily to inhibit activity of the Notch1 ICD. (Notch4 is also reported to inhibit Notch1 activity, but by a different mechanism (James et al. 2014).)

Many other facets of Notch signaling impact pathway activity and cell behavior, and these should be considered in modeling when relevant to the specific context under study. These include, but are not limited to: regulation of NICD stability (Braunreiter and Cole 2019); contact area of the signaling interface (Khait et al. 2016; Shaya et al. 2017); mechanical forces (Cohen and Sprinzak 2021); expression of noncanonical ligands (Brendan D'Souza, Meloty-Kapella, and Weinmaster 2010; Fiddes et al. 2018); possible ligand extracellular vesicle-mediated signaling (E. Tan, Asada, and Ge 2018; Sheldon et al. 2010); ligand extracellular domain shedding (Sun, Li, and Zolkiewska 2008; Six et al. 2003; Parr-Sturgess, Rushton, and Parkin 2010; LaVoie and Selkoe 2003); expression of ligand activity modifiers like E3 ubiquitin ligase Mindbomb1 (Mib1), which alters the balance of trans-activation vs. cis-inhibition (Baek et al. 2018; Troost et al. 2022); architecture of Notch cis-regulatory transcriptional enhancers, which can affect target gene sensitivities and temporal responses (Falo-Sanjuan et al. 2019) and NICD stability (Kuang et al. 2020); and feedback regulation, such as that which mediates Notch signaling oscillations in somitogenesis (Bochter et al. 2022; Takagi et al. 2020), neurogenesis (Shimojo, Ohtsuka, and Kageyama 2008), myogenesis (Sueda and Kageyama 2020; Lahmann et al. 2019), and pancreatic progenitors (Seymour et al. 2020).

3.3 Future work: Toward the rational perturbation of Notch signaling

Chapter 1.4 described the advantages of selectively blocking individual Notch proteins or specific ligand-receptor pairs, as opposed to broadly inhibiting Notch signaling, for therapeutic intervention in Notch-dependent cancers and other diseases. To predict the efficacy of drugs that inhibit individual Notch receptors, ligands, or block binding between specific ligand-receptor pairs

in any given cell context, we need a mathematical model (Section 3.2) with parameters fit, or at least constrained, using our quantitative analysis of Notch signaling interactions in Chapter 2. We also need single-cell expression data, ideally with spatial context, since receptor, ligand, and Fringe expression in any given cell provide no information about the ligands or receptors that may be interacting with that cell in trans. Spatial transcriptomics methods are rapidly improving (Ståhl et al. 2016; Asp, Bergenstråhle, and Lundeberg 2020; Zhaoyang Liu, Sun, and Wang 2022; Longo et al. 2021; Lee, Yoo, and Choi 2022), hastening the advent of such a dataset.

However, mRNA counts are limited as proxies for surface protein levels, and provide no information about surface protein dynamics. For example, if basal endocytosis rates differ for Dll1 and Dll4, their surface levels might differ even when the ligands have similar transcript counts. Additionally, some ligands are subject to complex spatial reorganization, as in endothelial cells, where Jag1 is removed from the surface and intracellularly compartmentalized during the application of shear stress (Driessen et al. 2018). Moreover, mature transcript counts obscure the underlying dynamics of Notch gene expression, which can exhibit short (2-3 hour) oscillations, as observed for Dll1 in muscle, pancreatic, and neural progenitor cells (Sueda and Kageyama 2020; Lahmann et al. 2019; Shimojo, Ohtsuka, and Kageyama 2008; Seymour et al. 2020). Nevertheless, rough estimates of Notch protein expression based on RNA expression levels should still be useful for identifying promising ligand-receptor pairs as candidates for rational perturbation of Notch signaling in therapeutic or tissue engineering applications.

Time-series single-cell RNA-sequencing (Ding, Sharon, and Bar-Joseph 2022; W. Chen et al. 2022) is another method that promises valuable insights into the functional roles of individual Notch components in complex expression modules. Such datasets will enable detection of correlations or anticorrelations between the expression of specific Notch signaling components and target genes. For example, if in time-series analysis of single cells, the upregulation of a Notch ligand is associated with upregulation of downstream target genes such as the widely accessible, Notch-responsive Nrarp gene (Duvall et al. 2022), this would supports the idea that the upregulated ligand has a signal-activating role in this context. However, the mechanism by which it mediates that activation cannot be assumed, since the complex dependencies of binding and activation parameters in a complete model of Notch signaling would prevent adequate parameter estimation even with the rich, combinatorial datasets presented in Chapter 2 (see Section 3.2). In principle,

strong, single-cell correlations between ligand and target gene expression would be consistent with cis-activation, but they would also be consistent with more indirect methods of activation such as the relief of inhibitory interactions between other ligand-receptor pairs. If slight anticorrelations are evident between ligand and target gene expression in single cells at the same time point, but these genes show a positive correlation through time, this could indicate that the ligand is predominantly trans-activating (Chapter 2.3.12). However, slight anticorrelations at a fixed time point might also be consistent with negative oscillatory feedback loops between activating ligands and repressor target genes, depending on the mRNA stability and dynamics of the genes in question. Similar ambiguities would prevent confident interpretation of molecular events where upregulation of a ligand is instead associated with downregulation of signaling. To complicate matters further, multiple Notch ligands, receptors, and Fringes are often up- or down-regulated in tandem (Castel et al. 2013; Negri et al. 2019), making it impossible to identify functional correlations between target genes and individual Notch signaling proteins in such cases.

Nevertheless, time-series scRNA-seq datasets, especially with spatial cell-type mapping (as described above), should provide valuable information that will substantially narrow the list of candidate receptor-ligand pairs (and binding orientations) to target for signaling perturbation in a given context. Further studies of interactions between receptors and ligands in more complex expression modules will continue to enhance the utility of these datasets for purposes of drug design.

References

Abe, Natsumi, Katsuto Hozumi, Ken-Ichi Hirano, Hideo Yagita, and Sonoko Habu. 2010. "Notch Ligands Transduce Different Magnitudes of Signaling Critical for Determination of T-Cell Fate." *European Journal of Immunology* 40 (9): 2608–17.

Álamo, David del, Hervé Rouault, and François Schweisguth. 2011. "Mechanism and Significance of Cis-Inhibition in Notch Signalling." *Current Biology: CB* 21 (1): R40–47.

Andrawes, Marie Blanke, Xiang Xu, Hong Liu, Scott B. Ficarro, Jarrod A. Marto, Jon C. Aster, and Stephen C. Blacklow. 2013. "Intrinsic Selectivity of Notch 1 for Delta-like 4 over Delta-like 1." *The Journal of Biological Chemistry* 288 (35): 25477–89.

Artavanis-Tsakonas, S., M. D. Rand, and R. J. Lake. 1999. "Notch Signaling: Cell Fate Control and Signal Integration in Development." *Science* 284 (5415): 770–76.

Asp, Michaela, Joseph Bergenstråhle, and Joakim Lundeberg. 2020. "Spatially Resolved Transcriptomes-Next Generation Tools for Tissue Exploration." *BioEssays: News and Reviews in Molecular, Cellular and Developmental Biology* 42 (10): e1900221.

Aster, Jon C., Warren S. Pear, and Stephen C. Blacklow. 2017. "The Varied Roles of Notch in Cancer." *Annual Review of Pathology* 12 (January): 245–75.

Baek, Chooyoung, Lucy Freem, Rosette Goïame, Helen Sang, Xavier Morin, and Samuel Tozer. 2018. "Mib1 Prevents Notch Cis-Inhibition to Defer Differentiation and Preserve Neuroepithelial Integrity during Neural Delamination." *PLoS Biology* 16 (4): e2004162.

Bardot, Boris, Lee-Peng Mok, Tristan Thayer, Francois Ahimou, and Cedric Wesley. 2005. "The Notch Amino Terminus Regulates Protein Levels and Delta-Induced Clustering of Drosophila Notch Receptors." *Experimental Cell Research* 304 (1): 202–23.

Beatus, P., J. Lundkvist, C. Oberg, and U. Lendahl. 1999. "The Notch 3 Intracellular Domain Represses Notch 1-Mediated Activation through Hairy/Enhancer of Split (HES) Promoters." *Development* 126 (17): 3925–35.

Becam, Isabelle, Ulla-Maj Fiuza, Alfonso Martínez Arias, and Marco Milán. 2010. "A Role of Receptor Notch in Ligand Cis-Inhibition in Drosophila." *Current Biology: CB* 20 (6): 554–60.

Benedito, Rui, Cristina Roca, Inga Sörensen, Susanne Adams, Achim Gossler, Marcus Fruttiger, and Ralf H. Adams. 2009. "The Notch Ligands Dll4 and Jagged1 Have Opposing Effects on Angiogenesis." *Cell* 137 (6): 1124–35.

Bochter, Matthew S., Dustin Servello, Shinako Kakuda, Rachel D'Amico, Meaghan F. Ebetino, Robert S. Haltiwanger, and Susan E. Cole. 2022. "Lfng and Dll3 Cooperate to Modulate Protein Interactions in Cis and Coordinate Oscillatory Notch Pathway Activation in the Segmentation Clock." *Developmental Biology* 487 (July): 42–56.

Braunreiter, Kara M., and Susan E. Cole. 2019. "A Tale of Two Clocks: Phosphorylation of NICD by CDKs Links Cell Cycle and Segmentation Clock." *EMBO Reports*.

Bray, Sarah J. 2016. “Notch Signalling in Context.” *Nature Reviews. Molecular Cell Biology* 17 (11): 722–35.

Cappellari, Ornella, Sara Benedetti, Anna Innocenzi, Francesco Saverio Tedesco, Artal Moreno-Fortuny, Gonzalo Ugarte, Maria Grazia Lampugnani, Graziella Messina, and Giulio Cossu. 2013. “Dll4 and PDGF-BB Convert Committed Skeletal Myoblasts to Pericytes without Erasing Their Myogenic Memory.” *Developmental Cell* 24 (6): 586–99.

Castel, David, Philippos Mourikis, Stefanie J. J. Bartels, Arie B. Brinkman, Shahragim Tajbakhsh, and Hendrik G. Stunnenberg. 2013. “Dynamic Binding of RBPJ Is Determined by Notch Signaling Status.” *Genes & Development* 27 (9): 1059–71.

Castillo-Hair, Sebastian M., John T. Sexton, Brian P. Landry, Evan J. Olson, Oleg A. Igoshin, and Jeffrey J. Tabor. 2016. “FlowCal: A User-Friendly, Open Source Software Tool for Automatically Converting Flow Cytometry Data from Arbitrary to Calibrated Units.” *ACS Synthetic Biology* 5 (7): 774–80.

Cattoni, Diego I., Osvaldo Chara, Sergio B. Kaufman, and F. Luis González Flecha. 2015. “Cooperativity in Binding Processes: New Insights from Phenomenological Modeling.” *PloS One* 10 (12): e0146043.

Chapman, Gavin, Duncan B. Sparrow, Elisabeth Kremmer, and Sally L. Dunwoodie. 2011. “Notch Inhibition by the Ligand DELTA-LIKE 3 Defines the Mechanism of Abnormal Vertebral Segmentation in Spondylocostal Dysostosis.” *Human Molecular Genetics* 20 (5): 905–16.

Chen, Daipeng, Zary Forghany, Xinxin Liu, Haijiang Wang, Roeland M. H. Merks, and David A. Baker. 2023. “A New Model of Notch Signalling: Control of Notch Receptor Cis-Inhibition via Notch Ligand Dimers.” *PLoS Computational Biology* 19 (1): e1010169.

Chen, Wanze, Orane Guillaume-Gentil, Pernille Yde Rainer, Christoph G. Gäbelein, Wouter Saelens, Vincent Gardeux, Amanda Klaeger, et al. 2022. “Live-Seq Enables Temporal Transcriptomic Recording of Single Cells.” *Nature* 608 (7924): 733–40.

Cohen, Roie, and David Sprinzak. 2021. “Mechanical Forces Shaping the Development of the Inner Ear.” *Biophysical Journal* 120 (19): 4142–48.

Collier, J. R., N. A. Monk, P. K. Maini, and J. H. Lewis. 1996. “Pattern Formation by Lateral Inhibition with Feedback: A Mathematical Model of Delta-Notch Intercellular Signalling.” *Journal of Theoretical Biology* 183 (4): 429–46.

Conlon, R. A., A. G. Reaume, and J. Rossant. 1995. “Notch1 Is Required for the Coordinate Segmentation of Somites.” *Development* 121 (5): 1533–45.

Cordle, Jemima, Steven Johnson, Joyce Zi Yan Tay, Pietro Roversi, Marian B. Wilkin, Beatriz Hernández de Madrid, Hideyuki Shimizu, et al. 2008. “A Conserved Face of the Jagged/Serrate DSL Domain Is Involved in Notch Trans-Activation and Cis-Inhibition.” *Nature Structural & Molecular Biology* 15 (8): 849–57.

Dahlqvist, Camilla, Andries Blokzijl, Gavin Chapman, Anna Falk, Karin Dannaeus, Carlos F. Ibâñez, and Urban Lendahl. 2003. “Functional Notch Signaling Is Required for BMP4-Induced Inhibition of Myogenic Differentiation.” *Development* 130 (24): 6089–99.

Dallas, Mari H., Barbara Varnum-Finney, Colleen Delaney, Keizo Kato, and Irwin D. Bernstein. 2005. "Density of the Notch Ligand Delta1 Determines Generation of B and T Cell Precursors from Hematopoietic Stem Cells." *The Journal of Experimental Medicine* 201 (9): 1361–66.

Del Real, Marissa Morales, and Ellen V. Rothenberg. 2013. "Architecture of a Lymphomyeloid Developmental Switch Controlled by PU.1, Notch and Gata3." *Development* 140 (6): 1207–19.

Ding, Jun, Nadav Sharon, and Ziv Bar-Joseph. 2022. "Temporal Modelling Using Single-Cell Transcriptomics." *Nature Reviews. Genetics* 23 (6): 355–68.

Driessen, R. C. H., O. M. J. A. Stassen, M. Sjöqvist, F. Suarez Rodriguez, J. Grolleman, C. V. C. Bouten, and C. M. Sahlgren. 2018. "Shear Stress Induces Expression, Intracellular Reorganization and Enhanced Notch Activation Potential of Jagged1." *Integrative Biology: Quantitative Biosciences from Nano to Macro* 10 (11): 719–26.

D'Souza, B., A. Miyamoto, and G. Weinmaster. 2008. "The Many Facets of Notch Ligands." *Oncogene* 27 (38): 5148–67.

D'Souza, Brendan, Laurence Meloty-Kapella, and Gerry Weinmaster. 2010. "Canonical and Non-Canonical Notch Ligands." *Current Topics in Developmental Biology* 92: 73–129.

Duke, Thomas, and Ian Graham. 2009. "Equilibrium Mechanisms of Receptor Clustering." *Progress in Biophysics and Molecular Biology* 100 (1-3): 18–24.

Duvall, Kathryn, Lauren Crist, Alison J. Perl, Naomi Pode Shakked, Praneet Chaturvedi, and Raphael Kopan. 2022. "Revisiting the Role of Notch in Nephron Segmentation Confirms a Role for Proximal Fate Selection during Mouse and Human Nephrogenesis." *Development* 149 (10). https://doi.org/10.1242/dev.200446.

Elowitz, Michael B., Leah A. Santat, and Nagarajan Nandagopal. 2018. "Cis-Activation in the Notch Signaling Pathway." *bioRxiv*. https://doi.org/10.1101/313171.

Engler, Anna, Chiara Rolando, Claudio Giachino, Ichiko Saotome, Andrea Erni, Callum Brien, Runrui Zhang, et al. 2018. "Notch2 Signaling Maintains NSC Quiescence in the Murine Ventricular-Subventricular Zone." *Cell Reports* 22 (4): 992–1002.

Evrard, Y. A., Y. Lun, A. Aulehla, L. Gan, and R. L. Johnson. 1998. "Lunatic Fringe Is an Essential Mediator of Somite Segmentation and Patterning." *Nature* 394 (6691): 377–81.

Falix, Farah A., Daniël C. Aronson, Wouter H. Lamers, and Ingrid C. Gaemers. 2012. "Possible Roles of DLK1 in the Notch Pathway during Development and Disease." *Biochimica et Biophysica Acta* 1822 (6): 988–95.

Falo-Sanjuan, Julia, and Sarah J. Bray. 2019. "Decoding the Notch Signal." *Development, Growth & Differentiation*, December. https://doi.org/10.1111/dgd.12644.

Falo-Sanjuan, Julia, Nicholas C. Lammers, Hernan G. Garcia, and Sarah J. Bray. 2019. "Enhancer Priming Enables Fast and Sustained Transcriptional Responses to Notch Signaling." *Developmental Cell* 50 (4): 411–25.e8.

Fiddes, Ian T., Gerrald A. Lodewijk, Meghan Mooring, Colleen M. Bosworth, Adam D. Ewing, Gary L. Mantalas, Adam M. Novak, et al. 2018. “Human-Specific NOTCH2NL Genes Affect Notch Signaling and Cortical Neurogenesis.” *Cell* 173 (6): 1356–69.e22.

Fiuza, Ulla-Maj, Thomas Klein, Alfonso Martinez Arias, and Penelope Hayward. 2010. “Mechanisms of Ligand-Mediated Inhibition in Notch Signaling Activity in Drosophila.” *Developmental Dynamics: An Official Publication of the American Association of Anatomists* 239 (3): 798–805.

Formosa-Jordan, Pau, and Marta Ibañes. 2014. “Competition in Notch Signaling with Cis Enriches Cell Fate Decisions.” *PloS One* 9 (4): e95744.

Gasperowicz, Malgorzata, Anshita Rai, and James C. Cross. 2013. “Spatiotemporal Expression of Notch Receptors and Ligands in Developing Mouse Placenta.” *Gene Expression Patterns: GEP* 13 (7): 249–54.

Gera, Sakshi, and Rajan R. Dighe. 2018. “The Soluble Ligand Ybox-1 Activates Notch3 Receptor by Binding to Epidermal Growth Factor like Repeats 20-23.” *Archives of Biochemistry and Biophysics*, October. https://doi.org/10.1016/j.abb.2018.10.009.

Gioftsidi, Stamatia, Frederic Relaix, and Philippos Mourikis. 2022. “The Notch Signaling Network in Muscle Stem Cells during Development, Homeostasis, and Disease.” *Skeletal Muscle* 12 (1): 9.

Golson, Maria L., John Le Lay, Nan Gao, Nuria Brämswig, Kathleen M. Loomes, Rebecca Oakey, Catherine L. May, Peter White, and Klaus H. Kaestner. 2009. “Jagged1 Is a Competitive Inhibitor of Notch Signaling in the Embryonic Pancreas.” *Mechanisms of Development* 126 (8-9): 687–99.

Gopalakrishnan, Manoj, Kimberly Forsten-Williams, Matthew A. Nugent, and Uwe C. Täuber. 2005. “Effects of Receptor Clustering on Ligand Dissociation Kinetics: Theory and Simulations.” *Biophysical Journal* 89 (6): 3686–3700.

Gordon, Wendy R., Brandon Zimmerman, Li He, Laura J. Miles, Jiuhong Huang, Kittichoat Tiyanont, Debbie G. McArthur, et al. 2015. “Mechanical Allostery: Evidence for a Force Requirement in the Proteolytic Activation of Notch.” *Developmental Cell* 33 (6): 729–36.

Granados, Alejandro A., Nivedita Kanrar, and Michael B. Elowitz. 2022. “Combinatorial Expression Motifs in Signaling Pathways.” *bioRxiv*. https://doi.org/10.1101/2022.08.21.504714.

Groot, Arjan J., Roger Habets, Sanaz Yahyanejad, Caroline M. Hodin, Karina Reiss, Paul Saftig, Jan Theys, and Marc Vooijs. 2014. “Regulated Proteolysis of NOTCH2 and NOTCH3 Receptors by ADAM10 and Presenilins.” *Molecular and Cellular Biology* 34 (15): 2822–32.

Guentchev, Marin, and Ronald D. G. McKay. 2006. “Notch Controls Proliferation and Differentiation of Stem Cells in a Dose-Dependent Manner.” *The European Journal of Neuroscience* 23 (9): 2289–96.

Hadjivasiliou, Zena, Ginger L. Hunter, and Buzz Baum. 2016. "A New Mechanism for Spatial Pattern Formation via Lateral and Protrusion-Mediated Lateral Signalling." *Journal of the Royal Society, Interface / the Royal Society* 13 (124). https://doi.org/10.1098/rsif.2016.0484.

Hamada, Y., Y. Kadokawa, M. Okabe, M. Ikawa, J. R. Coleman, and Y. Tsujimoto. 1999. "Mutation in Ankyrin Repeats of the Mouse Notch2 Gene Induces Early Embryonic Lethality." *Development* 126 (15): 3415–24.

Henrique, Domingos, and François Schweisguth. 2019. "Mechanisms of Notch Signaling: A Simple Logic Deployed in Time and Space." *Development* 146 (3). https://doi.org/10.1242/dev.172148.

Hicks, C., S. H. Johnston, G. diSibio, A. Collazo, T. F. Vogt, and G. Weinmaster. 2000. "Fringe Differentially Modulates Jagged1 and Delta1 Signalling through Notch1 and Notch2." *Nature Cell Biology* 2 (8): 515–20.

Hozumi, Katsuto. 2019. "Distinctive Properties of the Interactions between Notch and Notch Ligands." *Development, Growth & Differentiation*, December. https://doi.org/10.1111/dgd.12641.

James, A. C., J. O. Szot, K. Iyer, J. A. Major, S. E. Pursglove, G. Chapman, and S. L. Dunwoodie. 2014. "Notch4 Reveals a Novel Mechanism Regulating Notch Signal Transduction." *Biochimica et Biophysica Acta* 1843 (7): 1272–84.

Kageyama, Ryoichiro, Toshiyuki Ohtsuka, Hiromi Shimojo, and Itaru Imayoshi. 2008. "Dynamic Notch Signaling in Neural Progenitor Cells and a Revised View of Lateral Inhibition." *Nature Neuroscience* 11 (11): 1247–51.

Kakuda, Shinako, and Robert S. Haltiwanger. 2017. "Deciphering the Fringe-Mediated Notch Code: Identification of Activating and Inhibiting Sites Allowing Discrimination between Ligands." *Developmental Cell* 40 (2): 193–201.

Kakuda, Shinako, Rachel K. LoPilato, Atsuko Ito, and Robert S. Haltiwanger. 2020. "Canonical Notch Ligands and Fringes Have Distinct Effects on NOTCH1 and NOTCH2." *The Journal of Biological Chemistry* 295 (43): 14710–22.

Kamath, Binita Maya, Robert C. Bauer, Kathleen M. Loomes, Grace Chao, Jennifer Gerfen, Anne Hutchinson, Winita Hardikar, et al. 2012. "NOTCH2 Mutations in Alagille Syndrome." *Journal of Medical Genetics* 49 (2): 138–44.

Khait, Itzhak, Yuval Orsher, Ohad Golan, Udi Binshtok, Nadav Gordon-Bar, Liat Amir-Zilberstein, and David Sprinzak. 2016. "Quantitative Analysis of Delta-like 1 Membrane Dynamics Elucidates the Role of Contact Geometry on Notch Signaling." *Cell Reports* 14 (2): 225–33.

Kim, Mi-Yeon, Jane Jung, Jung-Soon Mo, Eun-Jung Ann, Ji-Seon Ahn, Ji-Hye Yoon, and Hee-Sae Park. 2011. "The Intracellular Domain of Jagged-1 Interacts with Notch1 Intracellular Domain and Promotes Its Degradation through Fbw7 E3 Ligase." *Experimental Cell Research* 317 (17): 2438–46.

Kitamoto, Takeo, Keikichi Takahashi, Hiroaki Takimoto, Kazuma Tomizuka, Michiko Hayasaka, Takeshi Tabira, and Kazunori Hanaoka. 2005. "Functional Redundancy of the Notch Gene Family during Mouse Embryogenesis: Analysis of Notch Gene Expression in Notch3-Deficient Mice." *Biochemical and Biophysical Research Communications* 331 (4): 1154–62.

Klein, T., K. Brennan, and A. M. Arias. 1997. "An Intrinsic Dominant Negative Activity of Serrate That Is Modulated during Wing Development in Drosophila." *Developmental Biology* 189 (1): 123–34.

Kopan, Raphael, and Maria Xenia G. Ilagan. 2009. "The Canonical Notch Signaling Pathway: Unfolding the Activation Mechanism." *Cell* 137 (2): 216–33.

Kovall, Rhett A., Brian Gebelein, David Sprinzak, and Raphael Kopan. 2017. "The Canonical Notch Signaling Pathway: Structural and Biochemical Insights into Shape, Sugar, and Force." *Developmental Cell* 41 (3): 228–41.

Kraman, Matthew, and Brent McCright. 2005. "Functional Conservation of Notch1 and Notch2 Intracellular Domains." *FASEB Journal: Official Publication of the Federation of American Societies for Experimental Biology* 19 (10): 1311–13.

Krebs, L. T., Y. Xue, C. R. Norton, J. R. Shutter, M. Maguire, J. P. Sundberg, D. Gallahan, et al. 2000. "Notch Signaling Is Essential for Vascular Morphogenesis in Mice." *Genes & Development* 14 (11): 1343–52.

Krebs, Luke T., Yingzi Xue, Christine R. Norton, John P. Sundberg, Paul Beatus, Urban Lendahl, Anne Joutel, and Thomas Gridley. 2003. "Characterization of Notch3-Deficient Mice: Normal Embryonic Development and Absence of Genetic Interactions with a Notch1 Mutation." *Genesis* 37 (3): 139–43.

Kuang, Yi, Ohad Golan, Kristina Preusse, Brittany Cain, Collin J. Christensen, Joseph Salomone, Ian Campbell, et al. 2020. "Enhancer Architecture Sensitizes Cell-Specific Responses to Notch Gene Dose via a Bind and Discard Mechanism." *eLife* 9 (April). https://doi.org/10.7554/eLife.53659.

Ladi, Ena, James T. Nichols, Weihong Ge, Alison Miyamoto, Christine Yao, Liang-Tung Yang, Jim Boulter, Yi E. Sun, Chris Kintner, and Gerry Weinmaster. 2005. "The Divergent DSL Ligand Dll3 Does Not Activate Notch Signaling but Cell Autonomously Attenuates Signaling Induced by Other DSL Ligands." *The Journal of Cell Biology* 170 (6): 983–92.

Lafkas, Daniel, Amy Shelton, Cecilia Chiu, Gladys de Leon Boenig, Yongmei Chen, Scott S. Stawicki, Christian Siltanen, et al. 2015. "Therapeutic Antibodies Reveal Notch Control of Transdifferentiation in the Adult Lung." *Nature* 528 (7580): 127–31.

Lahmann, Ines, Dominique Bröhl, Tatiana Zyrianova, Akihiro Isomura, Maciej T. Czajkowski, Varun Kapoor, Joscha Griger, et al. 2019. "Oscillations of MyoD and Hes1 Proteins Regulate the Maintenance of Activated Muscle Stem Cells." *Genes & Development* 33 (9-10): 524–35.

Langridge, Paul D., and Gary Struhl. 2017. "Epsin-Dependent Ligand Endocytosis Activates Notch by Force." *Cell* 171 (6): 1383–96.e12.

LaVoie, Matthew J., and Dennis J. Selkoe. 2003. “The Notch Ligands, Jagged and Delta, Are Sequentially Processed by Alpha-Secretase and Presenilin/gamma-Secretase and Release Signaling Fragments.” *The Journal of Biological Chemistry* 278 (36): 34427–37.

LeBon, Lauren, Tom V. Lee, David Sprinzak, Hamed Jafar-Nejad, and Michael B. Elowitz. 2014. “Fringe Proteins Modulate Notch-Ligand Cis and Trans Interactions to Specify Signaling States.” *eLife* 3 (September): e02950.

Lee, Jongwon, Minsu Yoo, and Jungmin Choi. 2022. “Recent Advances in Spatially Resolved Transcriptomics: Challenges and Opportunities.” *BMB Reports* 55 (3): 113–24.

Lehar, Sophie M., James Dooley, Andrew G. Farr, and Michael J. Bevan. 2005. “Notch Ligands Delta 1 and Jagged1 Transmit Distinct Signals to T-Cell Precursors.” *Blood* 105 (4): 1440–47.

Liang, Yu, Hui Han, Qiuchan Xiong, Chunlong Yang, Lu Wang, Jieyi Ma, Shuibin Lin, and Yi-Zhou Jiang. 2021. “METTL3-Mediated m6A Methylation Regulates Muscle Stem Cells and Muscle Regeneration by Notch Signaling Pathway.” *Stem Cells International* 2021 (May): 9955691.

Liu, Zhaoyang, Dongqing Sun, and Chenfei Wang. 2022. “Evaluation of Cell-Cell Interaction Methods by Integrating Single-Cell RNA Sequencing Data with Spatial Information.” *Genome Biology* 23 (1): 218.

Liu, Zhenyi, Eric Brunskill, Barbara Varnum-Finney, Chi Zhang, Andrew Zhang, Patrick Y. Jay, Irv Bernstein, Mitsuru Morimoto, and Raphael Kopan. 2015. “The Intracellular Domains of Notch1 and Notch2 Are Functionally Equivalent during Development and Carcinogenesis.” *Development* 142 (14): 2452–63.

Liu, Zhenyi, Shuang Chen, Scott Boyle, Yu Zhu, Andrew Zhang, David R. Piwnica-Worms, Ma Xenia G. Ilagan, and Raphael Kopan. 2013. “The Extracellular Domain of Notch2 Increases Its Cell-Surface Abundance and Ligand Responsiveness during Kidney Development.” *Developmental Cell* 25 (6): 585–98.

Longo, Sophia K., Margaret G. Guo, Andrew L. Ji, and Paul A. Khavari. 2021. “Integrating Single-Cell and Spatial Transcriptomics to Elucidate Intercellular Tissue Dynamics.” *Nature Reviews. Genetics* 22 (10): 627–44.

Lovendahl, Klaus N., Stephen C. Blacklow, and Wendy R. Gordon. 2018. “The Molecular Mechanism of Notch Activation.” *Advances in Experimental Medicine and Biology* 1066: 47–58.

Luca, Vincent C., Kevin M. Jude, Nathan W. Pierce, Maxence V. Nachury, Suzanne Fischer, and K. Christopher Garcia. 2015. “Structural Basis for Notch1 Engagement of Delta-like 4.” *Science* 347 (6224): 847–53.

Luca, Vincent C., Byoung Choul Kim, Chenghao Ge, Shinako Kakuda, Di Wu, Mehdi Roein-Peikar, Robert S. Haltiwanger, Cheng Zhu, Taekjip Ha, and K. Christopher Garcia. 2017. “Notch-Jagged Complex Structure Implicates a Catch Bond in Tuning Ligand Sensitivity.” *Science* 355 (6331): 1320–24.

Luna-Escalante, Juan C., Pau Formosa-Jordan, and Marta Ibañes. 2018. "Redundancy and Cooperation in Notch Intercellular Signaling." *Development* 145 (1). https://doi.org/10.1242/dev.154807.

Luther, Kelvin B., Hermann Schindelin, and Robert S. Haltiwanger. 2009. "Structural and Mechanistic Insights into Lunatic Fringe from a Kinetic Analysis of Enzyme Mutants." *The Journal of Biological Chemistry* 284 (5): 3294–3305.

Majumder, Samarpan, Judy S. Crabtree, Todd E. Golde, Lisa M. Minter, Barbara A. Osborne, and Lucio Miele. 2021. "Targeting Notch in Oncology: The Path Forward." *Nature Reviews. Drug Discovery* 20 (2): 125–44.

Martin, Alexandre P., Gary A. Bradshaw, Robyn J. Eisert, Emily D. Egan, Lena Tveriakhina, Julia M. Rogers, Andrew N. Dates, et al. 2022. "A Spatiotemporal Notch Interaction Map from Membrane to Nucleus." *bioRxiv*. https://doi.org/10.1101/2022.12.21.521435.

McCright, B., X. Gao, L. Shen, J. Lozier, Y. Lan, M. Maguire, D. Herzlinger, G. Weinmaster, R. Jiang, and T. Gridley. 2001. "Defects in Development of the Kidney, Heart and Eye Vasculature in Mice Homozygous for a Hypomorphic Notch2 Mutation." *Development* 128 (4): 491–502.

Micchelli, C. A., E. J. Rulifson, and S. S. Blair. 1997. "The Function and Regulation of Cut Expression on the Wing Margin of Drosophila: Notch, Wingless and a Dominant Negative Role for Delta and Serrate." *Development* 124 (8): 1485–95.

Miller, Adam C., Eric L. Lyons, and Tory G. Herman. 2009. "Cis-Inhibition of Notch by Endogenous Delta Biases the Outcome of Lateral Inhibition." *Current Biology: CB* 19 (16): 1378–83.

Mitra, Ankita, Sudarvili Shanthalingam, Heather L. Sherman, Khushboo Singh, Mine Canakci, Joe A. Torres, Rebecca Lawlor, et al. 2020. "CD28 Signaling Drives Notch Ligand Expression on CD4 T Cells." *Frontiers in Immunology* 11 (May): 735.

Moran, Jennifer L., Emily T. Shifley, John M. Levorse, Shyamala Mani, Kristin Ostmann, Ariadna Perez-Balaguer, Dawn M. Walker, Thomas F. Vogt, and Susan E. Cole. 2009. "Manic Fringe Is Not Required for Embryonic Development, and Fringe Family Members Do Not Exhibit Redundant Functions in the Axial Skeleton, Limb, or Hindbrain." *Developmental Dynamics: An Official Publication of the American Association of Anatomists* 238 (7): 1803–12.

Morsut, Leonardo, Kole T. Roybal, Xin Xiong, Russell M. Gordley, Scott M. Coyle, Matthew Thomson, and Wendell A. Lim. 2016. "Engineering Customized Cell Sensing and Response Behaviors Using Synthetic Notch Receptors." *Cell* 164 (4): 780–91.

Nandagopal, Nagarajan, Leah A. Santat, and Michael B. Elowitz. 2019. "Cis-Activation in the Notch Signaling Pathway." *eLife* 8 (January). https://doi.org/10.7554/eLife.37880.

Narui, Yoshie, and Khalid Salaita. 2013. "Membrane Tethered Delta Activates Notch and Reveals a Role for Spatio-Mechanical Regulation of the Signaling Pathway." *Biophysical Journal* 105 (12): 2655–65.

Negri, Victor A., Meike E. W. Logtenberg, Lisa M. Renz, Bénédicte Oules, Gernot Walko, and Fiona M. Watt. 2019. "Delta-like 1-Mediated Cis-Inhibition of Jagged1/2 Signalling Inhibits Differentiation of Human Epidermal Cells in Culture." *Scientific Reports* 9 (1): 10825.

Ninov, Nikolay, Maxim Borius, and Didier Y. R. Stainier. 2012. "Different Levels of Notch Signaling Regulate Quiescence, Renewal and Differentiation in Pancreatic Endocrine Progenitors." *Development* 139 (9): 1557–67.

Nofziger, D., A. Miyamoto, K. M. Lyons, and G. Weinmaster. 1999. "Notch Signaling Imposes Two Distinct Blocks in the Differentiation of C2C12 Myoblasts." *Development* 126 (8): 1689–1702.

Palmer, William Hunt, Dongyu Jia, and Wu-Min Deng. 2014. "Cis-Interactions between Notch and Its Ligands Block Ligand-Independent Notch Activity." *eLife* 3 (December). https://doi.org/10.7554/eLife.04415.

Parr-Sturgess, Catherine A., David J. Rushton, and Edward T. Parkin. 2010. "Ectodomain Shedding of the Notch Ligand Jagged1 Is Mediated by ADAM17, but Is Not a Lipid-Raft-Associated Event." *Biochemical Journal* 432 (2): 283–94.

Pedrosa, Ana-Rita, Alexandre Trindade, Ana-Carina Fernandes, Catarina Carvalho, Joana Gigante, Ana Teresa Tavares, Rodrigo Diéguez-Hurtado, Hideo Yagita, Ralf H. Adams, and António Duarte. 2015. "Endothelial Jagged1 Antagonizes Dll4 Regulation of Endothelial Branching and Promotes Vascular Maturation Downstream of Dll4/Notch1." *Arteriosclerosis, Thrombosis, and Vascular Biology* 35 (5): 1134–46.

Pennarubia, Florian, Alison V. Nairn, Megumi Takeuchi, Kelley W. Moremen, and Robert S. Haltiwanger. 2021. "Modulation of the NOTCH1 Pathway by LUNATIC FRINGE Is Dominant over That of MANIC or RADICAL FRINGE." *Molecules* 26 (19). https://doi.org/10.3390/molecules26195942.

Penton, Andrea L., Laura D. Leonard, and Nancy B. Spinner. 2012. "Notch Signaling in Human Development and Disease." *Seminars in Cell & Developmental Biology* 23 (4): 450–57.

Preuße, Kristina, Lena Tveriakhina, Karin Schuster-Gossler, Cláudia Gaspar, Alexandra Isabel Rosa, Domingos Henrique, Achim Gossler, and Michael Stauber. 2015. "Context-Dependent Functional Divergence of the Notch Ligands DLL1 and DLL4 In Vivo." *PLoS Genetics* 11 (6): e1005328.

Rabadán, M. A., J. Cayuso, G. Le Dréau, C. Cruz, M. Barzi, S. Pons, J. Briscoe, and E. Martí. 2012. "Jagged2 Controls the Generation of Motor Neuron and Oligodendrocyte Progenitors in the Ventral Spinal Cord." *Cell Death and Differentiation* 19 (2): 209–19.

Radhakrishnan, Krishnan, Ádám Halász, Meghan M. McCabe, Jeremy S. Edwards, and Bridget S. Wilson. 2012. "Mathematical Simulation of Membrane Protein Clustering for Efficient Signal Transduction." *Annals of Biomedical Engineering* 40 (11): 2307–18.

Ramos, Catarina, Susana Rocha, Claudia Gaspar, and Domingos Henrique. 2010. "Two Notch Ligands, Dll1 and Jag1, Are Differently Restricted in Their Range of Action to Control Neurogenesis in the Mammalian Spinal Cord." *PloS One* 5 (11): e15515.

Riccio, Orbicia, Marielle E. van Gijn, April C. Bezdek, Luca Pellegrinet, Johan H. van Es, Ursula Zimber-Strobl, Lothar J. Strobl, Tasuku Honjo, Hans Clevers, and Freddy Radtke. 2008. "Loss of Intestinal Crypt Progenitor Cells Owing to Inactivation of Both Notch1 and Notch2 Is Accompanied by Derepression of CDK Inhibitors p27Kip1 and p57Kip2." *EMBO Reports* 9 (4): 377–83.

Rios, Anne C., Olivier Serralbo, David Salgado, and Christophe Marcelle. 2011. "Neural Crest Regulates Myogenesis through the Transient Activation of NOTCH." *Nature* 473 (7348): 532–35.

Rocha, Susana Ferreira, Susana Santos Lopes, Achim Gossler, and Domingos Henrique. 2009. "Dll1 and Dll4 Function Sequentially in the Retina and pV2 Domain of the Spinal Cord to Regulate Neurogenesis and Create Cell Diversity." *Developmental Biology* 328 (1): 54–65.

Romero-Wolf, Maile, Boyoung Shin, Wen Zhou, Maria Koizumi, Ellen V. Rothenberg, and Hiroyuki Hosokawa. 2020. "Notch2 Complements Notch1 to Mediate Inductive Signaling That Initiates Early T Cell Development." *The Journal of Cell Biology* 219 (10). https://doi.org/10.1083/jcb.202005093.

Rusanescu, Gabriel, and Jianren Mao. 2014. "Notch3 Is Necessary for Neuronal Differentiation and Maturation in the Adult Spinal Cord." *Journal of Cellular and Molecular Medicine* 18 (10): 2103–16.

Sakata-Yanagimoto, Mamiko, Etsuko Nakagami-Yamaguchi, Toshiki Saito, Keiki Kumano, Koji Yasutomo, Seishi Ogawa, Mineo Kurokawa, and Shigeru Chiba. 2008. "Coordinated Regulation of Transcription Factors through *Notch2* Is an Important Mediator of Mast Cell Fate." *Proceedings of the National Academy of Sciences of the United States of America* 105 (22): 7839–44.

Sánchez-Iranzo, Héctor, Aliaksandr Halavatyi, and Alba Diz-Muñoz. 2022. "Strength of Interactions in the Notch Gene Regulatory Network Determines Patterning and Fate in the Notochord." *eLife* 11 (June). https://doi.org/10.7554/eLife.75429.

Sassoli, Chiara, Alessandro Pini, Flaminia Chellini, Benedetta Mazzanti, Silvia Nistri, Daniele Nosi, Riccardo Saccardi, Franco Quercioli, Sandra Zecchi-Orlandini, and Lucia Formigli. 2012. "Bone Marrow Mesenchymal Stromal Cells Stimulate Skeletal Myoblast Proliferation through the Paracrine Release of VEGF." *PloS One* 7 (7): e37512.

Sekine, Chiyoko, Akemi Koyanagi, Noriko Koyama, Katsuto Hozumi, Shigeru Chiba, and Hideo Yagita. 2012. "Differential Regulation of Osteoclastogenesis by Notch2/Delta-like 1 and Notch1/Jagged1 Axes." *Arthritis Research & Therapy* 14 (2): R45.

Serth, Katrin, Karin Schuster-Gossler, Elisabeth Kremmer, Birte Hansen, Britta Marohn-Köhn, and Achim Gossler. 2015. "O-Fucosylation of DLL3 Is Required for Its Function during Somitogenesis." *PloS One* 10 (4): e0123776.

Sewell, William, Duncan B. Sparrow, Allanceson J. Smith, Dorian M. Gonzalez, Eric F. Rappaport, Sally L. Dunwoodie, and Kenro Kusumi. 2009. "Cyclical Expression of the Notch/Wnt Regulator Nrarp Requires Modulation by Dll3 in Somitogenesis." *Developmental Biology* 329 (2): 400–409.

Seymour, Philip Allan, Caitlin Alexis Collin, Anuska la Rosa Egeskov-Madsen, Mette Christine Jørgensen, Hiromi Shimojo, Itaru Imayoshi, Kristian Honnens de Lichtenberg, Raphael Kopan, Ryoichiro Kageyama, and Palle Serup. 2020. "Jag1 Modulates an Oscillatory Dll1-Notch-Hes1 Signaling Module to Coordinate Growth and Fate of Pancreatic Progenitors." *Developmental Cell* 52 (6): 731–47.e8.

Shawber, C., D. Nofziger, J. J. Hsieh, C. Lindsell, O. Bögler, D. Hayward, and G. Weinmaster. 1996. "Notch Signaling Inhibits Muscle Cell Differentiation through a CBF1-Independent Pathway." *Development* 122 (12): 3765–73.

Shaya, Oren, Udi Binshtok, Micha Hersch, Dmitri Rivkin, Sheila Weinreb, Liat Amir-Zilberstein, Bassma Khamaisi, et al. 2017. "Cell-Cell Contact Area Affects Notch Signaling and Notch-Dependent Patterning." *Developmental Cell* 40 (5): 505–11.e6.

Sheldon, Helen, Emily Heikamp, Helen Turley, Rebecca Dragovic, Peter Thomas, Chern Ein Oon, Russell Leek, et al. 2010. "New Mechanism for Notch Signaling to Endothelium at a Distance by Delta-like 4 Incorporation into Exosomes." *Blood* 116 (13): 2385–94.

Shimizu, K., S. Chiba, T. Saito, K. Kumano, T. Takahashi, and H. Hirai. 2001. "Manic Fringe and Lunatic Fringe Modify Different Sites of the Notch2 Extracellular Region, Resulting in Different Signaling Modulation." *The Journal of Biological Chemistry* 276 (28): 25753–58.

Shimojo, Hiromi, Toshiyuki Ohtsuka, and Ryoichiro Kageyama. 2008. "Oscillations in Notch Signaling Regulate Maintenance of Neural Progenitors." *Neuron* 58 (1): 52–64.

Singh, Ankita, Helene F. Kildegaard, and Mikael R. Andersen. 2018. "An Online Compendium of CHO RNA-Seq Data Allows Identification of CHO Cell Line-Specific Transcriptomic Signatures." *Biotechnology Journal* 13 (10): e1800070.

Six, Emmanuelle, Delphine Ndiaye, Yacine Laabi, Christel Brou, Neetu Gupta-Rossi, Alain Israel, and Frederique Logeat. 2003. "The Notch Ligand Delta1 Is Sequentially Cleaved by an ADAM Protease and Gamma-Secretase." *Proceedings of the National Academy of Sciences of the United States of America* 100 (13): 7638–43.

Sjöqvist, Marika, and Emma R. Andersson. 2019. "Do as I Say, Not(ch) as I Do: Lateral Control of Cell Fate." *Developmental Biology* 447 (1): 58–70.

Song, Yinghui, Vivek Kumar, Hua-Xing Wei, Ju Qiu, and Pamela Stanley. 2016. "Lunatic, Manic, and Radical Fringe Each Promote T and B Cell Development." *Journal of Immunology* 196 (1): 232–43.

Sprinzak, David, Amit Lakhanpal, Lauren Lebon, Leah A. Santat, Michelle E. Fontes, Graham A. Anderson, Jordi Garcia-Ojalvo, and Michael B. Elowitz. 2010. "Cis-Interactions between Notch and Delta Generate Mutually Exclusive Signalling States." *Nature* 465 (7294): 86–90.

Ståhl, Patrik L., Fredrik Salmén, Sanja Vickovic, Anna Lundmark, José Fernández Navarro, Jens Magnusson, Stefania Giacomello, et al. 2016. "Visualization and Analysis of Gene Expression in Tissue Sections by Spatial Transcriptomics." *Science* 353 (6294): 78–82.

Stanley, Pamela. 2007. "Regulation of Notch Signaling by Glycosylation." *Current Opinion in Structural Biology* 17 (5): 530–35.

Stanley, Pamela, and Cynthia J. Guidos. 2009. “Regulation of Notch Signaling during T- and B-Cell Development by O-Fucose Glycans.” *Immunological Reviews* 230 (1): 201–15.

Sueda, Risa, and Ryoichiro Kageyama. 2020. “Regulation of Active and Quiescent Somatic Stem Cells by Notch Signaling.” *Development, Growth & Differentiation* 62 (1): 59–66.

Sun, Danqiong, Hui Li, and Anna Zolkiewska. 2008. “The Role of Delta-like 1 Shedding in Muscle Cell Self-Renewal and Differentiation.” *Journal of Cell Science* 121 (Pt 22): 3815–23.

Swiatek, P. J., C. E. Lindsell, F. F. del Amo, G. Weinmaster, and T. Gridley. 1994. “Notch1 Is Essential for Postimplantation Development in Mice.” *Genes & Development* 8 (6): 707–19.

Taghon, Tom, Inge Van de Walle, Greet De Smet, Magda De Smedt, Georges Leclercq, Bart Vandekerckhove, and Jean Plum. 2009. “Notch Signaling Is Required for Proliferation but Not for Differentiation at a Well-Defined Beta-Selection Checkpoint during Human T-Cell Development.” *Blood* 113 (14): 3254–63.

Takagi, Akari, Akihiro Isomura, Kumiko Yoshioka-Kobayashi, and Ryoichiro Kageyama. 2020. “Dynamic Delta-like1 Expression in Presomitic Mesoderm Cells during Somite Segmentation.” *Gene Expression Patterns: GEP* 35 (January): 119094.

Tan, Evan, Harry H. Asada, and Ruowen Ge. 2018. “Extracellular Vesicle-Carried Jagged-1 Inhibits HUVEC Sprouting in a 3D Microenvironment.” *Angiogenesis* 21 (3): 571–80.

Tan, G. Christopher, Esteban O. Mazzoni, and Hynek Wichterle. 2016. “Iterative Role of Notch Signaling in Spinal Motor Neuron Diversification.” *Cell Reports* 16 (4): 907–16.

Taylor, Paul, Hideyuki Takeuchi, Devon Sheppard, Chandramouli Chillakuri, Susan M. Lea, Robert S. Haltiwanger, and Penny A. Handford. 2014. “Fringe-Mediated Extension of O-Linked Fucose in the Ligand-Binding Region of Notch1 Increases Binding to Mammalian Notch Ligands.” *Proceedings of the National Academy of Sciences of the United States of America* 111 (20): 7290–95.

Tetzlaff, Fabian, M. Gordian Adam, Anja Feldner, Iris Moll, Amitai Menuchin, Juan Rodriguez-Vita, David Sprinzak, and Andreas Fischer. 2018. “MPDZ Promotes DLL4-Induced Notch Signaling during Angiogenesis.” *eLife* 7 (April). https://doi.org/10.7554/eLife.32860.

Troost, Tobias, Udi Binshtok, David Sprinzak, and Thomas Klein. 2022. “Cis-Inhibition Suppresses Basal Notch Signalling during Sensory Organ Precursor Selection.” *bioRxiv*. https://doi.org/10.1101/2022.07.19.500683.

Tveriakhina, Lena, Karin Schuster-Gossler, Sanchez M. Jarrett, Marie B. Andrawes, Meike Rohrbach, Stephen C. Blacklow, and Achim Gossler. 2018. “The Ectodomains Determine Ligand Function in Vivo and Selectivity of DLL1 and DLL4 toward NOTCH1 and NOTCH2 in Vitro.” *eLife* 7 (October). https://doi.org/10.7554/eLife.40045.

Van de Walle, Inge, Greet De Smet, Martina Gärtner, Magda De Smedt, Els Waegemans, Bart Vandekerckhove, Georges Leclercq, et al. 2011. “Jagged2 Acts as a Delta-like Notch Ligand during Early Hematopoietic Cell Fate Decisions.” *Blood* 117 (17): 4449–59.

Varshney, Shweta, and Pamela Stanley. 2017. “Notch Ligand Binding Assay Using Flow Cytometry.” *Bio-Protocol* 7 (23). https://doi.org/10.21769/BioProtoc.2637.

Xu, Xiaochan, Philip Allan Seymour, Kim Sneppen, Ala Trusina, Anuska la Rosa Egeskov-Madsen, Mette Christine Jørgensen, Mogens Høgh Jensen, and Palle Serup. 2023. "Jag1-Notch Cis-Interaction Determines Cell Fate Segregation in Pancreatic Development." *Nature Communications* 14 (1): 348.

Yang, Liang-Tung, James T. Nichols, Christine Yao, Jennifer O. Manilay, Ellen A. Robey, and Gerry Weinmaster. 2005. "Fringe Glycosyltransferases Differentially Modulate Notch1 Proteolysis Induced by Delta1 and Jagged1." *Molecular Biology of the Cell* 16 (2): 927–42.

Yao, Erica, Chuwen Lin, Qingzhe Wu, Kuan Zhang, Hai Song, and Pao-Tien Chuang. 2018. "Notch Signaling Controls Transdifferentiation of Pulmonary Neuroendocrine Cells in Response to Lung Injury." *Stem Cells* 36 (3): 377–91.

Yatsenko, Andriy S., and Halyna R. Shcherbata. 2021. "Distant Activation of Notch Signaling Induces Stem Cell Niche Assembly." *PLoS Genetics* 17 (3): e1009489.

Yu, Jungeun, and Ernesto Canalis. 2020. "Notch and the Regulation of Osteoclast Differentiation and Function." *Bone*, June, 115474.

Zamfirescu, Ana-Maria, Andriy S. Yatsenko, and Halyna R. Shcherbata. 2022. "Notch Signaling Sculpts the Stem Cell Niche." *Frontiers in Cell and Developmental Biology* 10 (December): 1027222.

Zhang, Nian, Christine R. Norton, and Thomas Gridley. 2002. "Segmentation Defects of Notch Pathway Mutants and Absence of a Synergistic Phenotype in Lunatic Fringe/radical Fringe Double Mutant Mice." *Genesis* 33 (1): 21–28.

Zhou, Binghan, Wanling Lin, Yaling Long, Yunkai Yang, Huan Zhang, Kongming Wu, and Qian Chu. 2022. "Notch Signaling Pathway: Architecture, Disease, and Therapeutics." *Signal Transduction and Targeted Therapy* 7 (1): 95.

Andrawes MB, Xu X, Liu H, Ficarro SB, Marto JA, Aster JC, Blacklow SC. 2013. Intrinsic selectivity of Notch 1 for Delta-like 4 over Delta-like 1. J Biol Chem 288:25477–25489.

Baek C, Freem L, Goïame R, Sang H, Morin X, Tozer S. 2018. Mib1 prevents Notch Cis-inhibition to defer differentiation and preserve neuroepithelial integrity during neural delamination. PLoS Biol 16:e2004162.

Becam I, Fiuza U-M, Arias AM, Milán M. 2010. A role of receptor Notch in ligand cis-inhibition in Drosophila. Curr Biol 20:554–560.

Benedito R, Roca C, Sörensen I, Adams S, Gossler A, Fruttiger M, Adams RH. 2009. The notch ligands Dll4 and Jagged1 have opposing effects on angiogenesis. Cell 137:1124–1135.

Bochter MS, Servello D, Kakuda S, D'Amico R, Ebetino MF, Haltiwanger RS, Cole SE. 2022. Lfng and Dll3 cooperate to modulate protein interactions in cis and coordinate oscillatory Notch pathway activation in the segmentation clock. Dev Biol 487:42–56.

Chen D, Forghany Z, Liu X, Wang H, Merks RMH, Baker DA. 2023. A new model of Notch signalling: Control of Notch receptor cis-inhibition via Notch ligand dimers. PLoS Comput Biol 19:e1010169.

Cordle J, Johnson S, Tay JZY, Roversi P, Wilkin MB, de Madrid BH, Shimizu H, Jensen S, Whiteman P, Jin B, Redfield C, Baron M, Lea SM, Handford PA. 2008. A conserved face of the Jagged/Serrate DSL domain is involved in Notch trans-activation and cis-inhibition. Nat Struct Mol Biol 15:849–857.

Dahlqvist C, Blokzijl A, Chapman G, Falk A, Dannaeus K, Ibâñez CF, Lendahl U. 2003. Functional Notch signaling is required for BMP4-induced inhibition of myogenic differentiation. Development 130:6089–6099.

del Álamo D, Rouault H, Schweisguth F. 2011. Mechanism and significance of cis-inhibition in Notch signalling. Curr Biol 21:R40–7.

Del Real MM, Rothenberg EV. 2013. Architecture of a lymphomyeloid developmental switch controlled by PU.1, Notch and Gata3. Development 140:1207–1219.

D'Souza B, Miyamoto A, Weinmaster G. 2008. The many facets of Notch ligands. Oncogene 27:5148–5167.

Elowitz MB, Santat LA, Nandagopal N. 2018. Cis-activation in the Notch signaling pathway. bioRxiv. doi:10.1101/313171

Falix FA, Aronson DC, Lamers WH, Gaemers IC. 2012. Possible roles of DLK1 in the Notch pathway during development and disease. Biochim Biophys Acta 1822:988–995.

Falo-Sanjuan J, Lammers NC, Garcia HG, Bray SJ. 2019. Enhancer Priming Enables Fast and Sustained Transcriptional Responses to Notch Signaling. Dev Cell 50:411–425.e8.

Fiddes IT, Lodewijk GA, Mooring M, Bosworth CM, Ewing AD, Mantalas GL, Novak AM, van den Bout A, Bishara A, Rosenkrantz JL, Lorig-Roach R, Field AR, Haeussler M, Russo L, Bhaduri A, Nowakowski TJ, Pollen AA, Dougherty ML, Nuttle X, Addor M-C, Zwolinski S, Katzman S, Kriegstein A, Eichler EE, Salama SR, Jacobs FMJ, Haussler D. 2018. Human-Specific NOTCH2NL Genes Affect Notch Signaling and Cortical Neurogenesis. Cell 173:1356–1369.e22.

Fiuza U-M, Klein T, Martinez Arias A, Hayward P. 2010. Mechanisms of ligand-mediated inhibition in Notch signaling activity in Drosophila. Dev Dyn 239:798–805.

Fleming RJ, Hori K, Sen A, Filloramo GV, Langer JM, Obar RA, Artavanis-Tsakonas S, Maharaj-Best AC. 2013. An extracellular region of Serrate is essential for ligand-induced cis-inhibition of Notch signaling. Development 140:2039–2049.

Gama-Norton L, Ferrando E, Ruiz-Herguido C, Liu Z, Guiu J, Islam ABMMK, Lee S-U, Yan M, Guidos CJ, López-Bigas N, Maeda T, Espinosa L, Kopan R, Bigas A. 2015. Notch signal strength controls cell fate in the haemogenic endothelium. Nat Commun 6:8510.

Gera S, Dighe RR. 2018. The soluble ligand Ybox-1 activates Notch3 receptor by binding to epidermal growth factor like repeats 20-23. Arch Biochem Biophys. doi:10.1016/j.abb.2018.10.009

Gioftsidi S, Relaix F, Mourikis P. 2022. The Notch signaling network in muscle stem cells during development, homeostasis, and disease. Skelet Muscle 12:9.

Golson ML, Le Lay J, Gao N, Brämswig N, Loomes KM, Oakey R, May CL, White P, Kaestner KH. 2009. Jagged1 is a competitive inhibitor of Notch signaling in the embryonic pancreas. Mech Dev 126:687–699.

Granados AA, Kanrar N, Elowitz MB. 2022. Combinatorial expression motifs in signaling pathways. bioRxiv. doi:10.1101/2022.08.21.504714

Groot AJ, Habets R, Yahyanejad S, Hodin CM, Reiss K, Saftig P, Theys J, Vooijs M. 2014. Regulated proteolysis of NOTCH2 and NOTCH3 receptors by ADAM10 and presenilins. Mol Cell Biol 34:2822–2832.

Guentchev M, McKay RDG. 2006. Notch controls proliferation and differentiation of stem cells in a dose-dependent manner. Eur J Neurosci 23:2289–2296.

Hadjivasiliou Z, Hunter GL, Baum B. 2016. A new mechanism for spatial pattern formation via lateral and protrusion-mediated lateral signalling. J R Soc Interface 13. doi:10.1098/rsif.2016.0484

Hicks C, Johnston SH, diSibio G, Collazo A, Vogt TF, Weinmaster G. 2000. Fringe differentially modulates Jagged1 and Delta1 signalling through Notch1 and Notch2. Nat Cell Biol 2:515–520.

James AC, Szot JO, Iyer K, Major JA, Pursglove SE, Chapman G, Dunwoodie SL. 2014. Notch4 reveals a novel mechanism regulating Notch signal transduction. Biochim Biophys Acta 1843:1272–1284.

Kakuda S, Haltiwanger RS. 2017. Deciphering the Fringe-Mediated Notch Code: Identification of Activating and Inhibiting Sites Allowing Discrimination between Ligands. Dev Cell 40:193–201.

Kakuda S, LoPilato RK, Ito A, Haltiwanger RS. 2020. Canonical Notch ligands and Fringes have distinct effects on NOTCH1 and NOTCH2. J Biol Chem 295:14710–14722.

Kim M-Y, Jung J, Mo J-S, Ann E-J, Ahn J-S, Yoon J-H, Park H-S. 2011. The intracellular domain of Jagged-1 interacts with Notch1 intracellular domain and promotes its degradation through Fbw7 E3 ligase. Exp Cell Res 317:2438–2446.

Kitamoto T, Takahashi K, Takimoto H, Tomizuka K, Hayasaka M, Tabira T, Hanaoka K. 2005. Functional redundancy of the Notch gene family during mouse embryogenesis: analysis of Notch gene expression in Notch3-deficient mice. Biochem Biophys Res Commun 331:1154–1162.

Krebs LT, Xue Y, Norton CR, Shutter JR, Maguire M, Sundberg JP, Gallahan D, Closson V, Kitajewski J, Callahan R, Smith GH, Stark KL, Gridley T. 2000. Notch signaling is essential for vascular morphogenesis in mice. Genes Dev 14:1343–1352.

Krebs LT, Xue Y, Norton CR, Sundberg JP, Beatus P, Lendahl U, Joutel A, Gridley T. 2003. Characterization of Notch3-deficient mice: normal embryonic development and absence of genetic interactions with a Notch1 mutation. Genesis 37:139–143.

Ladi E, Nichols JT, Ge W, Miyamoto A, Yao C, Yang L-T, Boulter J, Sun YE, Kintner C, Weinmaster G. 2005. The divergent DSL ligand Dll3 does not activate Notch signaling but cell autonomously attenuates signaling induced by other DSL ligands. J Cell Biol 170:983–992.

Lafkas D, Shelton A, Chiu C, de Leon Boenig G, Chen Y, Stawicki SS, Siltanen C, Reichelt M, Zhou M, Wu X, Eastham-Anderson J, Moore H, Roose-Girma M, Chinn Y, Hang JQ, Warming S, Egen J, Lee WP, Austin C, Wu Y, Payandeh J, Lowe JB, Siebel CW. 2015. Therapeutic antibodies reveal Notch control of transdifferentiation in the adult lung. Nature 528:127–131.

Langridge PD, Struhl G. 2017. Epsin-Dependent Ligand Endocytosis Activates Notch by Force. Cell 171:1383–1396.e12.

LeBon L, Lee TV, Sprinzak D, Jafar-Nejad H, Elowitz MB. 2014. Fringe proteins modulate Notch-ligand cis and trans interactions to specify signaling states. Elife 3:e02950.

Lehar SM, Dooley J, Farr AG, Bevan MJ. 2005. Notch ligands Delta 1 and Jagged1 transmit distinct signals to T-cell precursors. Blood 105:1440–1447.

Liang Y, Han H, Xiong Q, Yang C, Wang L, Ma J, Lin S, Jiang Y-Z. 2021. METTL3-Mediated m6A Methylation Regulates Muscle Stem Cells and Muscle Regeneration by Notch Signaling Pathway. Stem Cells Int 2021:9955691.

Lovendahl KN, Blacklow SC, Gordon WR. 2018. The Molecular Mechanism of Notch Activation. Adv Exp Med Biol 1066:47–58.

Luca VC, Kim BC, Ge C, Kakuda S, Wu D, Roein-Peikar M, Haltiwanger RS, Zhu C, Ha T, Garcia KC. 2017. Notch-Jagged complex structure implicates a catch bond in tuning ligand sensitivity. Science 355:1320–1324.

Luna-Escalante JC, Formosa-Jordan P, Ibañes M. 2018. Redundancy and cooperation in Notch intercellular signaling. Development 145. doi:10.1242/dev.154807

Luther KB, Schindelin H, Haltiwanger RS. 2009. Structural and mechanistic insights into lunatic fringe from a kinetic analysis of enzyme mutants. J Biol Chem 284:3294–3305.

Mitra A, Shanthalingam S, Sherman HL, Singh K, Canakci M, Torres JA, Lawlor R, Ran Y, Golde TE, Miele L, Thayumanavan S, Minter LM, Osborne BA. 2020. CD28 Signaling Drives Notch Ligand Expression on CD4 T Cells. Front Immunol 11:735.

Nandagopal N, Santat LA, Elowitz MB. 2019. Cis-activation in the Notch signaling pathway. Elife 8. doi:10.7554/eLife.37880

Narui Y, Salaita K. 2013. Membrane tethered delta activates notch and reveals a role for spatio-mechanical regulation of the signaling pathway. Biophys J 105:2655–2665.

Ninov N, Borius M, Stainier DYR. 2012. Different levels of Notch signaling regulate quiescence, renewal and differentiation in pancreatic endocrine progenitors. Development 139:1557–1567.

Nofziger D, Miyamoto A, Lyons KM, Weinmaster G. 1999. Notch signaling imposes two distinct blocks in the differentiation of C2C12 myoblasts. Development 126:1689–1702.

Pedrosa A-R, Trindade A, Fernandes A-C, Carvalho C, Gigante J, Tavares AT, Diéguez-Hurtado R, Yagita H, Adams RH, Duarte A. 2015. Endothelial Jagged1 antagonizes Dll4 regulation of endothelial branching and promotes vascular maturation downstream of Dll4/Notch1. Arterioscler Thromb Vasc Biol 35:1134–1146.

Pennarubia F, Nairn AV, Takeuchi M, Moremen KW, Haltiwanger RS. 2021. Modulation of the NOTCH1 Pathway by LUNATIC FRINGE Is Dominant over That of MANIC or RADICAL FRINGE. Molecules 26. doi:10.3390/molecules26195942

Preuße K, Tveriakhina L, Schuster-Gossler K, Gaspar C, Rosa AI, Henrique D, Gossler A, Stauber M. 2015. Context-Dependent Functional Divergence of the Notch Ligands DLL1 and DLL4 In Vivo. PLoS Genet 11:e1005328.

Romero-Wolf M, Shin B, Zhou W, Koizumi M, Rothenberg EV, Hosokawa H. 2020. Notch2 complements Notch1 to mediate inductive signaling that initiates early T cell development. J Cell Biol 219. doi:10.1083/jcb.202005093

Sakata-Yanagimoto M, Nakagami-Yamaguchi E, Saito T, Kumano K, Yasutomo K, Ogawa S, Kurokawa M, Chiba S. 2008. Coordinated regulation of transcription factors through Notch2 is an important mediator of mast cell fate. Proc Natl Acad Sci U S A 105:7839–7844.

Sánchez-Iranzo H, Halavatyi A, Diz-Muñoz A. 2022. Strength of interactions in the Notch gene regulatory network determines patterning and fate in the notochord. Elife 11. doi:10.7554/eLife.75429

Sassoli C, Pini A, Chellini F, Mazzanti B, Nistri S, Nosi D, Saccardi R, Quercioli F, Zecchi-Orlandini S, Formigli L. 2012. Bone marrow mesenchymal stromal cells stimulate skeletal myoblast proliferation through the paracrine release of VEGF. PLoS One 7:e37512.

Serth K, Schuster-Gossler K, Kremmer E, Hansen B, Marohn-Köhn B, Gossler A. 2015. O-fucosylation of DLL3 is required for its function during somitogenesis. PLoS One 10:e0123776.

Sewell W, Sparrow DB, Smith AJ, Gonzalez DM, Rappaport EF, Dunwoodie SL, Kusumi K. 2009. Cyclical expression of the Notch/Wnt regulator Nrarp requires modulation by Dll3 in somitogenesis. Dev Biol 329:400–409.

Shawber C, Nofziger D, Hsieh JJ, Lindsell C, Bögler O, Hayward D, Weinmaster G. 1996. Notch signaling inhibits muscle cell differentiation through a CBF1-independent pathway. Development 122:3765–3773.

Shimizu K, Chiba S, Saito T, Kumano K, Takahashi T, Hirai H. 2001. Manic fringe and lunatic fringe modify different sites of the Notch2 extracellular region, resulting in different signaling modulation. J Biol Chem 276:25753–25758.

Singh A, Kildegaard HF, Andersen MR. 2018. An Online Compendium of CHO RNA-Seq Data Allows Identification of CHO Cell Line-Specific Transcriptomic Signatures. Biotechnol J 13:e1800070.

Song Y, Kumar V, Wei H-X, Qiu J, Stanley P. 2016. Lunatic, Manic, and Radical Fringe Each Promote T and B Cell Development. J Immunol 196:232–243.

Sprinzak D, Lakhanpal A, Lebon L, Santat LA, Fontes ME, Anderson GA, Garcia-Ojalvo J, Elowitz MB. 2010. Cis-interactions between Notch and Delta generate mutually exclusive signalling states. Nature 465:86–90.

Stanley P, Guidos CJ. 2009. Regulation of Notch signaling during T- and B-cell development by O-fucose glycans. Immunol Rev 230:201–215.

Sun D, Li H, Zolkiewska A. 2008. The role of Delta-like 1 shedding in muscle cell self-renewal and differentiation. J Cell Sci 121:3815–3823.

Taghon T, Van de Walle I, De Smet G, De Smedt M, Leclercq G, Vandekerckhove B, Plum J. 2009. Notch signaling is required for proliferation but not for differentiation at a well-defined beta-selection checkpoint during human T-cell development. Blood 113:3254–3263.

Taylor P, Takeuchi H, Sheppard D, Chillakuri C, Lea SM, Haltiwanger RS, Handford PA. 2014. Fringe-mediated extension of O-linked fucose in the ligand-binding region of Notch1 increases binding to mammalian Notch ligands. Proc Natl Acad Sci U S A 111:7290–7295.

Tveriakhina L, Schuster-Gossler K, Jarrett SM, Andrawes MB, Rohrbach M, Blacklow SC, Gossler A. 2018. The ectodomains determine ligand function in vivo and selectivity of DLL1 and DLL4 toward NOTCH1 and NOTCH2 in vitro. Elife 7. doi:10.7554/eLife.40045

Varshney S, Stanley P. 2017. Notch Ligand Binding Assay Using Flow Cytometry. Bio Protoc 7. doi:10.21769/BioProtoc.2637

Xu X, Seymour PA, Sneppen K, Trusina A, Egeskov-Madsen A la R, Jørgensen MC, Jensen MH, Serup P. 2023. Jag1-Notch cis-interaction determines cell fate segregation in pancreatic development. Nat Commun 14:348.

Yang L-T, Nichols JT, Yao C, Manilay JO, Robey EA, Weinmaster G. 2005. Fringe glycosyltransferases differentially modulate Notch1 proteolysis induced by Delta1 and Jagged1. Mol Biol Cell 16:927–942.

Yatsenko AS, Shcherbata HR. 2021. Distant activation of Notch signaling induces stem cell niche assembly. PLoS Genet 17:e1009489.

Zamfirescu A-M, Yatsenko AS, Shcherbata HR. 2022. Notch signaling sculpts the stem cell niche. Front Cell Dev Biol 10:1027222.